VIRGINIA TECH

COLLEGE OF ENGINEERING
BRADLEY DEPARTMENT OF ELECTRICAL AND COMPUTER ENGINEERING
VIRGINIA TECH

TUTORIAL PRESENTATION

REMOTE MEASUREMENT OF VITAL SIGNS USING AI FOR HEALTH MONITORING AND COGNITION

ABHIJIT SARKAR AND LYNN ABBOTT

AHFE 2023 International Conference

INTRODUCTION

PURPOSE OF THIS TUTORIAL

- To describe new technologies for measuring vital signs, particularly noncontact ("remote") methods
- To describe how remote measurement of vital signs might be useful for applications beyond monitoring of a person's health

RESEARCH TEAM

- Abhijit Sarkar
- Lynn Abbott
- Yogesh Deshpande
- Surendrabikram Thapa
- Fulan Li





VIRGINIA TECH

A. LYNN ABBOTT, PHD

PROFESSOR, DEPARTMENT OF ECE, VIRGINIA TECH

ABOUT VIRGINIA TECH

- Virginia Polytechnic Institute and State University
- Founded in 1872
- 37,000 students
- 2,575 instructional faculty members (both full and part-time)
- $521 million in research expenditures (ranks 24th among public research universities in National Science Foundation's annual survey of higher education research expenditures)
- Departments represented here:
  - Electrical and Computer Engineering
  - Computer Science

VIRGINIA TECH

ABHIJIT SARKAR, PHD

SENIOR RESEARCH ASSOCIATE, TEAM LEADER
VTTI

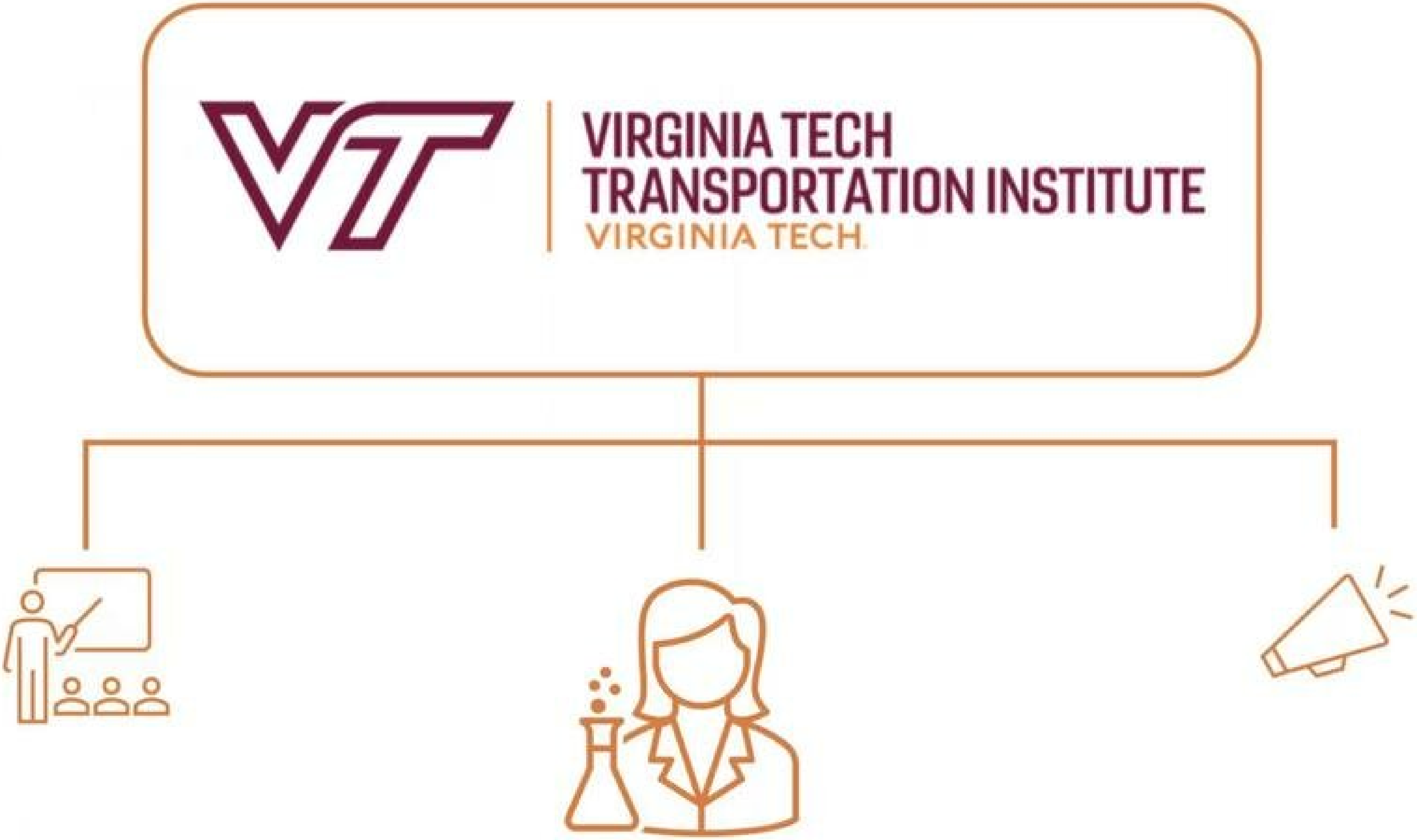
VIRGINIA TECH
TRANSPORTATION INSTITUTE
VIRGINIA TECH

With a legacy of innovation and pioneering approaches, we are the global destination for mobility research.

300+	researchers dedicating their lives to saving lives
$1B	of infrastructure accessible to VTTI and partners
$150M	in infrastructure managed by VTTI
$50M	annual research portfolio supporting 100s of sponsors
70M	miles of naturalistic driving data
>1M	hours of car naturalistic driving data
3,000	studies completed
4,000	instrumented vehicles
30,000	hours of data collected on Virginia Smart Roads

UT PROSIM

VIRGINIA TECH TRANSPORTATION INSTITUTE

For VTTI, innovation is a team sport.

VDOT GM Qualcomm Transurban SAFE-D NEC Ford AMERICAN TOWER DBi SERVICES JBG SMITH Google DAIMLER NISSAN GOODYEAR BMW HONDA CISCO PHILIPS MICHELIN TOYOTA SIEMENS AT&T WAYMO SPIN U.S. DEPARTMENT OF ENERGY Audi leidos e.g.

For a more complete list of our 200+ partners, check out our website at: https://www.vtti.vt.edu/about/partners-sponsors.html

Facilities & Resources

Virginia Smart Roads

- Opened in 2000; co-sponsored with VDOT and operated by VTTI
- First road built specifically with research in mind
- Nearly 14 miles of closed test track among the combined sections
- DGPS; 8 DSRC and 4 C-V2X / 5G RSUs

Other Test Track Resources

- Virginia International Raceway (Alton, VA)
- Several of our strong partners have world-class test tracks and proving grounds available to support task order research

Surface Street
(urban)
Intersections, merging areas, roundabouts, ADS compatible pavement markings (temporary)

Highway
Weather-making capabilities (rain, snow, and fog), variable lighting, full DGPS

Rural Roadway
Built to older standards with more challenging roadway environments

Smart Roads Capabilities

Rural Roadway




Highway




TUTORIAL AGENDA

REMOTE MEASUREMENT OF VITAL SIGNS

- Scope : 30 min (Abbott)
- Application: 30 min (Sarkar)
- Existing Methods: 30 min (Abbott)
- Break
- Camera based rPPG methods : 1 hr 15 min (Sarkar)
- Resources and discussion: 30 min

(END OF PART 1)

AHFE 2023 International Conference

July 20-24, 2023 - San Francisco, California, USA

VIRGINIA TECH TRANSPORTATION INSTITUTE
VIRGINIA TECH

COLLEGE OF ENGINEERING
BRADLEY DEPARTMENT OF ELECTRICAL AND COMPUTER ENGINEERING
VIRGINIA TECH

End of slide show, click to exit.

COLLEGE OF ENGINEERING
BRADLEY DEPARTMENT OF ELECTRICAL AND COMPUTER ENGINEERING
VIRGINIA TECH

TUTORIAL PRESENTATION (PART 2)

REMOTE MEASUREMENT OF VITAL SIGNS USING AI FOR HEALTH MONITORING AND COGNITION

ABHIJIT SARKAR AND LYNN ABBOTT

AHFE 2023 International Conference
July 20-24, 2023 - San Francisco, California, USA

SCOPE OF THIS TUTORIAL

WHAT VITAL SIGNS WILL BE DISCUSSED?

- Heart rate
- Pulse rate
- Respiration rate
- Blood pressure
- . . .

COMMON CONTACT-BASED SENSING METHODS

- Heart rate
- Pulse rate
- Respiration rate
- Blood pressure

[Source: health.clevelandclinic.org]

[Source: healthline.com]

[Source: biopac.com]

[Source: fitbit.com]

NON-CONTACT SENSING METHODS

- Heart rate
- Pulse rate
- Respiration rate
- Blood pressure

POTENTIAL APPLICATIONS OF NON-CONTACT SENSING

- Continuous health monitoring

POTENTIAL APPLICATIONS OF NON-CONTACT SENSING

- Continuous health monitoring
- Performance monitoring (cognitive load, physical load)
- Automotive safety
- Biometric authentication
- Surveillance and law enforcement

(END OF PART 2)

AHFE 2023 International Conference

July 20-24, 2023 - San Francisco, California, USA

VIRGINIA TECH

VIRGINIA TECH TRANSPORTATION INSTITUTE
VIRGINIA TECH

COLLEGE OF ENGINEERING
BRADLEY DEPARTMENT OF ELECTRICAL AND COMPUTER ENGINEERING
VIRGINIA TECH

APPLICATIONS

SESSION 3

WE ARE INCREASINGLY AWARE OF OUR HEALTH

COGNITIVE AND PHYSICAL LOAD

- Monitor psychophysiology
  - Improve performance
  - Improve safety
  - Improve lifestyle
- How to measure them?
  - Individually
  - Collectively
  - Continuously

Images from: amazon.com, flickr.com

WEARABLES ARE GREAT SOURCE OF INFORMATION ABOUT OUR HEALTH AND LIFESTYLE

WHAT CAN WE MEASURE?

- Heart rate
- Pulse rate
- Breathing rate
- Galvanic skin response
- Electrical activity in brain
- Heart rate variability
- Sleep
- Stress
- Step counts
- SpO2
- Gyroscopic data
- Blood glucose level
- Blood pressure
- …

Non Invasive measurement – greater usability

WHY SHOULD WE MEASURE?
DRIVING EXAMPLE

- Understand psychophysiological condition of a person
  - Cognitive load
  - Drowsiness
  - Effect of Alcohol/ drug / other impairment
  - Customer Satisfaction
  - Effectivity of training
  - Chronic depression

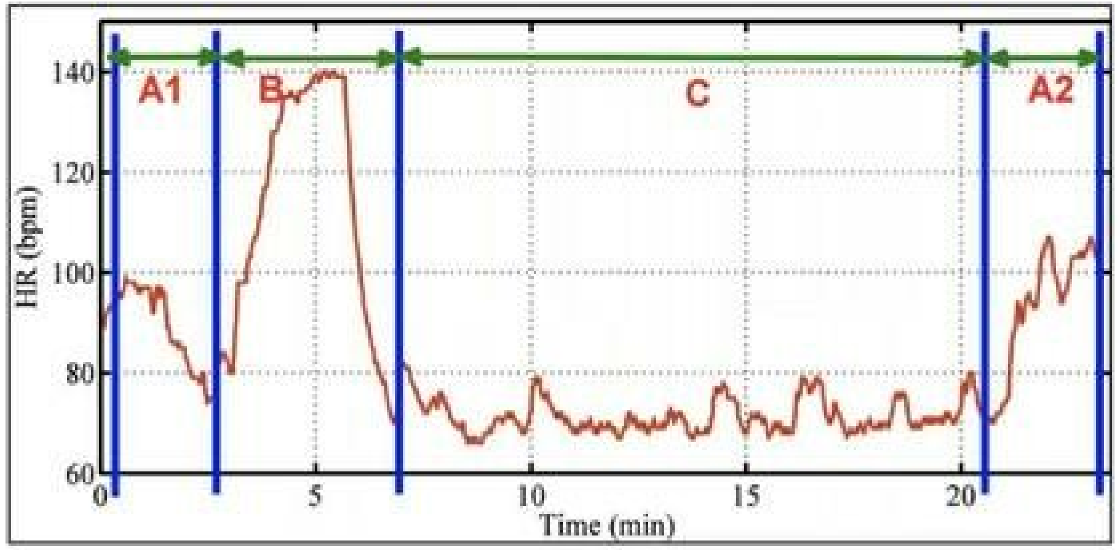

A1 and A2 – City driving – high cognitive load
C – Interstate driving – low cognitive load
B – Panic – High cognitive load

A. Sarkar, A. L. Abbott and Z. Doerzaph, "Assessment of psychophysiological characteristics using heart rate from naturalistic face video data," *IEEE International Joint Conference on Biometrics*, 2014, pp. 1-6, doi: 10.1109/BTAS.2014.6996264.

UBIQUITOUS HEALTH MONITORING

- Connecting multiple technology and service providers
- Use the power of data

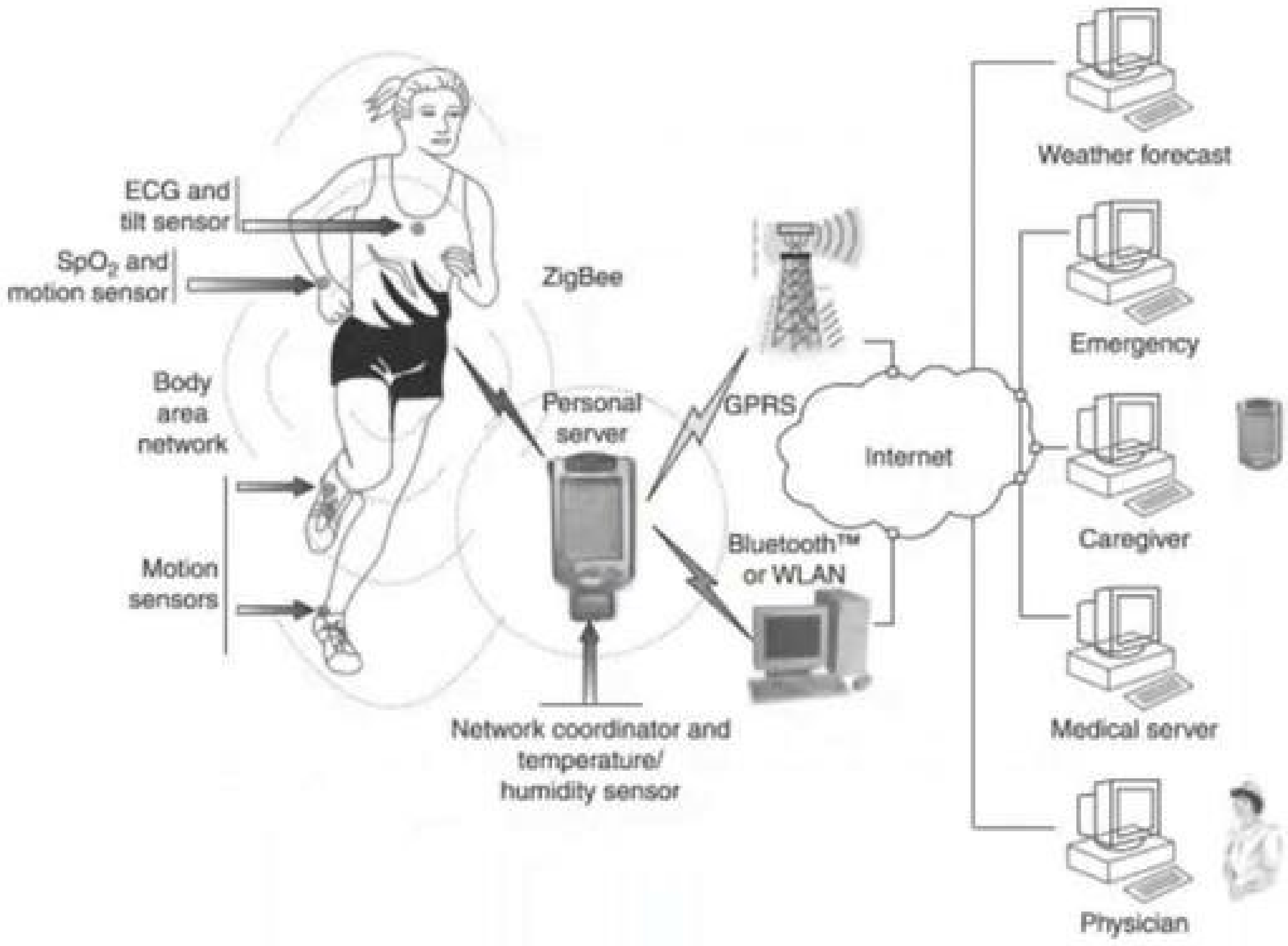

Crean, C., Mcgeouge, C., & O'kennedy, R. (2012). Wearable biosensors for medical applications. In *Biosensors for Medical Applications* (pp. 301-330). Woodhead publishing.

COMMERCIAL DRIVER SAFETY RISK FACTORS STUDY

- Goal: examine driver and situational factors that impact CMV safety
  - Demographic characteristics, work experience, lifestyle and behavioral habits, medical conditions
  - Identify personal, medical, and situational factors that increase crash or violation risk
  - Identify factors associated with presence of obstructive sleep apnea (OSA)
  - Follow CMV drivers' safety records for up to three years
- Demographics
  - 29% overweight; 58% obese
  - 88% not or sometimes on a regular sleep schedule
- Predictive factors for OSA: BMI, hypertension, age, and Berlin Questionnaire
- Drivers being treated for medical conditions were no riskier than drivers without the same medical conditions
  - OSA treatment reduced crash risk ~40%
  - non-treatment increased risk by ~200%

DRIVING HEALTHY WEBSITE AND SOCIAL MEDIA

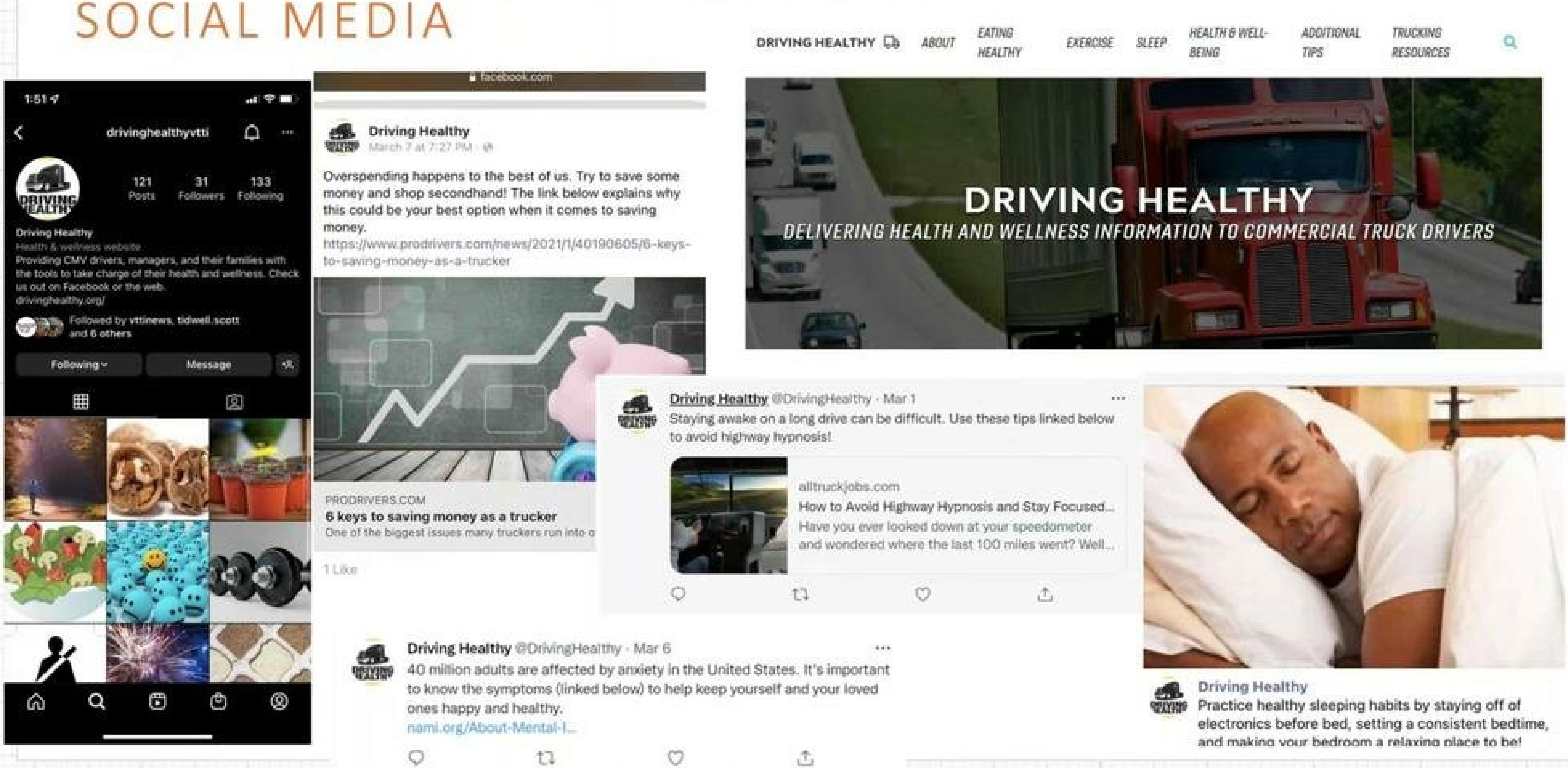

DRIVER APPLICATION IN MODERN VEHICLE

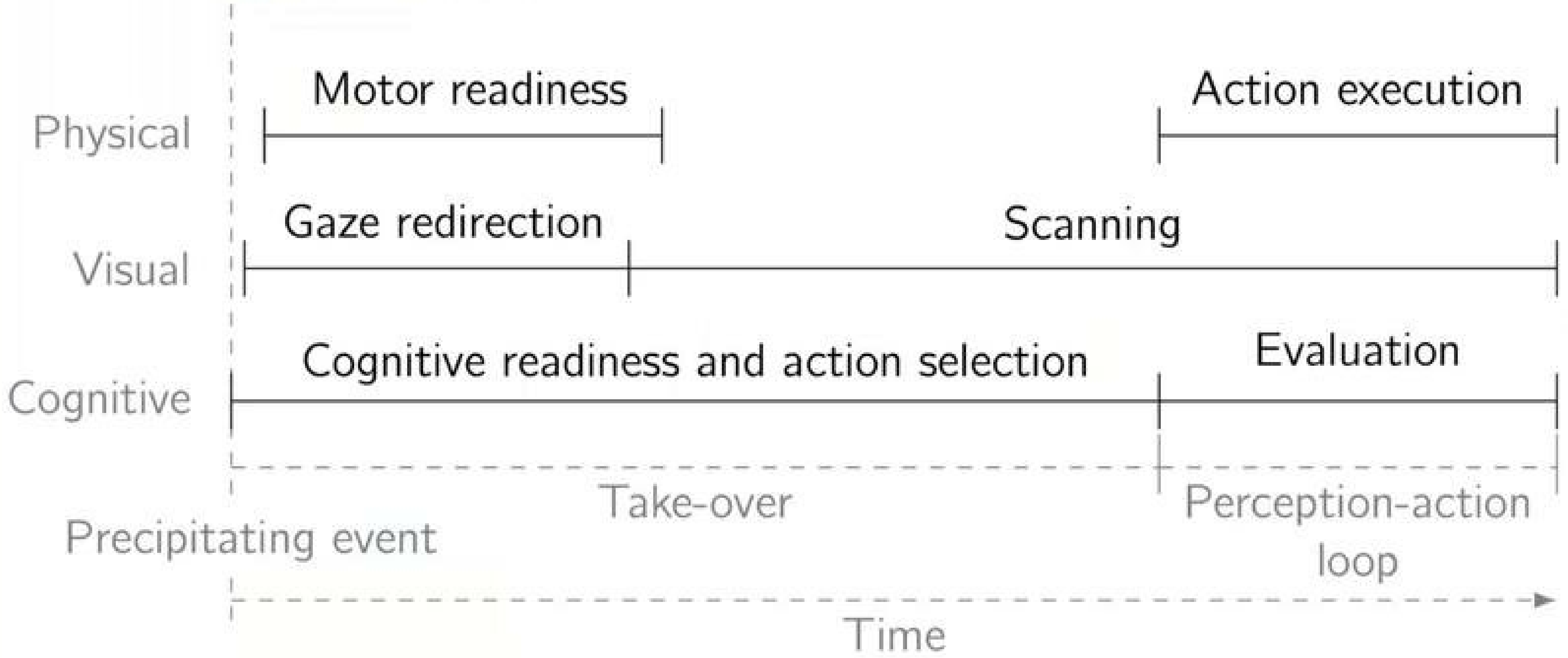

PATIENT MONITORING

- Continuous monitoring of patients
- Sleep monitoring
- Telehealth
- Health screening (airport)
- Biometrics

STRESS MEASUREMENT

- Stress has three major components:
  - Psychological, behavioral, physical
- Biosignal features are involuntary
- Surveys can be biased and manipulated

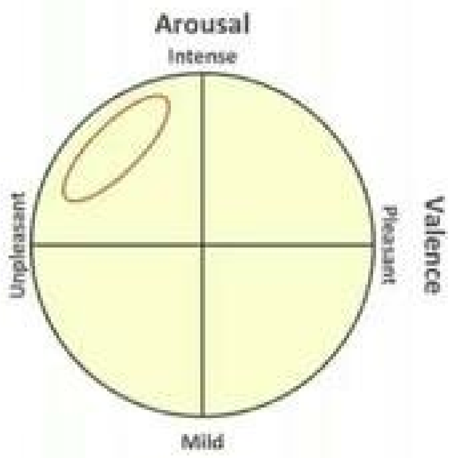

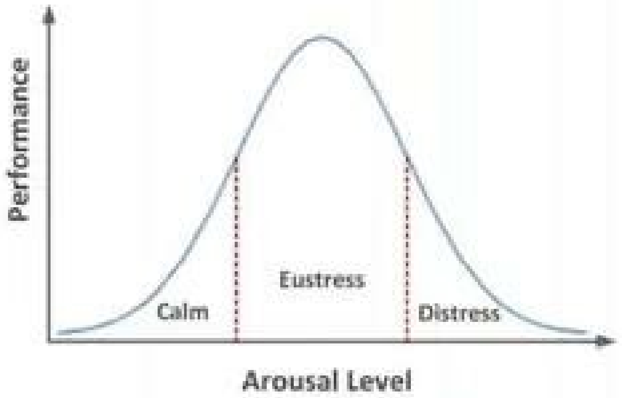

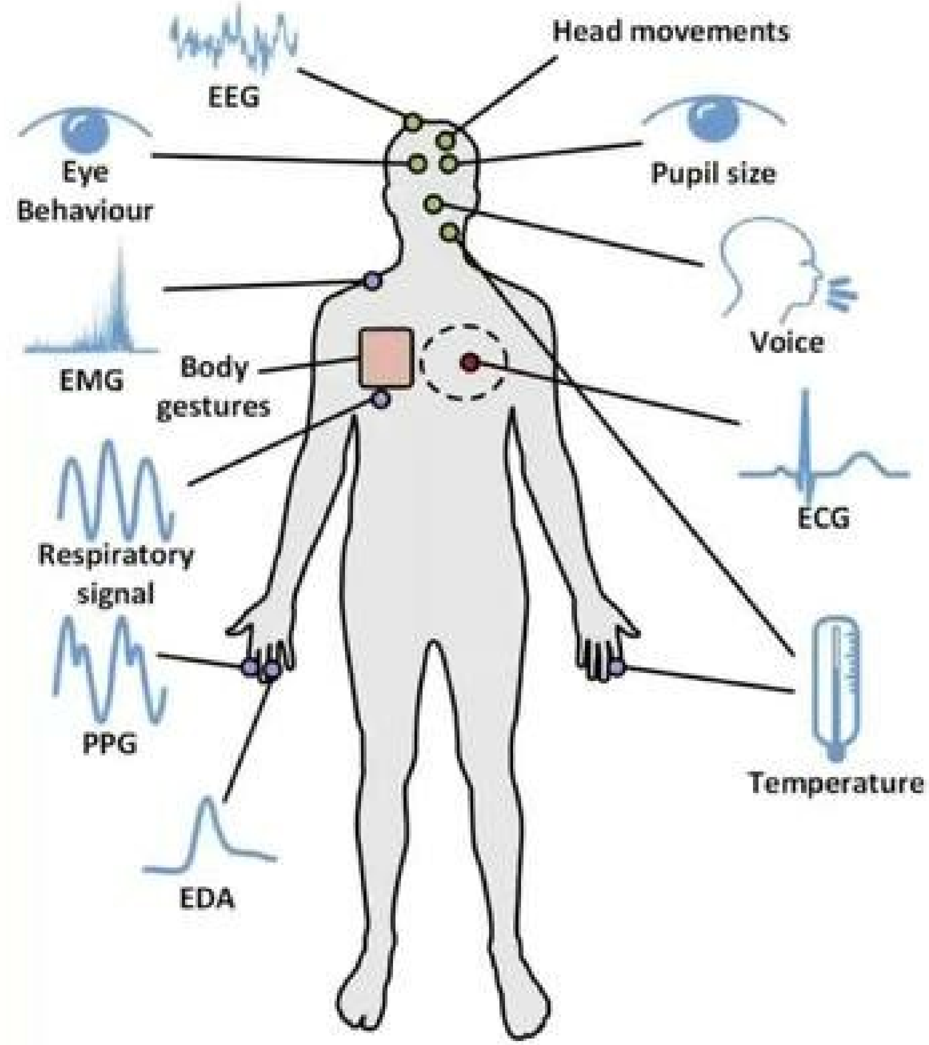

AUTONOMIC NERVOUS SYSTEM

- Parasympathetic and sympathetic balance
- Flight or Fight Vs Relax
- Involuntary response
- Reflects stress level

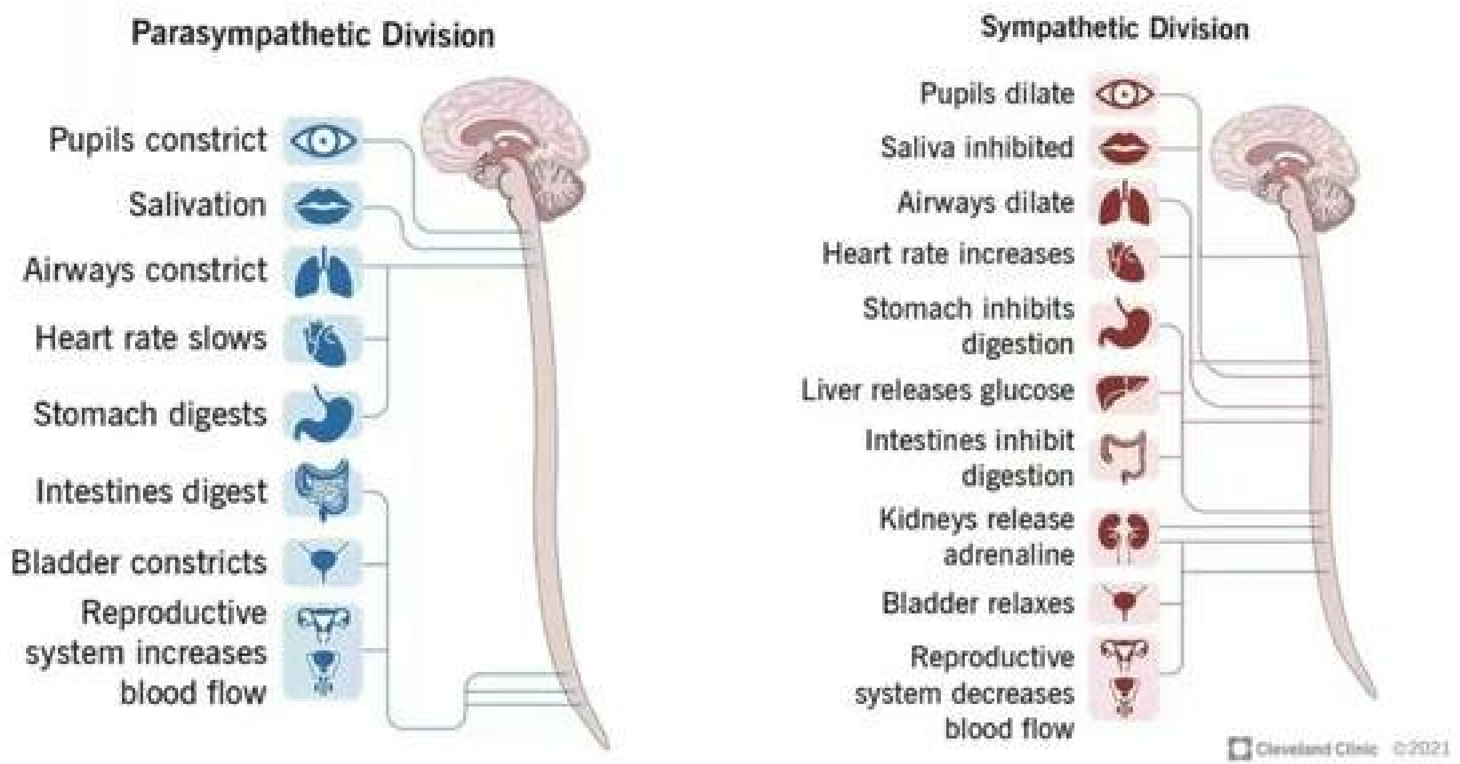

Image: https://my.clevelandclinic.org/health/body/23273-autonomic-nervous-system

THERMAL IMAGING

Temperature Features from Different Body ROI Used in Automatic Stress Detection and Significant Changes During Stress Conditions

Feature	Studies	↑	↓	=
Body	1 [129]	1	0	0
Finger	5 [127], [130], [131], [132], [133]	0	4	1
Whole Facial	5 [130], [131], [134], [135], [136]	4	1	0
Temp variability	1 [133]	0	1	0
Forehead	5 [131], [137], [138], [139]	3	0	2
Periorbital	2 [110], [131]	1	0	1
Nose	3 [131], [132], [140]	0	3	0
Maxillary	2 [135], [139]	0	2	0

↑: significant increase ($p < 0.05$) during stress.
↓: significant decrease ($p < 0.05$) during stress.
=: no difference.

HEART RATE VARIABILITY

- HRV is the measure of the variations of the heart beat
- Our consecutive heart rate varies

HEART RATE VARIABILITY

DIFFERENT MEASUREMENTS OF HRV

	Measure	Units	Description	References
Time-Domain	$\overline{RR}$	[ms]	The mean of RR intervals	
	STD RR (SDNN)	[ms]	Standard deviation of RR intervals [Eq. (3.1)]	
	$\overline{HR}$	[1/min]	The mean heart rate	
	STD HR	[1/min]	Standard deviation of intantaneous heart rate values	
	RMSSD	[ms]	Square root of the mean squared differences between successive RR intervals [Eq. (3.3)]	
	NN50		Number of successive RR interval pairs that differ more than 50 ms	
	pNN50	[%]	NN50 divided by the total number of RR intervals [Eq. (3.4)]	
	HRV triangular index		The integral of the RR interval histogram divided by the height of the histogram [44]	
	TINN	[ms]	Baseline width of the RR interval histogram	[44]

Tarvainen, M. P., & Niskanen, J. P. (2012). Kubios HRV. *Finland: Biosignal Analysis and Medical Imaging Group (BSAMIG), Department of Applied Physics, University of Eastern Finland, 39.*

HEART RATE VARIABILITY
DIFFERENT MEASUREMENTS OF HRV

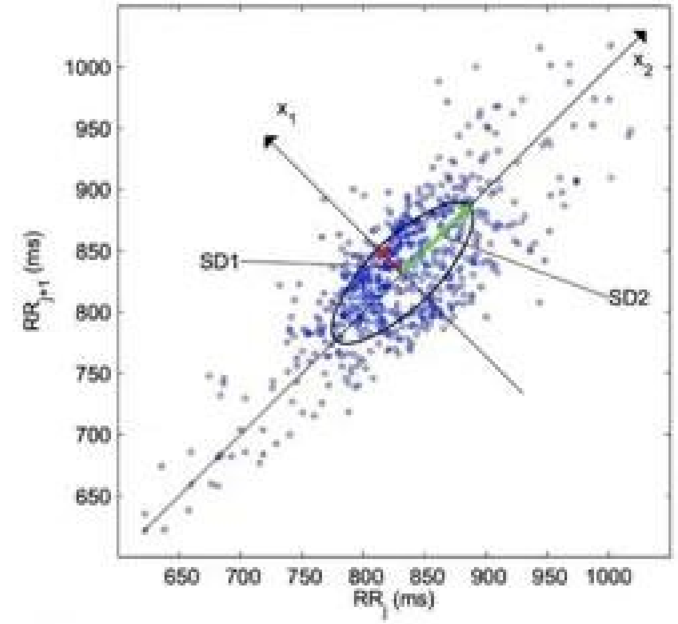

Nonlinear	SD1, SD2	[ms]	The standard deviation of the Poincaré plot perpendicular to (SD1) and along (SD2) the line-of-identity	[6, 7]
	ApEn		Approximate entropy [Eq. (3.11)]	[41, 14]
	SampEn		Sample entropy [Eq. (3.14)]	[41]
	D_2		Correlation dimension [Eq. (3.21)]	[17, 19]
	DFA		Detrended fluctuation analysis:	[37, 38]
	α_1		Short term fluctuation slope	
	α_2		Long term fluctuation slope	
	RPA		Recurrence plot analysis:	[47, 9, 49]
	Lmean	[beats]	Mean line length [Eq. (3.26)]	
	Lmax	[beats]	Maximum line length	
	REC	[%]	Recurrence rate [Eq. (3.24)]	
	DET	[%]	Determinism [Eq. (3.27)]	
	ShanEn		Shannon entropy [Eq. (3.28)]	

Tarvainen, M. P., & Niskanen, J. P. (2012). Kubios HRV. *Finland: Biosignal Analysis and Medical Imaging Group (BSAMIG), Department of Applied Physics, University of Eastern Finland, 39.*

HEART RATE VARIABILITY

DIFFERENT MEASUREMENTS OF HRV

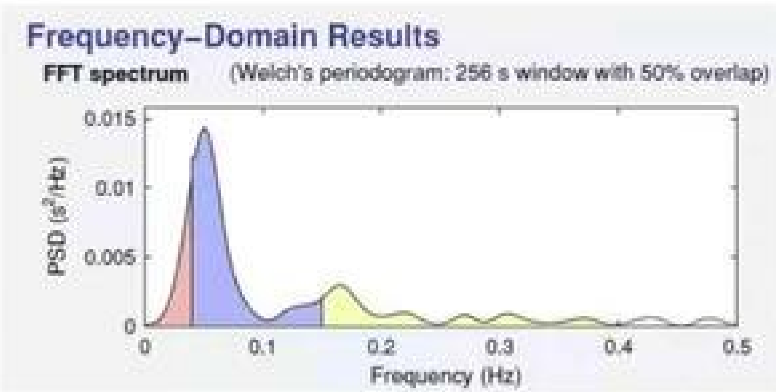

VLF → < 0.04 Hz
LF → > 0.04 Hz and <0.15 Hz
HF → > 0.15 Hz and <0.4 Hz

Frequency-Domain		
Peak frequency	[Hz]	VLF, LF, and HF band peak frequencies
Absolute power	[ms^2]	Absolute powers of VLF, LF, and HF bands
Relative power	[%]	Relative powers of VLF, LF, and HF bands $\text{VLF}\,[\%] = \text{VLF}\,[\text{ms}^2]/\text{total power}\,[\text{ms}^2] \times 100\%$ $\text{LF}\,[\%] = \text{LF}\,[\text{ms}^2]/\text{total power}\,[\text{ms}^2] \times 100\%$ $\text{HF}\,[\%] = \text{HF}\,[\text{ms}^2]/\text{total power}\,[\text{ms}^2] \times 100\%$
Normalized power	[n.u.]	Powers of LF and HF bands in normalized units $\text{LF}\,[\text{n.u.}] = \text{LF}\,[\text{ms}^2]/(\text{total power}\,[\text{ms}^2] - \text{VLF}\,[\text{ms}^2])$ $\text{HF}\,[\text{n.u.}] = \text{HF}\,[\text{ms}^2]/(\text{total power}\,[\text{ms}^2] - \text{VLF}\,[\text{ms}^2])$
LF/HF		Ratio between LF and HF band powers

Tarvainen, M. P., & Niskanen, J. P. (2012). Kubios HRV. *Finland: Biosignal Analysis and Medical Imaging Group (BSAMIG), Department of Applied Physics, University of Eastern Finland, 39*.

Feature	Studies	↑	↓	=
HR	23 [109], [131], [132], [151], [154], [160], [165], [180], [182], [187], [188], [189], [190], [191], [192], [193], [194], [195], [196], [197], [198], [199], [200]	18	0	5
STD HR	1 [198]	0	0	1
RR	8 [180], [198], [200], [201], [202], [203], [204], [205]	0	6	2
SDNN	12 [180], [187], [193], [194], [197], [198], [200], [201], [203], [204], [205], [206]	1	7	4
RMSSD	6 [187], [190], [197], [198], [203], [204]	0	5	1
NN50	2 [187], [200]	0	2	0
pNN50	6 [116], [194], [198], [200], [203], [207]	0	6	0
HRV triangular	2 [198], [200]	0	1	1
Total power	4 [133], [197], [204], [206]	0	4	0
VLF	3 [187], [204]	0	0	3
LF	12 [180], [187], [192], [193], [194], [195], [197], [199], [203], [204], [205], [208]	5	3	4
HF	14 [180], [187], [192], [193], [194], [197], [199], [201], [203], [204], [205], [208], [209], [210]	1	6	7
LF/HF	17 [165], [180], [187], [188], [192], [193], [194], [198], [199], [200], [202], [203], [204], [207], [208], [209], [210]	10	0	7

Feature	Studies	↑	↓	=
VLF relative	2 [187], [188]	2	0	0
LF relative	8 [187], [188], [200], [201], [202], [204], [208]	4	1	3
HF relative	7 [187], [200], [201], [202], [204], [208]	0	4	3
SD1	1 [211]	0	0	1
SD2	1 [211]	0	1	0
D2	2 [211]	0	2	0
BR	5 [165], [180], [193], [199], [204]	2	0	3
SBP	15 [129], [132], [151], [154], [160], [188], [189], [190], [191], [195], [201], [206], [212], [213], [214]	15	0	0
DBP	15 [129], [132], [151], [154], [160], [188], [189], [190], [191], [195], [201], [209], [212], [213], [214]	15	0	0
BP HF	1 [206]	1	0	0
ApEn	1 [211]	0	1	0
SampEn	1 [192]	0	0	1

↑: significant increase ($p < 0.05$) during stress.
↓: significant decrease ($p < 0.05$) during stress.
=: no significant difference.

HEART RATE VARIABILITY, BLOOD PRESSURE

DILATION, BLINKING

CHALLENGES AND CONSIDERATION

- Accessibility
- Privacy and data security
- Subjective biases
- Absolute vs relative measurements
- Complex environment and external stimuli

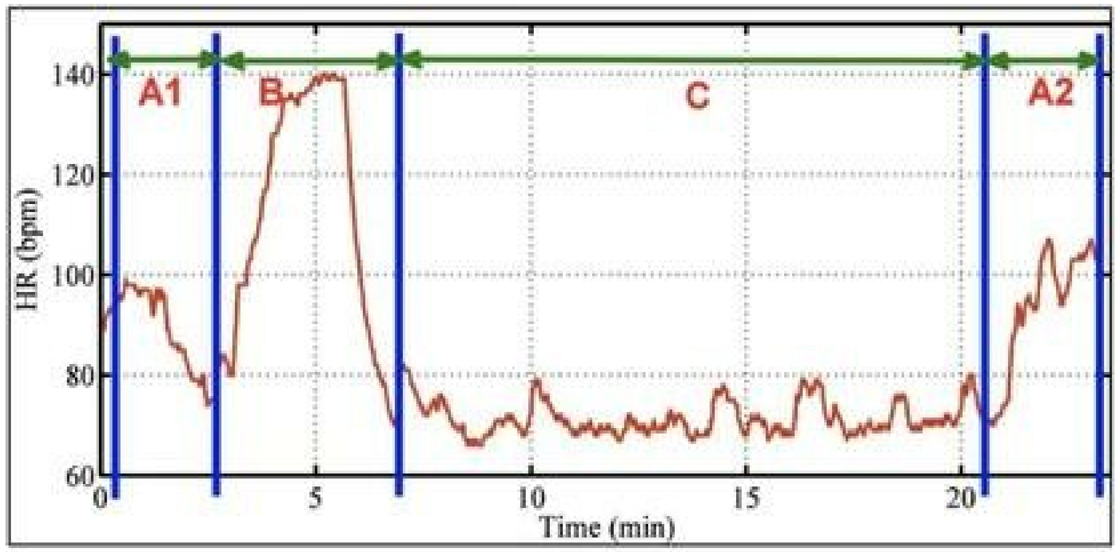

HRV AND RPPG

POSSIBILITIES

- What if we can use rPPG to measure HRV?
  - We need accurate instantaneous HR information

Asarcikli, L. D., Hayiroglu, M. İ., Osken, A., Keskin, K., Kolak, Z., & Aksu, T. (2022). Heart rate variability and cardiac autonomic functions in post-COVID period. *Journal of Interventional Cardiac Electrophysiology*, *63*(3), 715-721.

BREATHING PATTERNS

PULSE SIGNAL

COLLEGE OF ENGINEERING
BRADLEY DEPARTMENT OF ELECTRICAL AND COMPUTER ENGINEERING
VIRGINIA TECH

TUTORIAL PRESENTATION (PART 4)

REMOTE MEASUREMENT OF VITAL SIGNS USING AI FOR HEALTH MONITORING AND COGNITION

ABHIJIT SARKAR AND LYNN ABBOTT

AHFE 2023 International Conference
July 20-24, 2023 - San Francisco, California, USA

ELECTROMAGNETIC SPECTRUM

Video cameras

Radar

Wi-fi and ultra-wideband

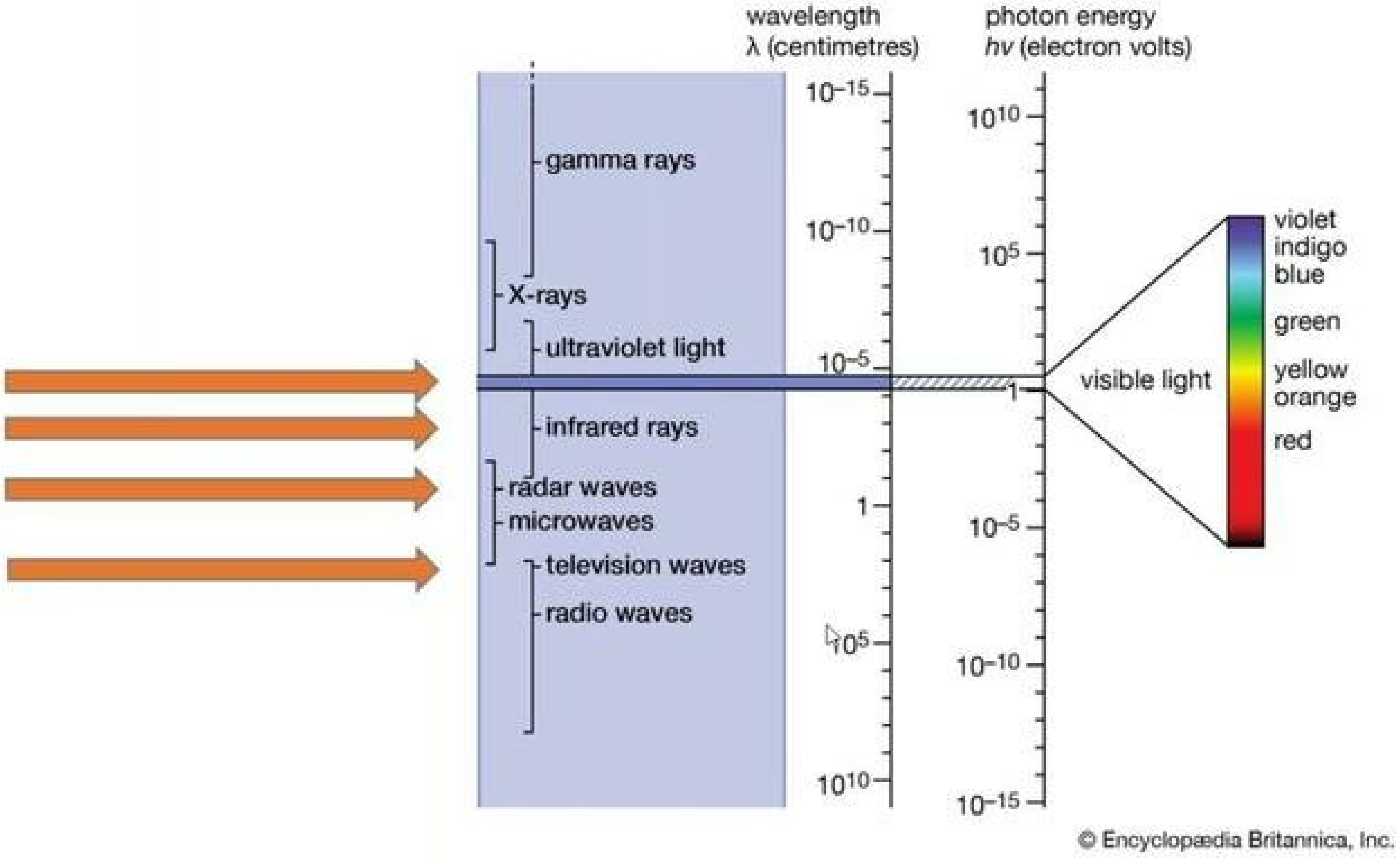

NON-CONTACT SENSING METHODS

- Video camera (visible-light)
- Video camera (infrared)
- Laser Doppler vibrometry (LDV)
- Radar
- Ultra-wideband impulse radio (UWB-IR)
- Wi-Fi

Sense changes in reflectance

Sense motion

PHOTOPLETHYSMOGRAPHY (PPG)

USE LIGHT TO DETECT
VOLUMETRIC CHANGES IN BLOOD IN PERIPHERAL CIRCULATION

- Contact-based PPG

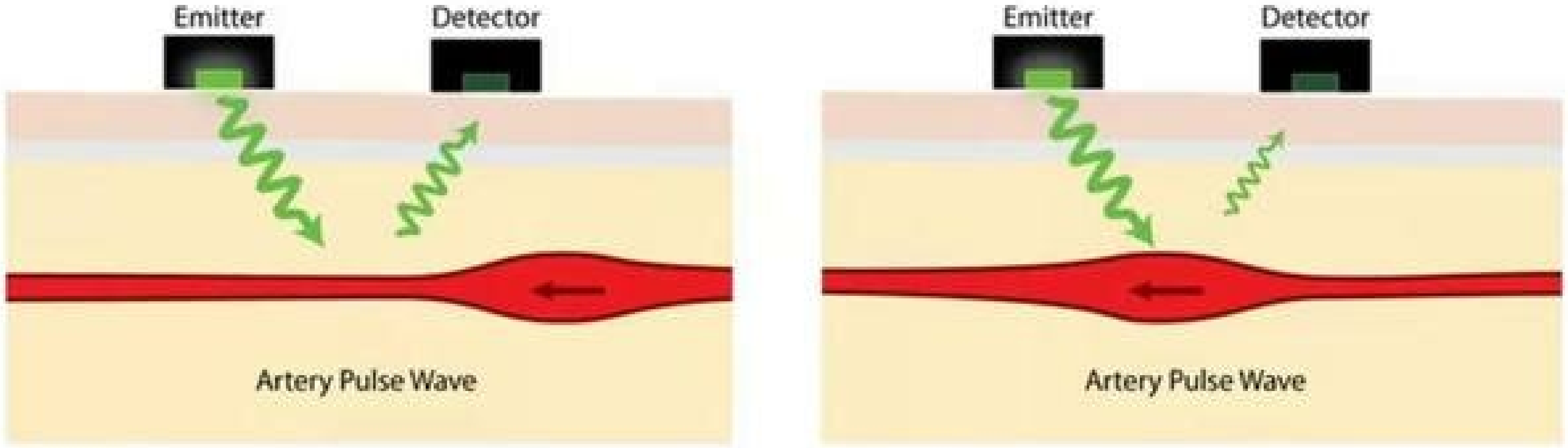

BVP: Blood Volume Pulse

[Source: Collins, TheConversation.com]

[Source: biopac.com]

NON-CONTACT SENSING METHODS

- Video camera (visible-light)
- Video camera (infrared)
- Laser Doppler vibrometry (LDV)
- Radar
- Ultra-wideband impulse radio (UWB-IR)
- Wi-Fi

Sense changes in reflectance

Sense motion

LASER DOPPLER VIBROMETRY (LDV)

Method:

- Aim a safe, low-power laser at skin overlying a carotid artery
- Blood volume pulses (BVP) cause movement of tissue and skin near these arteries
- Skin movements cause Doppler shifts in reflected laser light, and these shifts can be sensed

[Source: Miami Vascular Specialists]

Reference: A. D. Kaplan, J. A. O'Sullivan, E. J. Sirevaag, P.-H. Lai, and J. W. Rohrbaugh. Hidden state models for noncontact measurements of the carotid pulse using a laser Doppler vibrometer. IEEE Trans. On Biomedical Engineering, 59(3):744–753, 2011.

LASER DOPPLER VIBROMETRY (LDV)

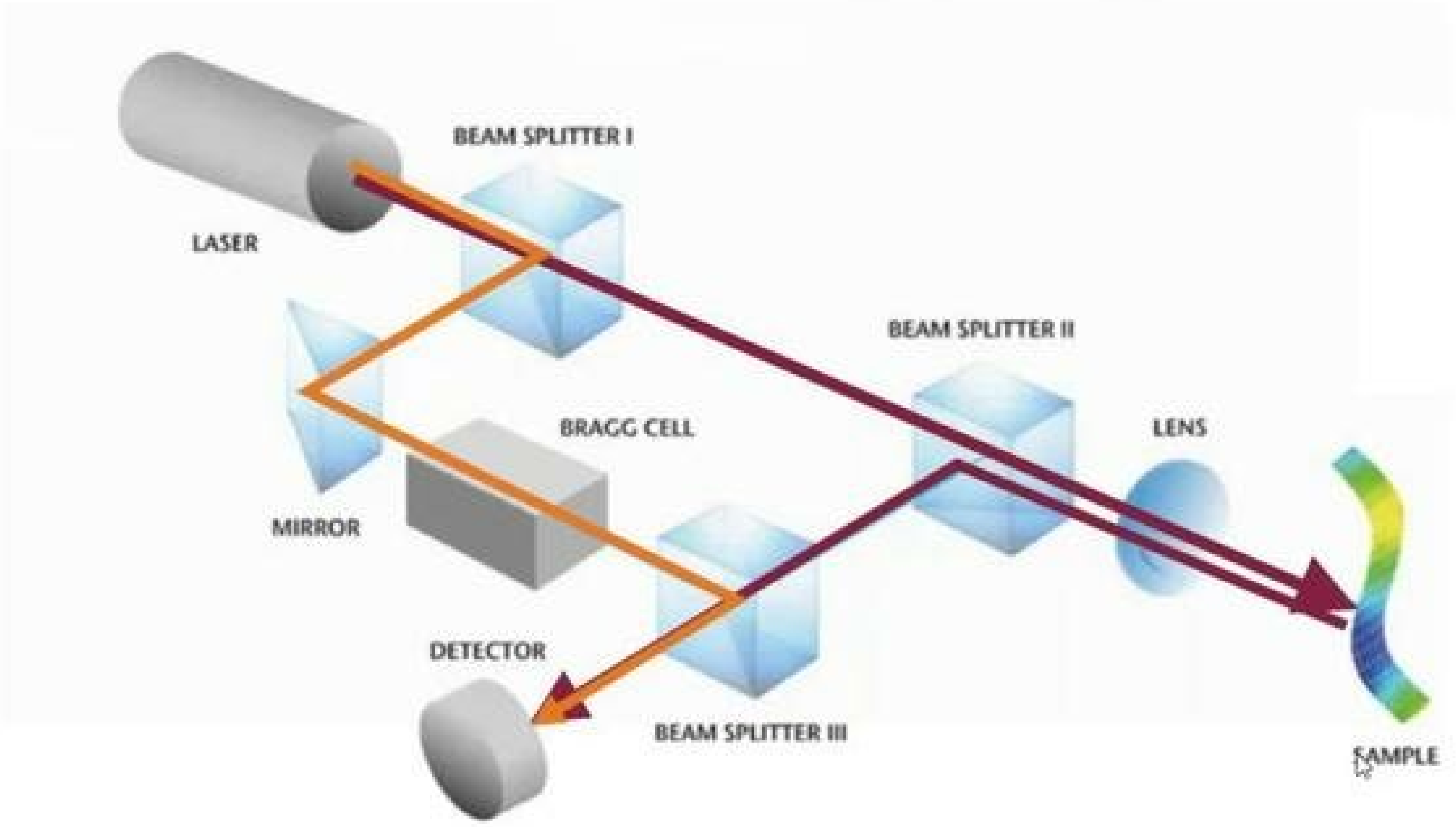

Basic measurement principle of vibrometry and setup of a laser Doppler vibrometer

[Source: polytec.com]

LASER DOPPLER VIBROMETRY (LDV)

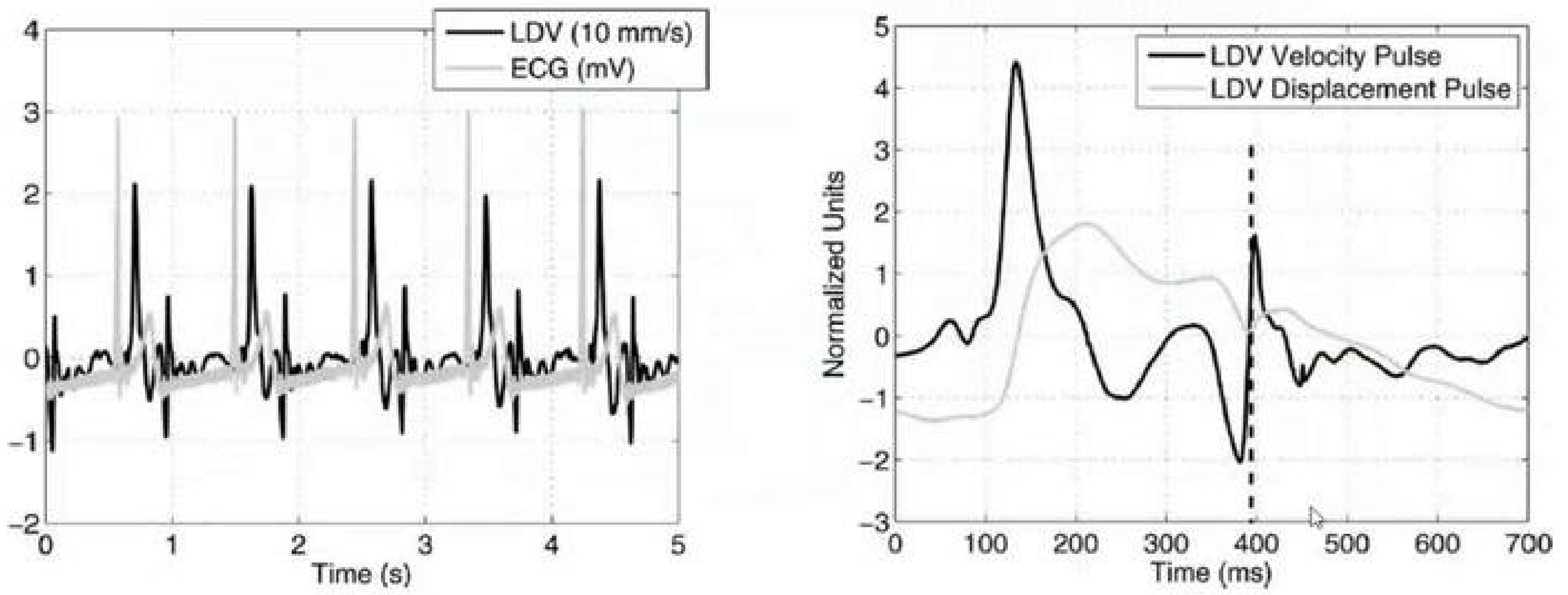

Reference: A. D. Kaplan, J. A. O'Sullivan, E. J. Sirevaag, P.-H. Lai, and J. W. Rohrbaugh. Hidden state models for noncontact measurements of the carotid pulse using a laser Doppler vibrometer. IEEE Trans. On Biomedical Engineering, 59(3):744–753, 2011.

LDV: PROS AND CONS

PRO

- Noncontact
- Relatively noninvasive
- LDV has also been used to infer arterial stiffness and respiration

CON

- Has only been tested with very large arteries (carotid)
- Need careful aim; primarily limited to subjects who are still
- Sensor may be relatively expensive

NON-CONTACT SENSING METHODS

- Video camera (visible-light)
- Video camera (infrared)
- Laser Doppler vibrometry (LDV)
- Radar
- Ultra-wideband impulse radio (UWB-IR)
- Wi-Fi

Sense changes in reflectance

Sense motion

RADAR-BASED SENSING OF THE HEART

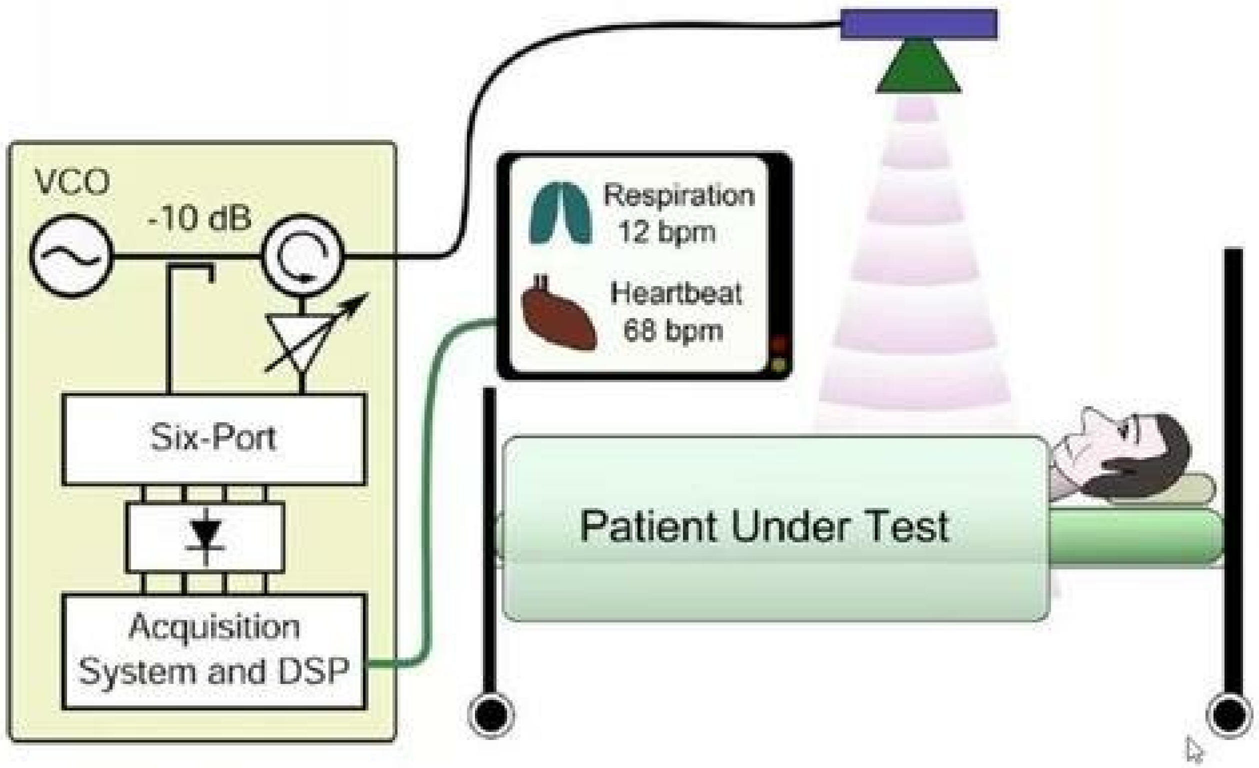

Fig. 1. System concept of the proposed sensor device.

Reference: G. Vinci, S. Lindner, F. Barbon, S. Mann, M. Hofmann, A. Duda, R. Weigel, and A. Koelpin. "Six-port radar sensor for remote respiration rate and heartbeat vital-sign monitoring." *IEEE Transactions on Microwave Theory and Techniques* 61, no. 5 (2013): 2093-2100.

RADAR-BASED SENSING OF THE HEART

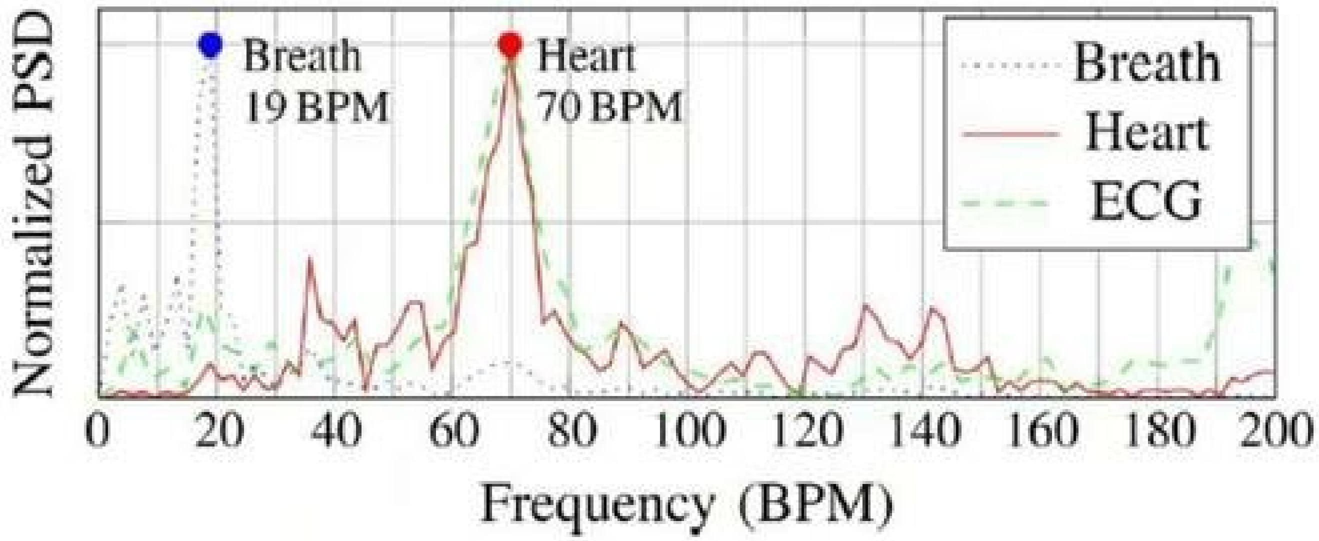

Fig. 11. Normalized PSD of the measured breath and heart-rate signals compared with the PSD of a reference ECG.

Reference: G. Vinci, S. Lindner, F. Barbon, S. Mann, M. Hofmann, A. Duda, R. Weigel, and A. Koelpin. "Six-port radar sensor for remote respiration rate and heartbeat vital-sign monitoring." *IEEE Transactions on Microwave Theory and Techniques* 61, no. 5 (2013): 2093-2100.

RADAR-BASED SENSING OF THE HEART

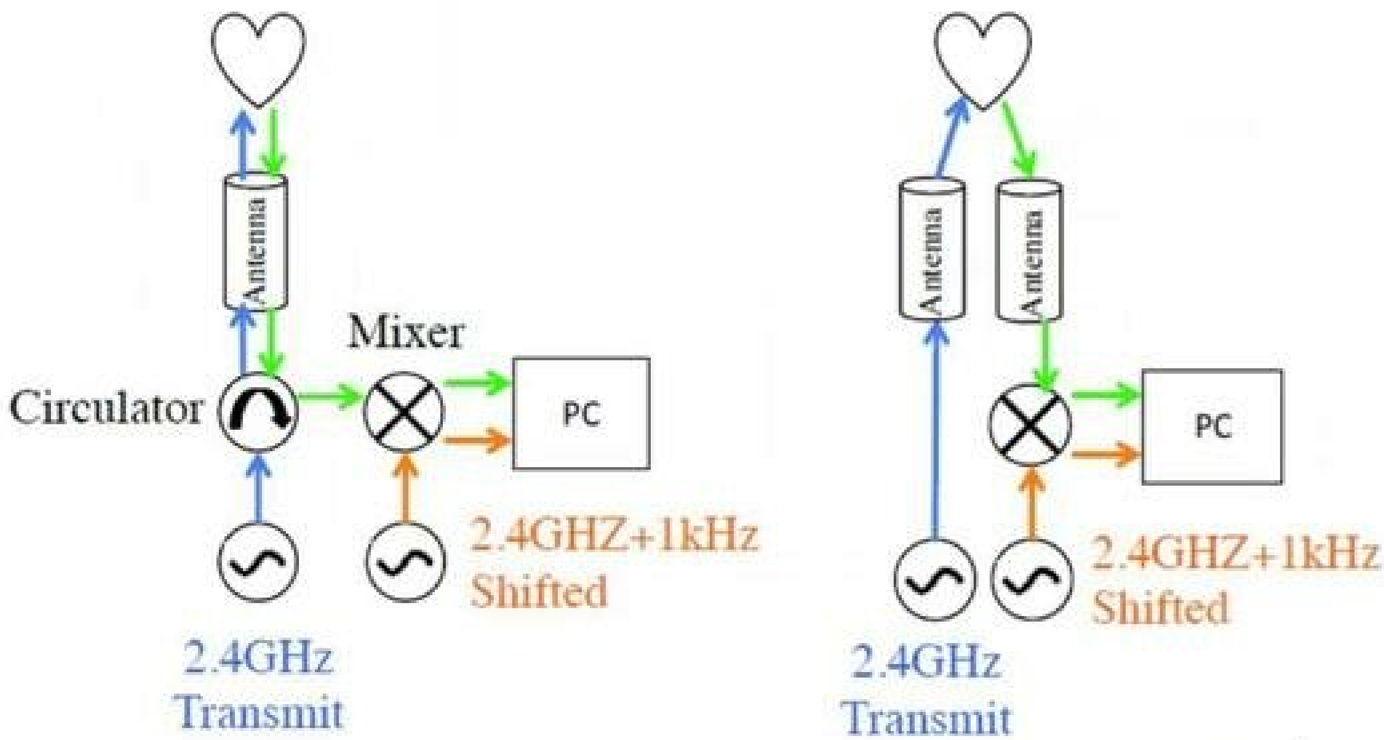

Figure 1: Cardiac Radar Setup: Monostatic Configuration (Left) and Bistatic Configuration (Right)

Reference: D. Rissacher, D. Galy, S. Schuckers, W. Zhang, M. Southcott, L. Rumbaugh, and W. Jemison. Cardiac radar for biometric identification using nearest neighbour of continuous wavelet transform peaks. In Proc. IEEE Intl. Conf. on Identity, Security and Behavior Analysis (ISBA), 2015.

RADAR-BASED SENSING OF THE HEART

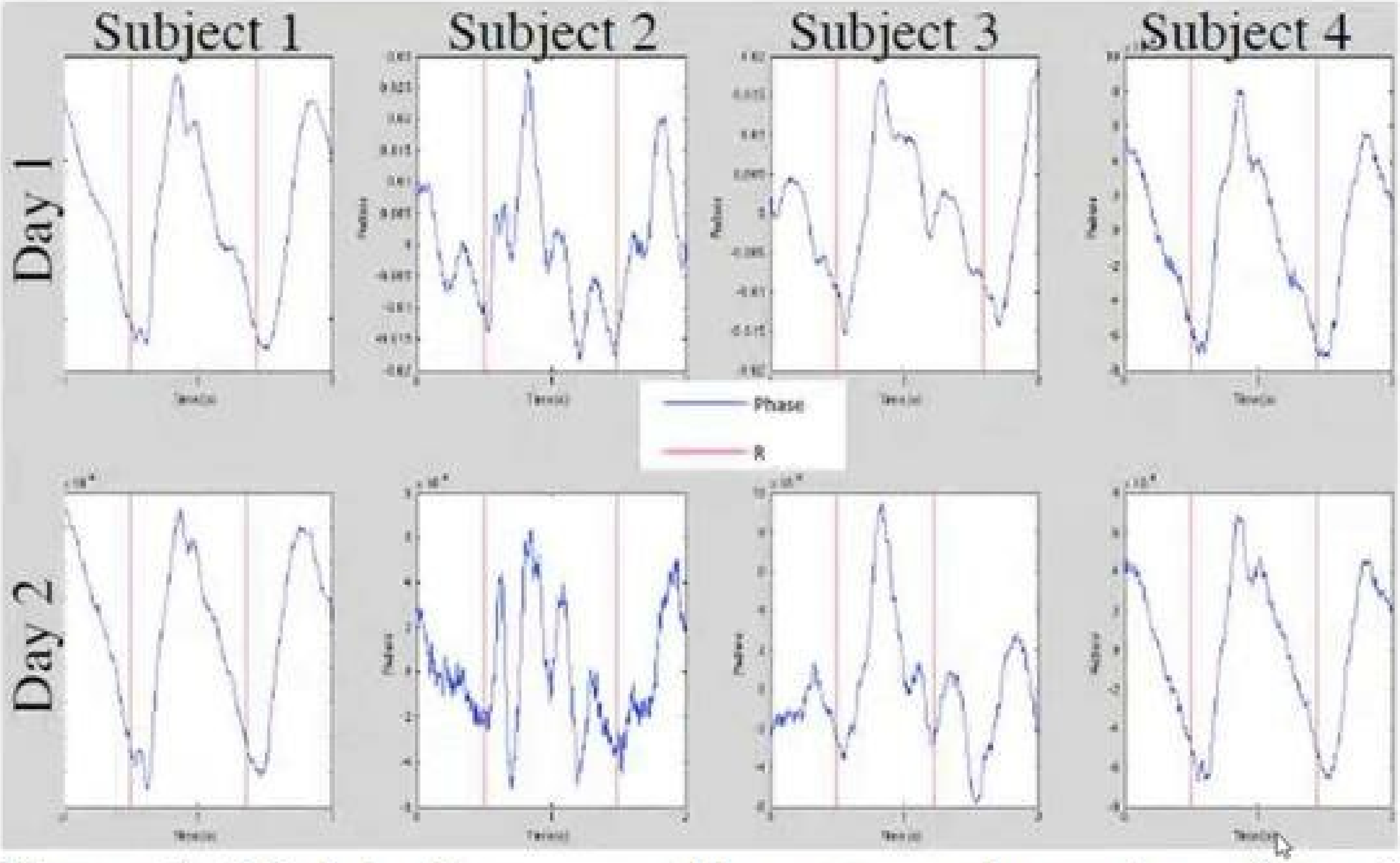

Figure 7: Trial 1 phase ensemble average shown here for a 2 second window to visualize approximately 2 cardiac cycles.

Reference: D. Rissacher, D. Galy, S. Schuckers, W. Zhang, M. Southcott, L. Rumbaugh, and W. Jemison. Cardiac radar for biometric identification using nearest neighbour of continuous wavelet transform peaks. In Proc. IEEE Intl. Conf. on Identity, Security and Behavior Analysis (ISBA), 2015.

RADAR: PROS AND CONS

PRO

- Noncontact
- Relatively noninvasive
- Requires no subject cooperation or knowledge
- Can be used through clothes and potentially through walls
- Long-range use may be feasible
- Feasibility for biometric identification has been demonstrated

CON

- Sensor may be relatively expensive
- Current sensors are not portable
- Safety: need to consider FCC Maximum Permissible Exposure (MPE)

NON-CONTACT SENSING METHODS

- Video camera (visible-light)
- Video camera (infrared)
- Laser Doppler vibrometry (LDV)
- Radar
- Ultra-wideband impulse radio (UWB-IR)
- Wi-Fi

Sense changes in reflectance

Sense motion

WI-FI & ULTRA-WIDEBAND IMPULSE RADIO (UWB-IR)

RESPIRATION MONITORING

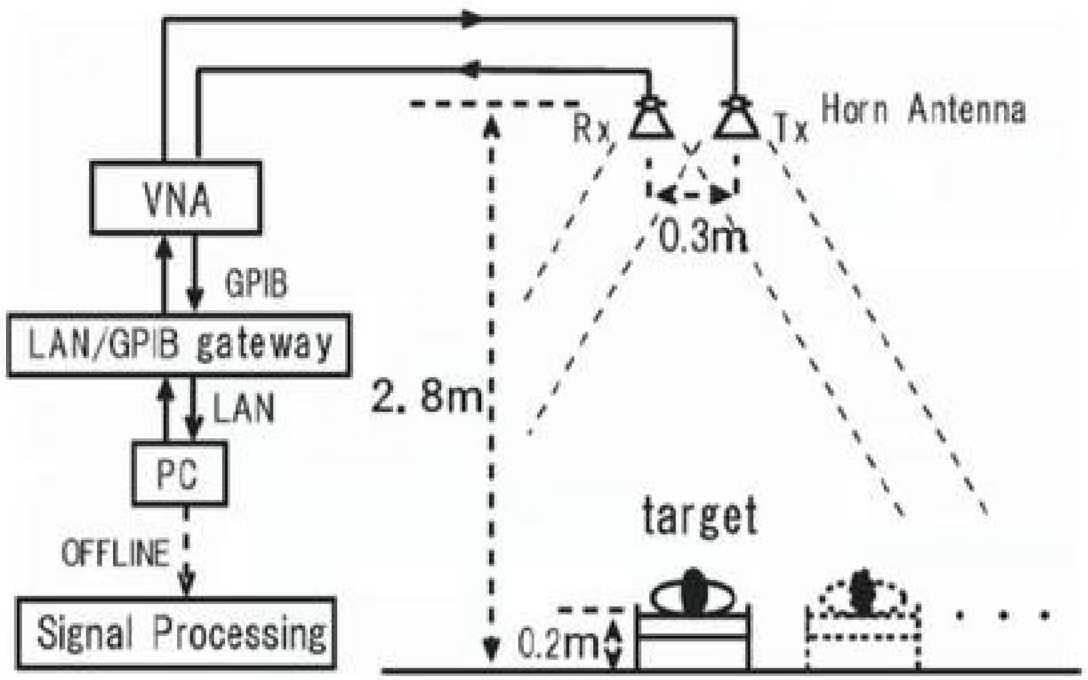

Fig. 2. Measurement environment.

Reference: K. Higashikaturagi, Y. Nakahata, I. Matsunami, and A. Kajiwara. Non-invasive respiration monitoring sensor using UWB-IR. In IEEE Intl. Conf. on Ultra-Wideband, volume 1, pages 101–104, 2008.

WI-FI & ULTRA-WIDEBAND IMPULSE RADIO (UWB-IR)

RESPIRATION MONITORING

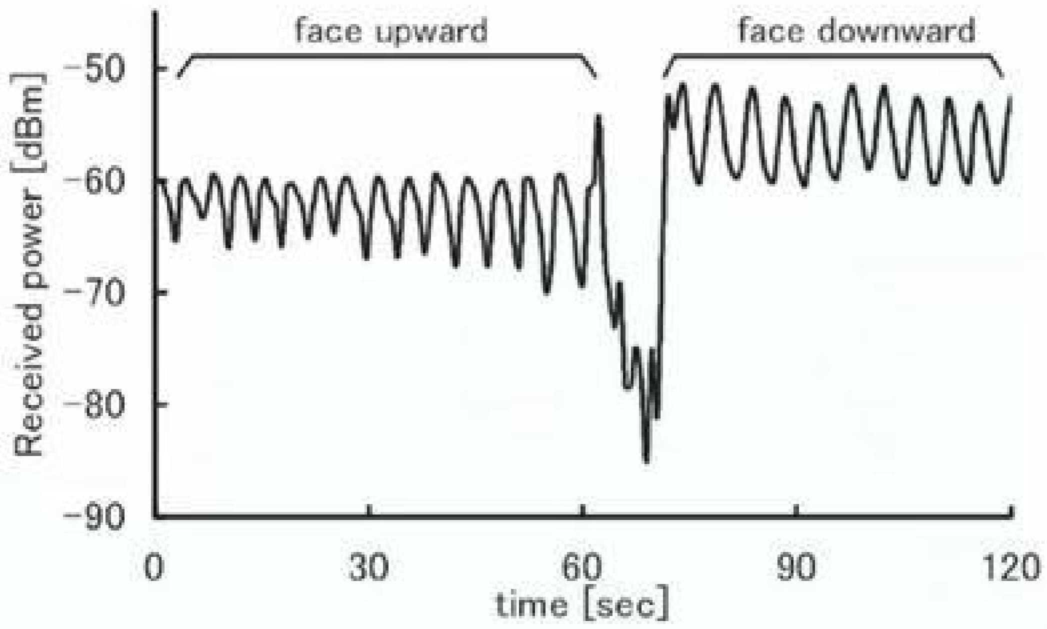

Fig. 6. Respiratory waveforms from face upward to downward.

Reference: K. Higashikaturagi, Y. Nakahata, I. Matsunami, and A. Kajiwara. Non-invasive respiration monitoring sensor using UWB-IR. In IEEE Intl. Conf. on Ultra-Wideband, volume 1, pages 101–104, 2008.

UWB-IR: PROS AND CONS

PRO

- Noncontact
- Relatively noninvasive
- Requires no subject cooperation or knowledge
- Can be used through clothes and blankets

CON

- Current sensors are not portable
- Safety: need to consider FCC Maximum Permissible Exposure (MPE)

SUMMARY

- Contact sensing vs. noncontact (remote) sensing
- Several noncontact methods have been developed for measuring vital signs (heart rate, pulse rate, respiration rate, blood pressure,)
- Most are still in the exploratory stage
- Several applications can benefit from these new techniques

- Invasive sensing vs. noninvasive sensing
  - Some contact-based methods are considered to be noninvasive
  - Some noncontact-based methods might be considered to be invasive (e.g., unwanted video recording of a person's face)

SELECTED REFERENCES

- D. Castaneda, A. Esparza, M. Ghamari, C. Soltanpur, and H. Nazeran. A review on wearable photoplethysmography sensors and their potential future applications in health care. *Int J. Biosens. Bioelectronics*. 4(4):195-202, 2019.
- M. Elgendi, R. Fletcher, Y. Liang, *et al.* The use of photoplethysmography for assessing hypertension. *NPJ Digit. Med.* 2, 60 (2019).
- W. Wang, A. C. den Brinker, S. Stuijk, and G. de Haan. Algorithmic principles of remote PPG. *IEEE Transactions on Biomedical Engineering*, *64*(7), pp.1479-1491, 2006.
- H.-Y. Wu, M. Rubinstein, E. Shih, J. Guttag, F. Durand, and W. Freeman. Eulerian video magnification for revealing subtle changes in the world. *ACM Trans. on Graphics,* 31, no. 4, pp. 1-8, 2012.
- A. D. Kaplan, J. A. O'Sullivan, E. J. Sirevaag, P.-H. Lai, and J. W. Rohrbaugh. Hidden state models for noncontact measurements of the carotid pulse using a laser Doppler vibrometer. *IEEE Trans. on Biomedical Engineering*, 59(3):744–753, 2011.
- G. Vinci, S. Lindner, F. Barbon, S. Mann, M. Hofmann, A. Duda, R. Weigel, and A. Koelpin. "Six-port radar sensor for remote respiration rate and heartbeat vital-sign monitoring." *IEEE Transactions on Microwave Theory and Techniques* 61, no. 5 (2013): 2093-2100.
- D. Rissacher, D. Galy, S. Schuckers, W. Zhang, M. Southcott, L. Rumbaugh, and W. Jemison. Cardiac radar for biometric identification using nearest neighbour of continuous wavelet transform peaks. In *Proc. IEEE Intl. Conf. on Identity, Security and Behavior Analysis*, 2015.
- K. Higashikaturagi, Y. Nakahata, I. Matsunami, and A. Kajiwara. Non-invasive respiration monitoring sensor using UWB-IR. In *Proc. IEEE Intl. Conf. on Ultra-Wideband*, vol. 1, pp. 101–104, 2008.

CAMERA BASED METHODS (FOCUS HEART RATE)

CAMERA BASED METHODS (FOCUS HEART RATE)

SESSION OVERVIEW

- Current state of research
- First we'll discuss how data from RGB and NIR cameras contains blood volume pulse information from human face.
- Next we'll discuss challenges from motion and ambient illumination and methods to address those challenges.
- Next, we'll show how advance computer vision, signal processing and machine learning methods including deep learning are used to extract blood volume pulse, and respiration rate.
- Retrieve different vital signs
- Finally, we'll discuss the open questions

RESEARCH TREND

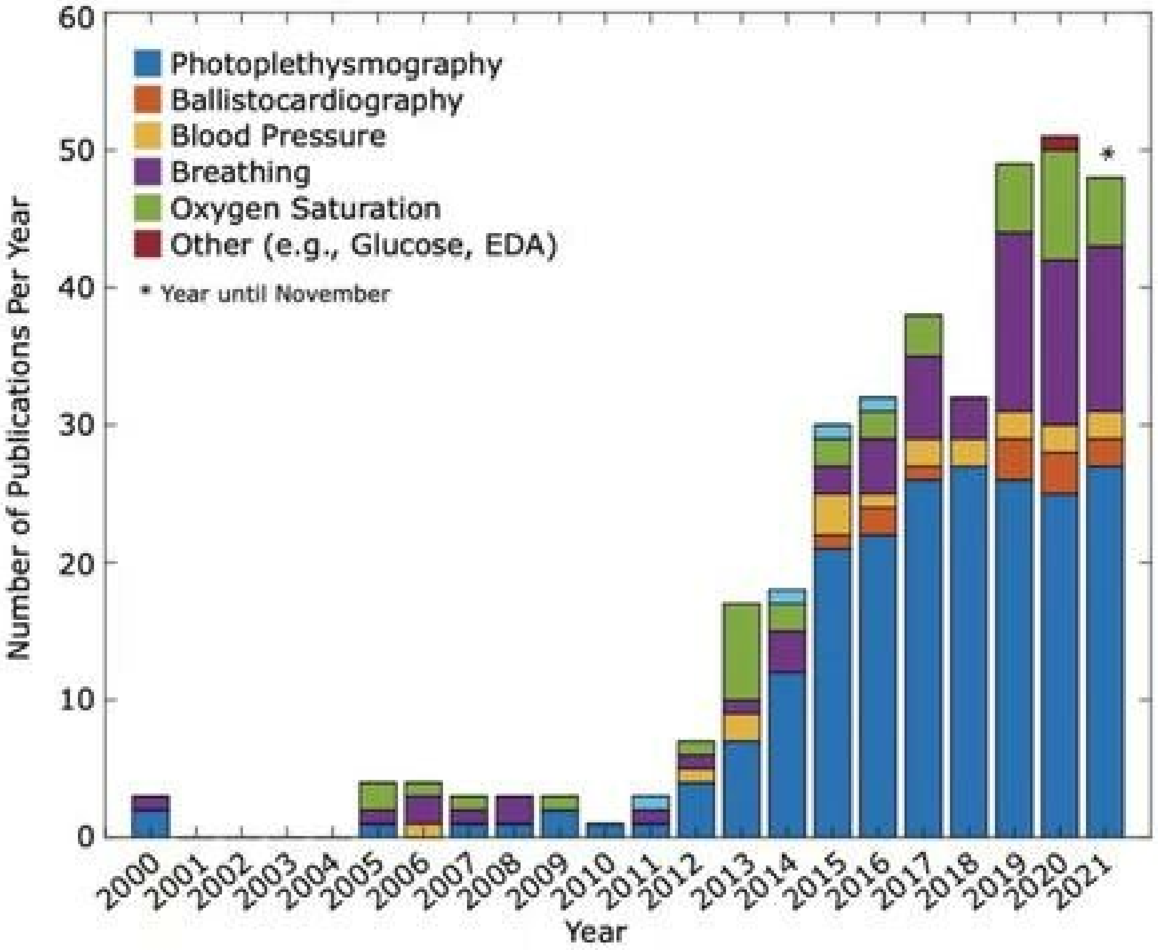

McDuff, D. (2023). Camera measurement of physiological vital signs. *ACM Computing Surveys*, *55*(9), 1-40.

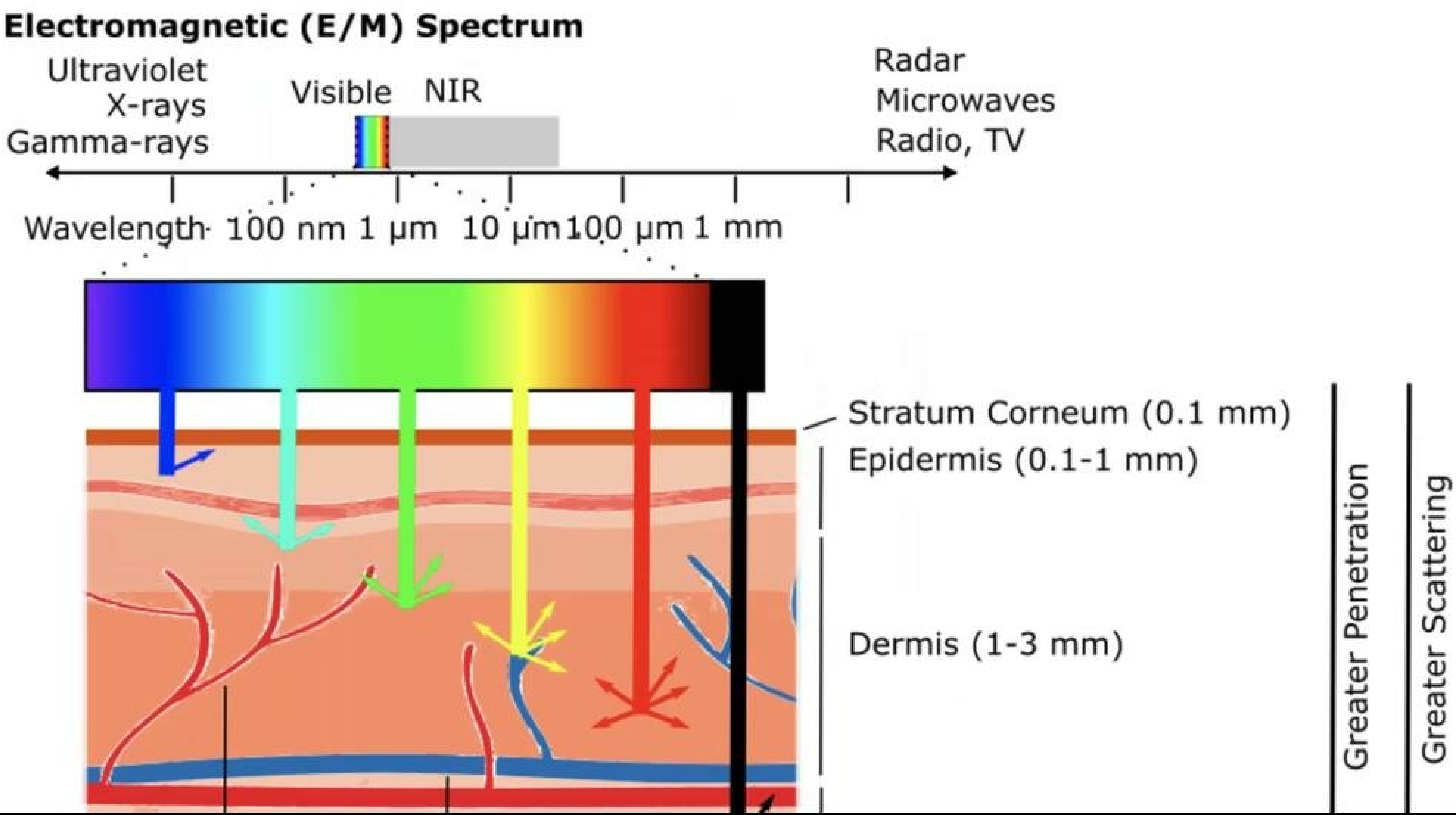
Electromagnetic (E/M) Spectrum
Ultraviolet
X-rays
Gamma-rays
Visible
NIR
Radar
Microwaves
Radio, TV
Wavelength
100 nm
1 μm
10 μm
100 μm
1 mm
Stratum Corneum (0.1 mm)
Epidermis (0.1-1 mm)
Dermis (1-3 mm)
Greater Penetration
Greater Scattering

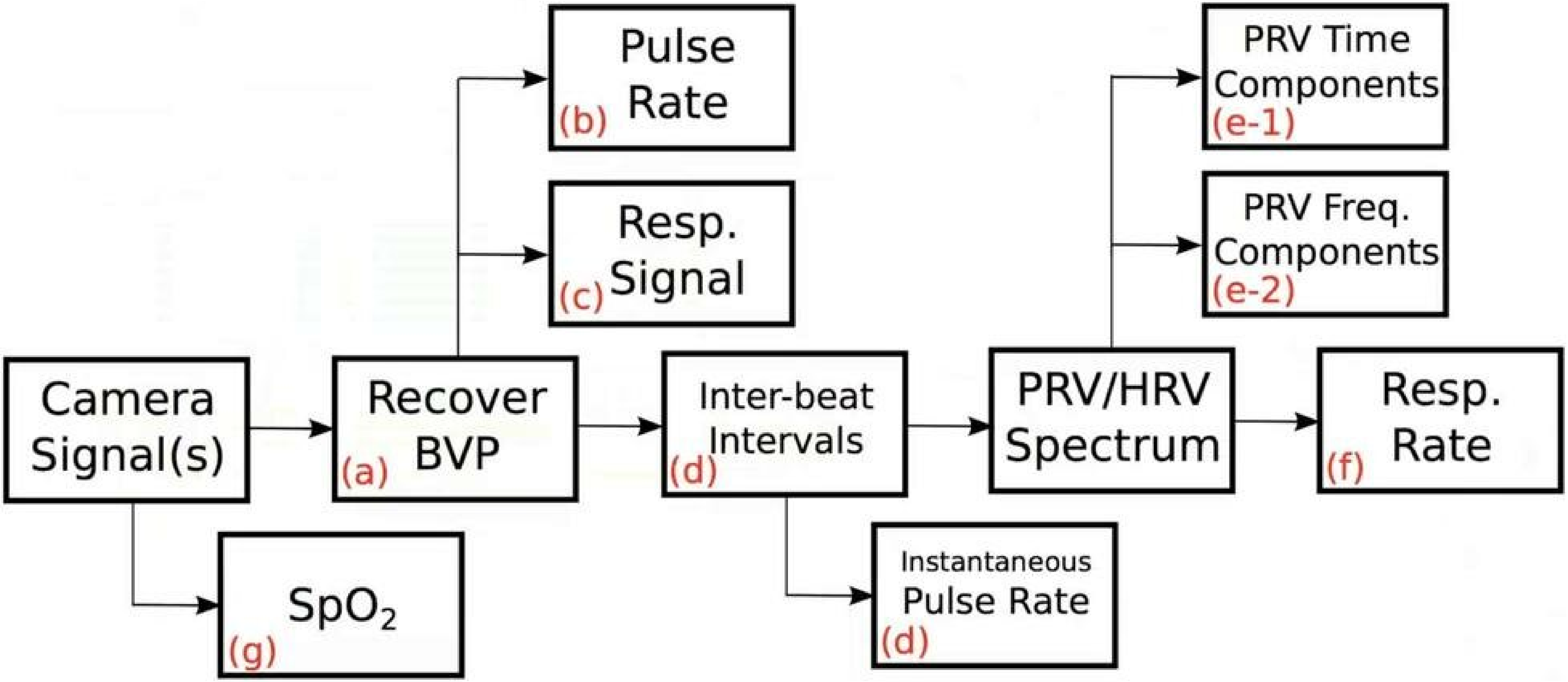
Camera Signal(s)
Recover BVP (a)
Pulse Rate (b)
Resp. Signal (c)
Inter-beat Intervals (d)
Instantaneous Pulse Rate (d)
PRV/HRV Spectrum
PRV Time Components (e-1)
PRV Freq. Components (e-2)
Resp. Rate (f)
SpO2 (g)

Optical Model

Robert Collins
CSE486, Penn State

Sketch: Light Transport

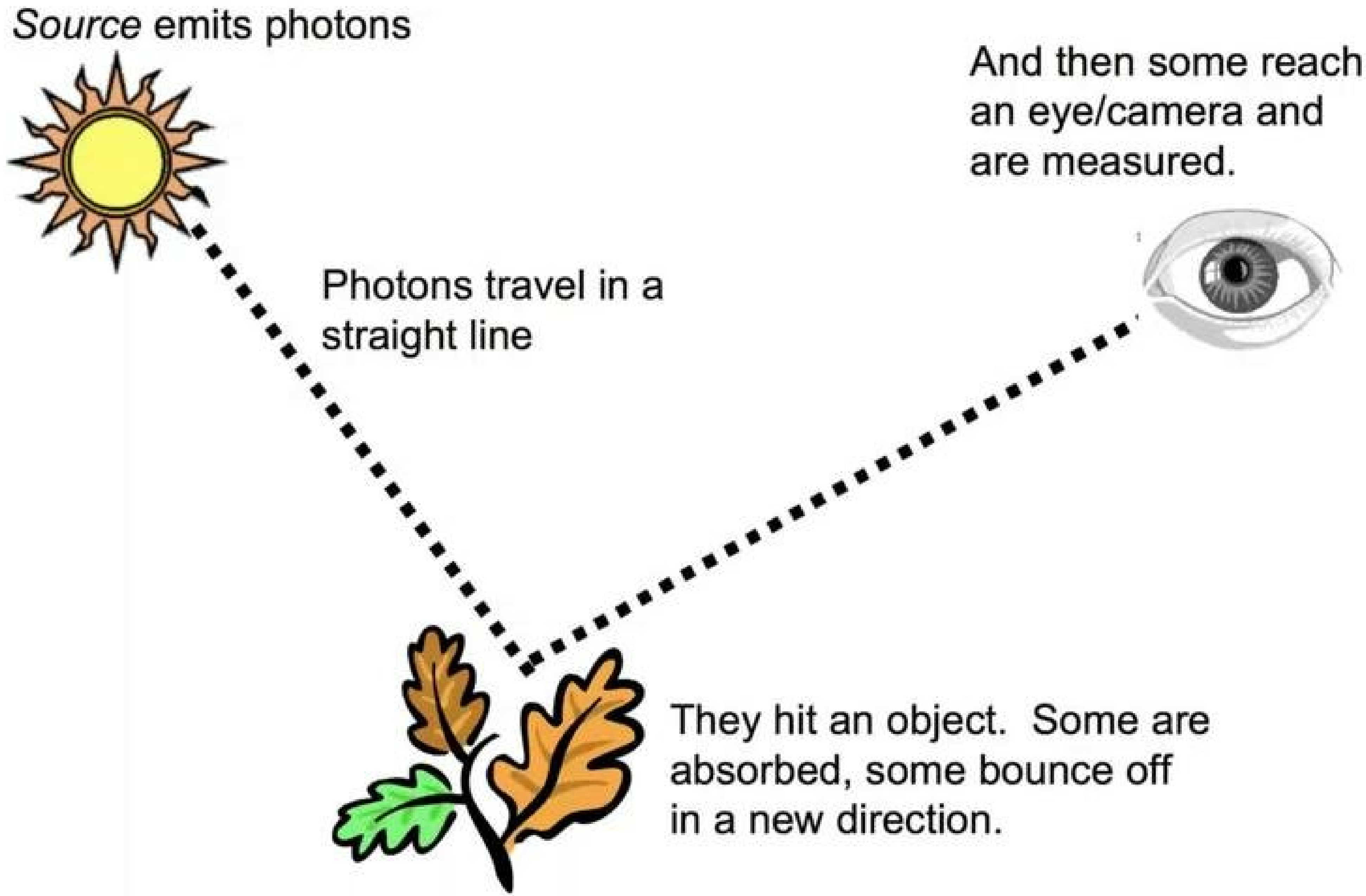

Robert Collins
CSE486, Penn State

Light Transport

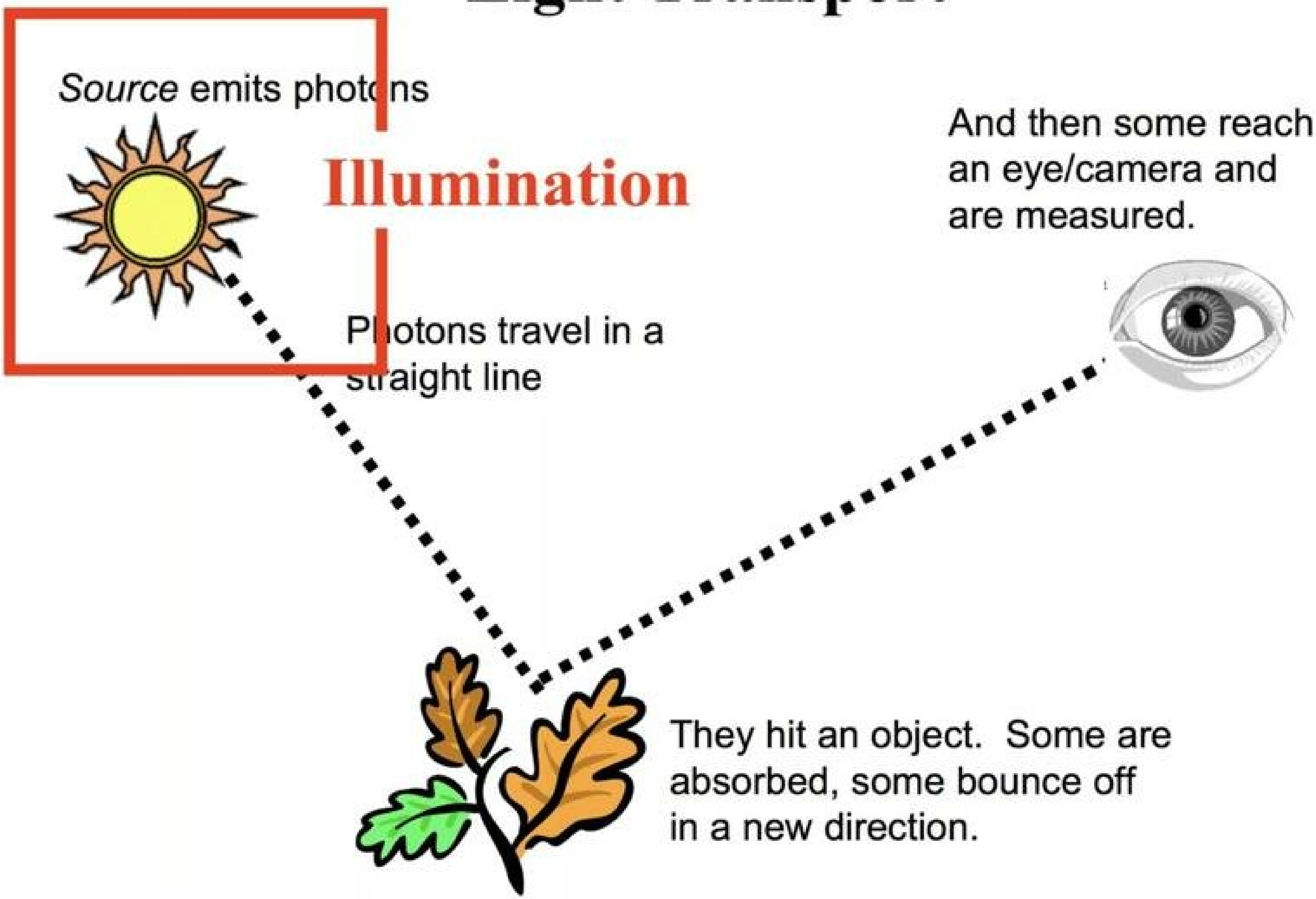

Light Transport

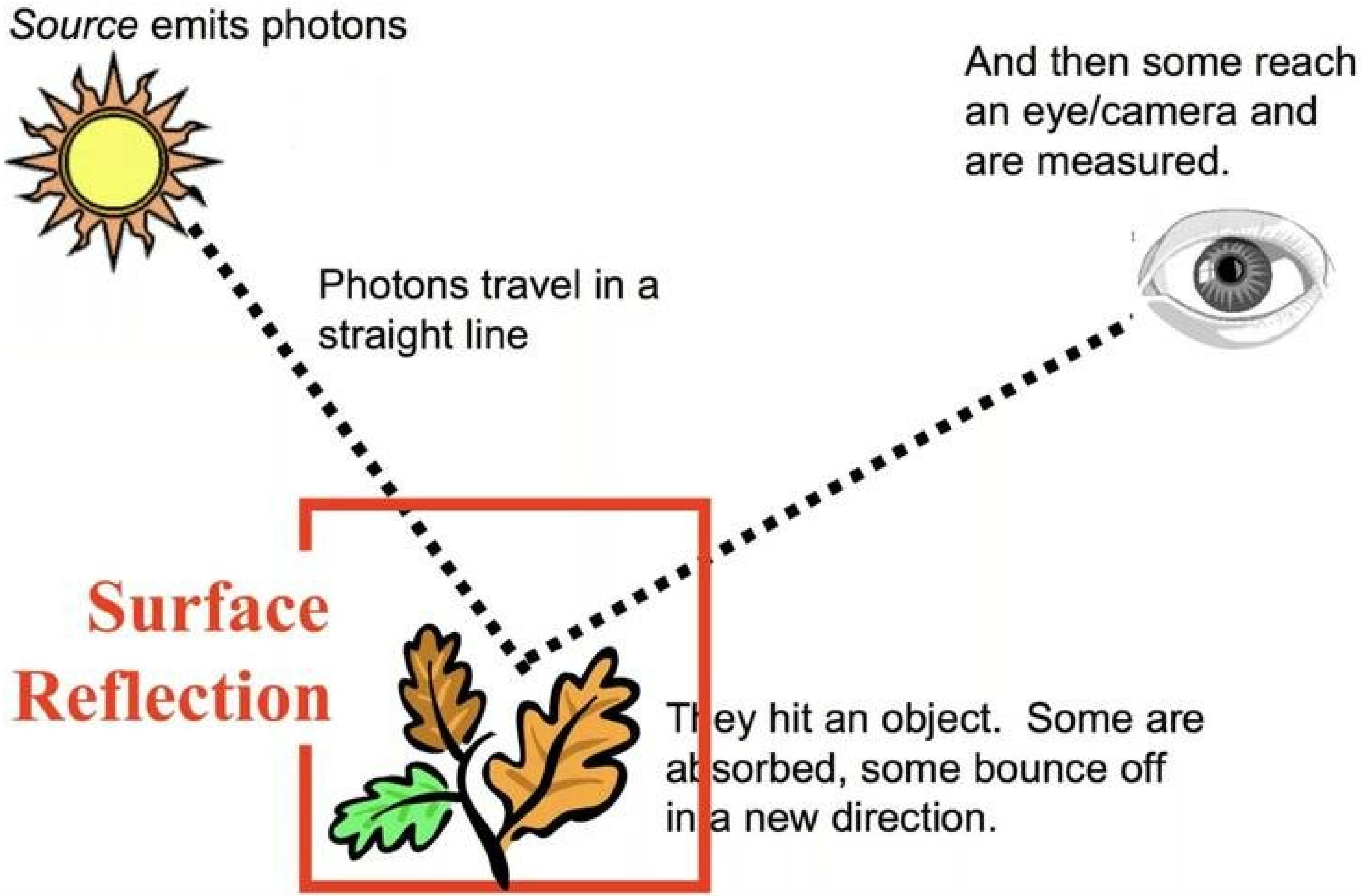

Robert Collins
CSE486, Penn State

Light Transport

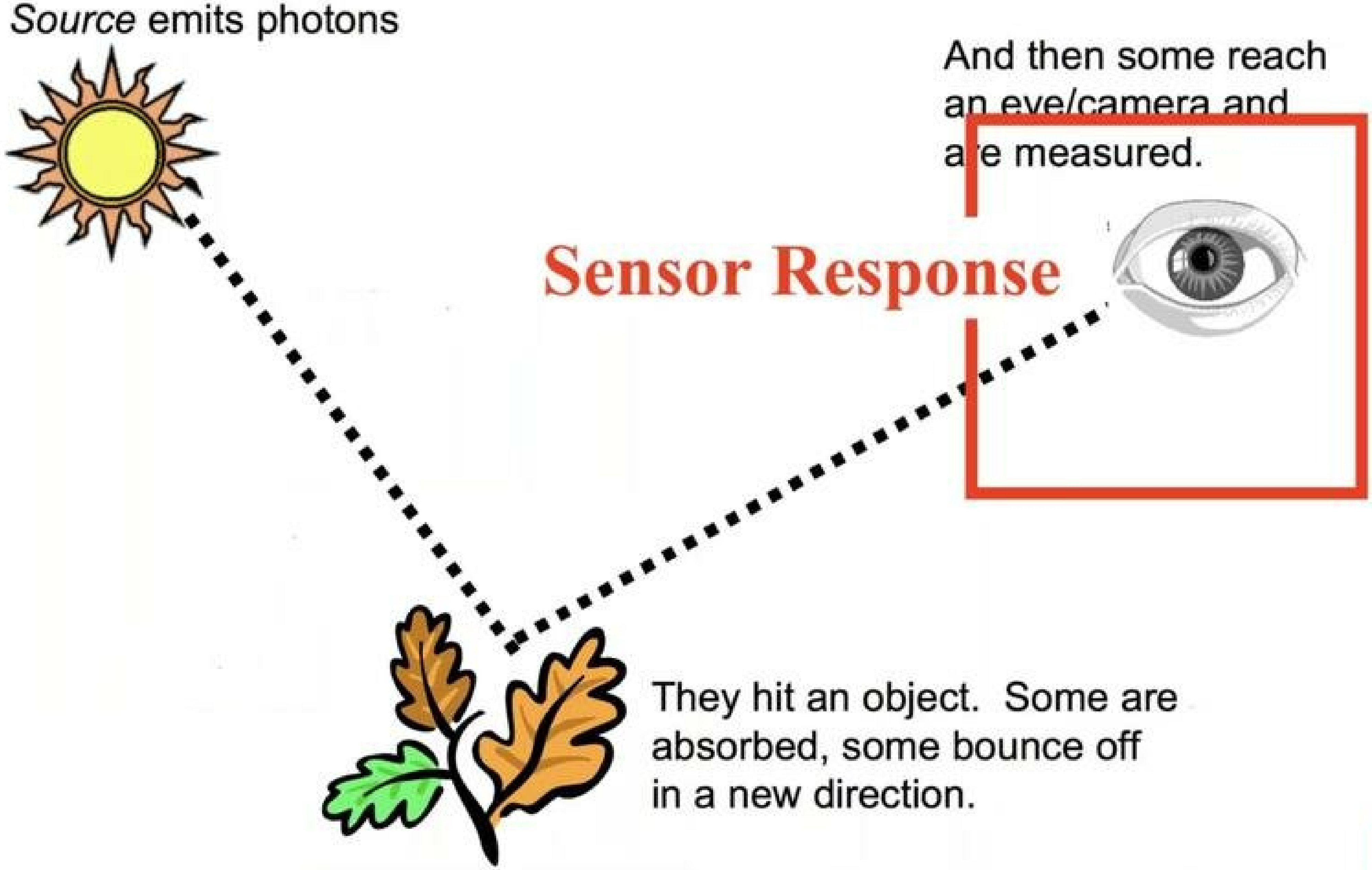

Robert Collins
CSE486

Skin Reflectance Model

Skin is well-modeled by a dichromatic reflectance model.
- **transparent medium (dermis)**
- **pigmentations (hemaglobin, melanin)**
- **specular reflection (oil on skin)**

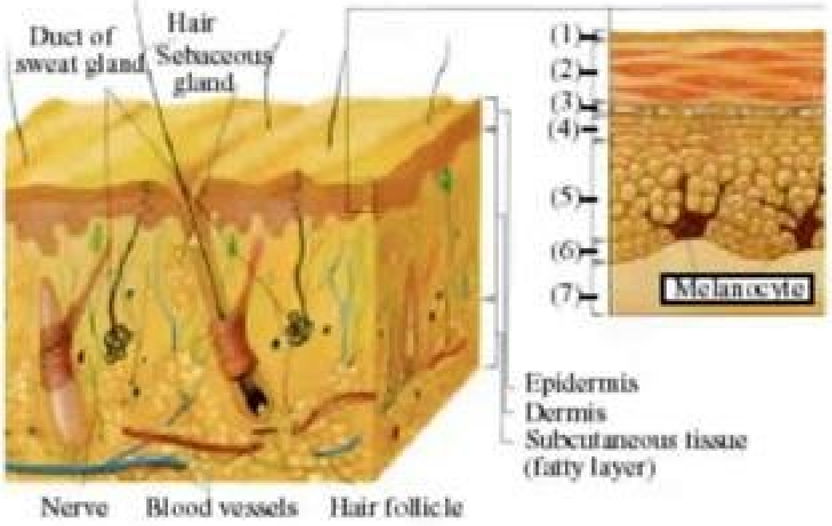

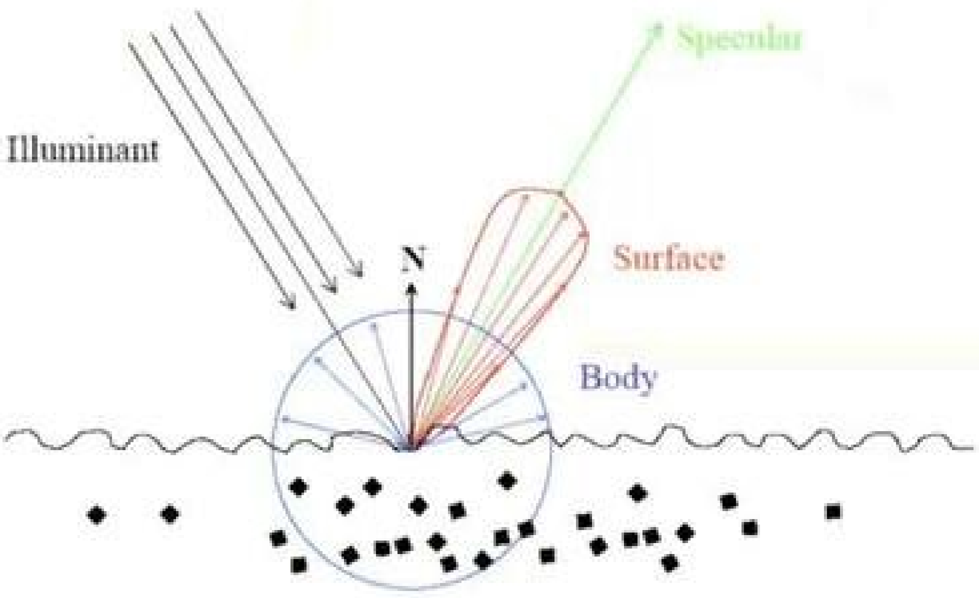

Dichromatic reflectance model

Robert Collins
CSE486, Penn State

Some Light Source SPDs

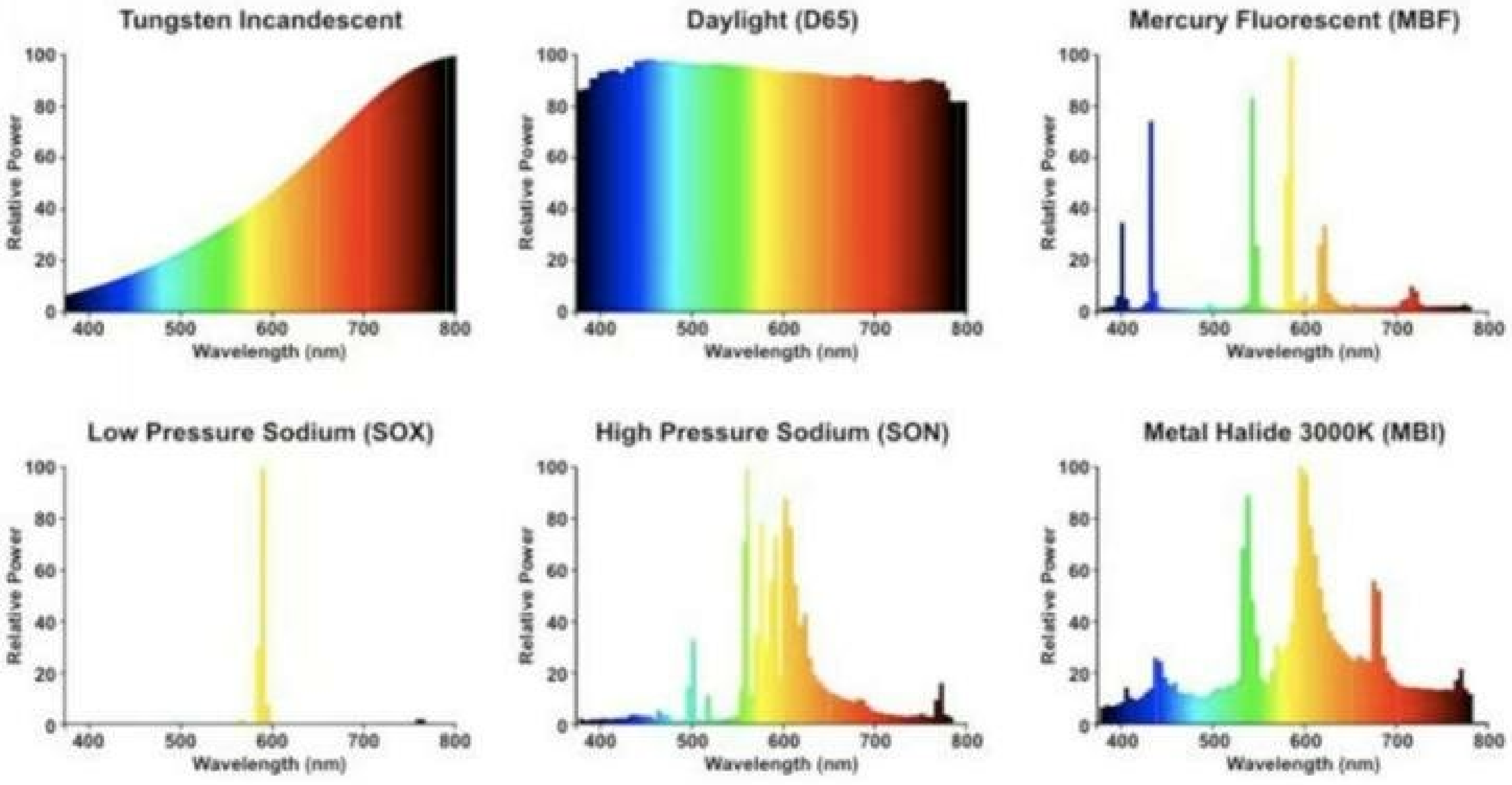

Skin reflectance

Ambient Light Spectra

Camera Sensitivity channel 'k'

Constant

$$
\begin{aligned}
I &= \int R_s(\lambda) a_l L(\lambda) C_k(\lambda) d\lambda \\
&= a_m a_l \int R_m(\lambda) L(\lambda) C_k(\lambda) d\lambda \\
&+ a_h a_l \int R_h(\lambda) L(\lambda) C_k(\lambda) d\lambda \\
I(t) &= a_m a_l(t) \int R_m(\lambda) L(\lambda, t) C_k(\lambda) d\lambda \\
&+ a_h(t) a_l(t) \int R_h(\lambda, t) L(\lambda, t) C_k(\lambda) d\lambda
\end{aligned}
$$

$$R_s(\lambda) = a_m R_m(\lambda) + a_h R_h(\lambda)$$

Spectral reflectance of Melanin

Spectral reflectance of Hemoglobin

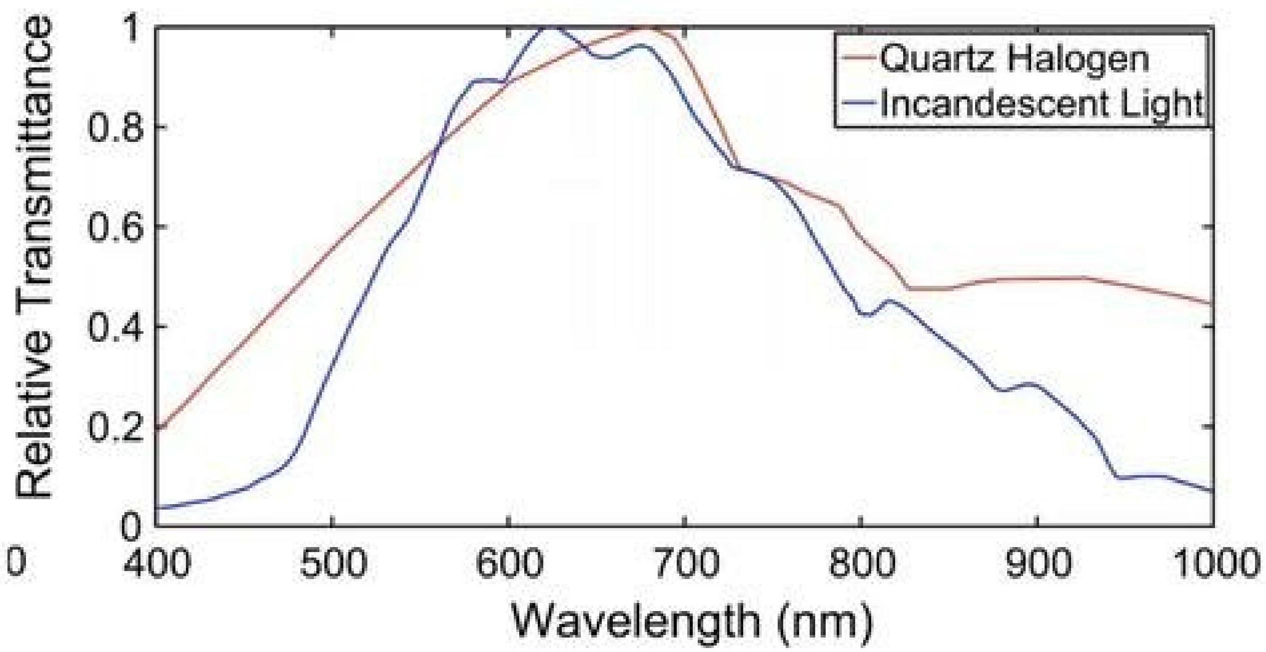
Quartz Halogen
Incandescent Light
Relative Transmittance
Wavelength (nm)
0
0.2
0.4
0.6
0.8
1
400
500
600
700
800
900
1000

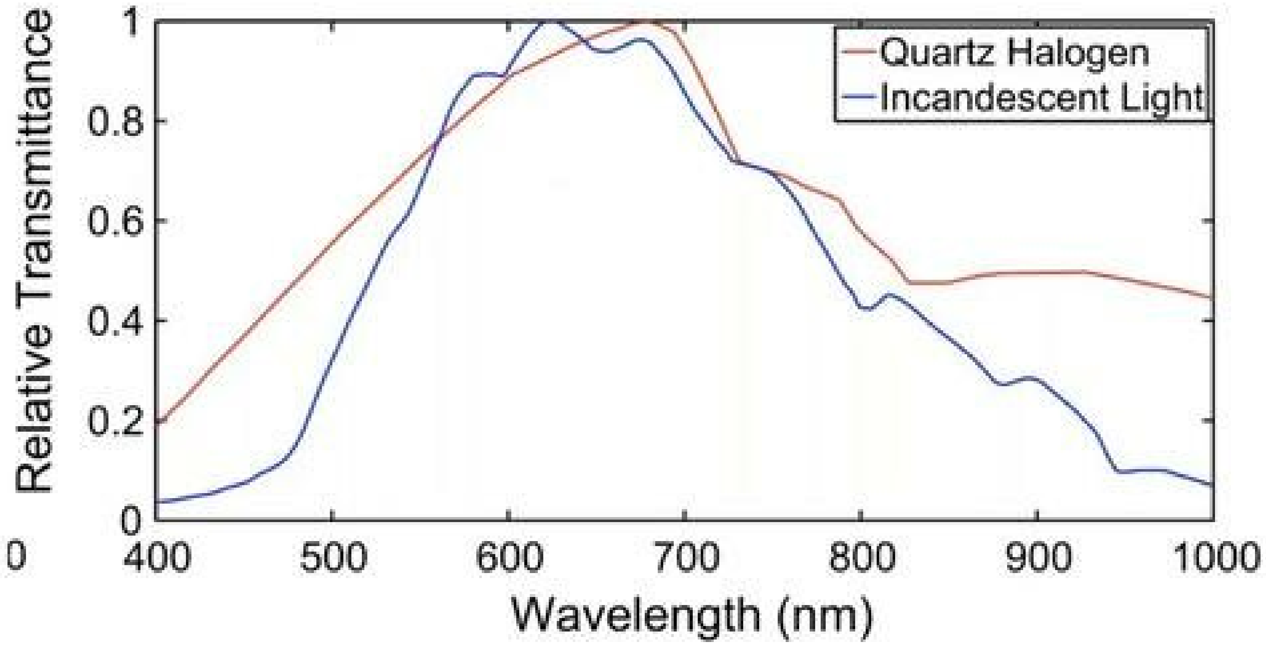
Quartz Halogen
Incandescent Light
Relative Transmittance
Wavelength (nm)

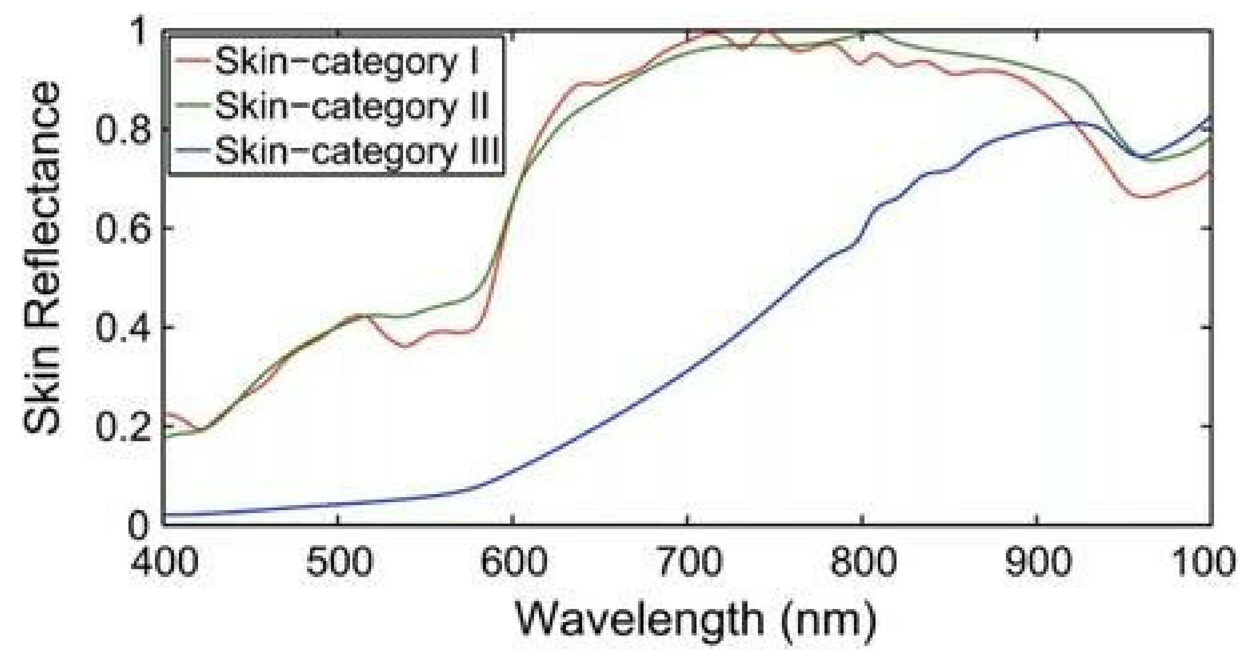
Skin−category I
Skin−category II
Skin−category III
Skin Reflectance
Wavelength (nm)

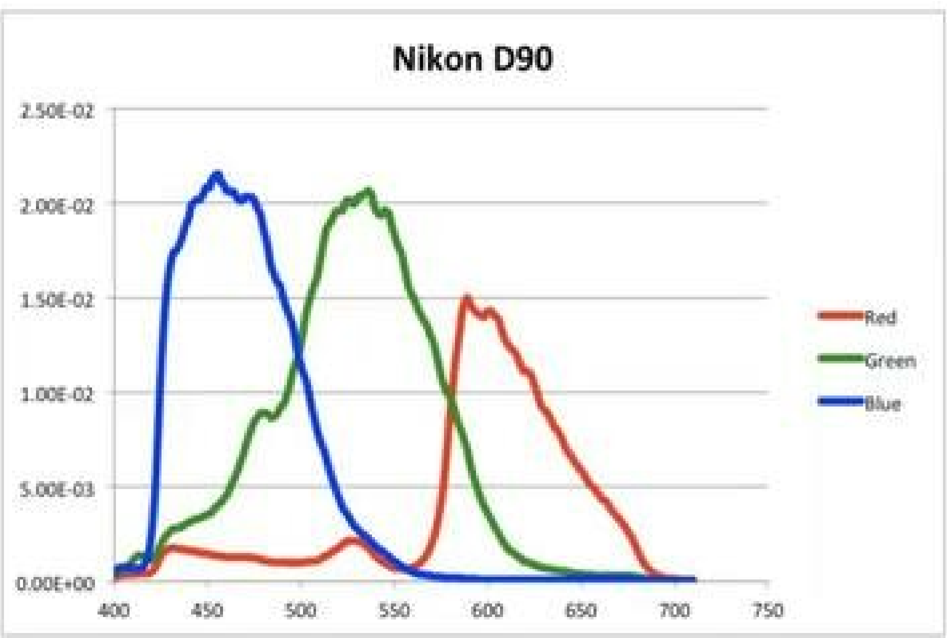
Nikon D90
Red
Green
Blue

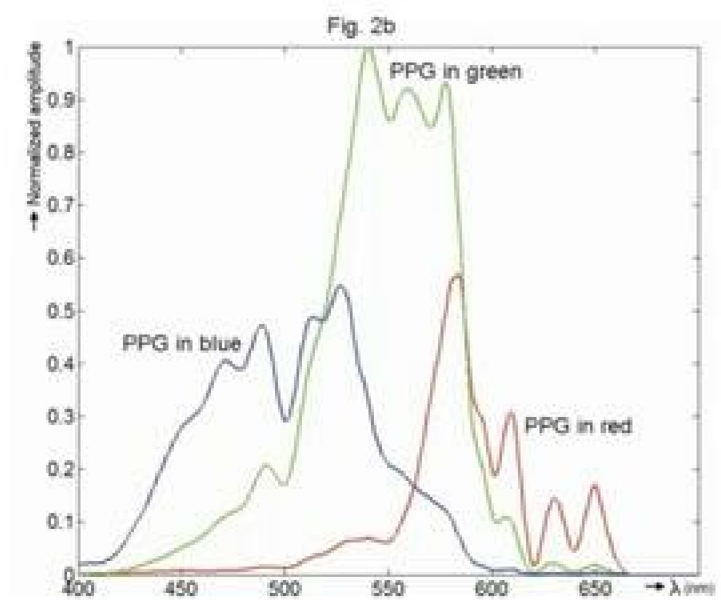
Fig. 2b
PPG in green
PPG in blue
PPG in red
Normalized amplitude

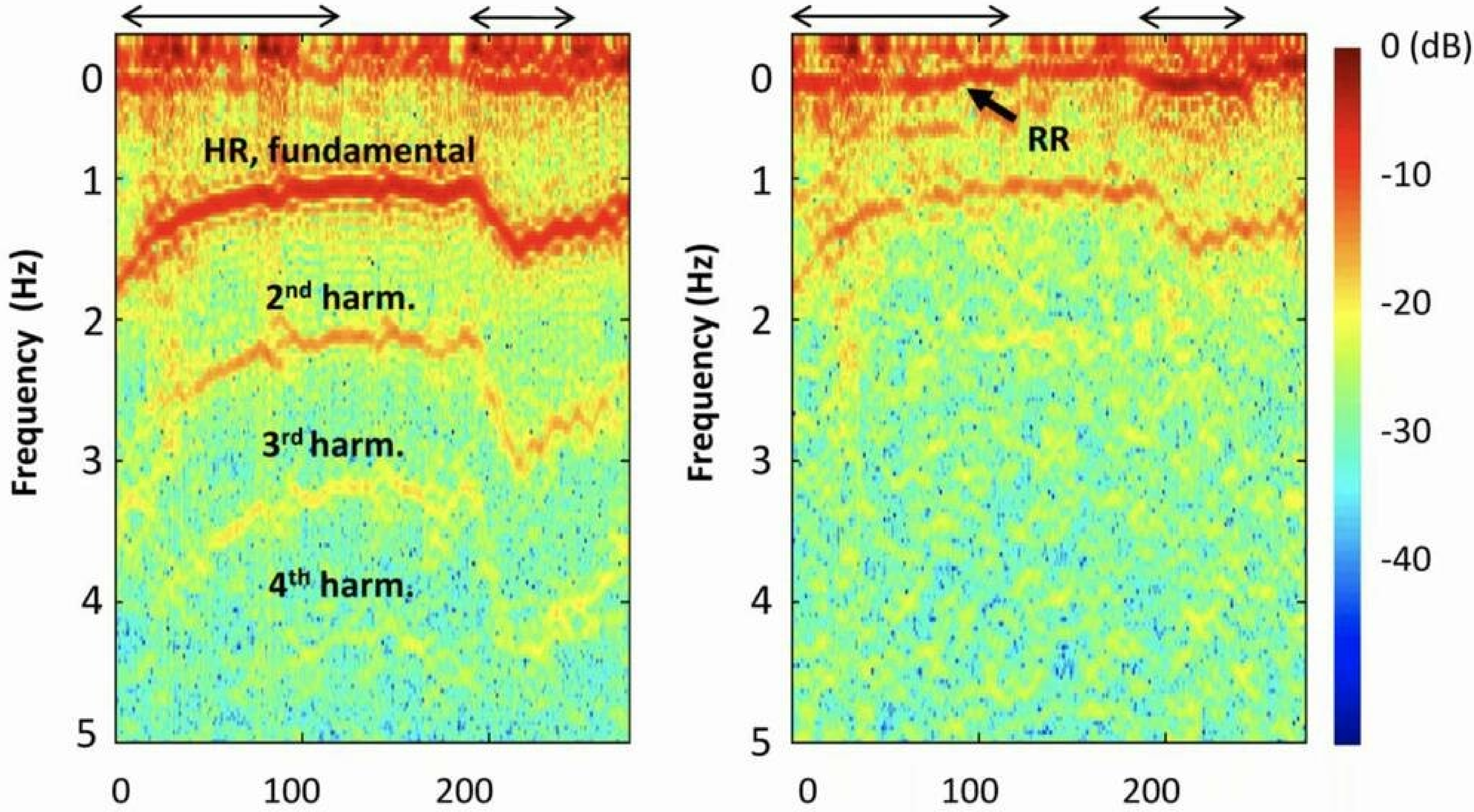

HR, fundamental
2nd harm.
3rd harm.
4th harm.
RR
Frequency (Hz)
0
1
2
3
4
5
0
100
200
0 (dB)
-10
-20
-30
-40

WHAT IS VIDEO MAGNIFICATION

- Blood volume pulses are imperceptible to normal vision

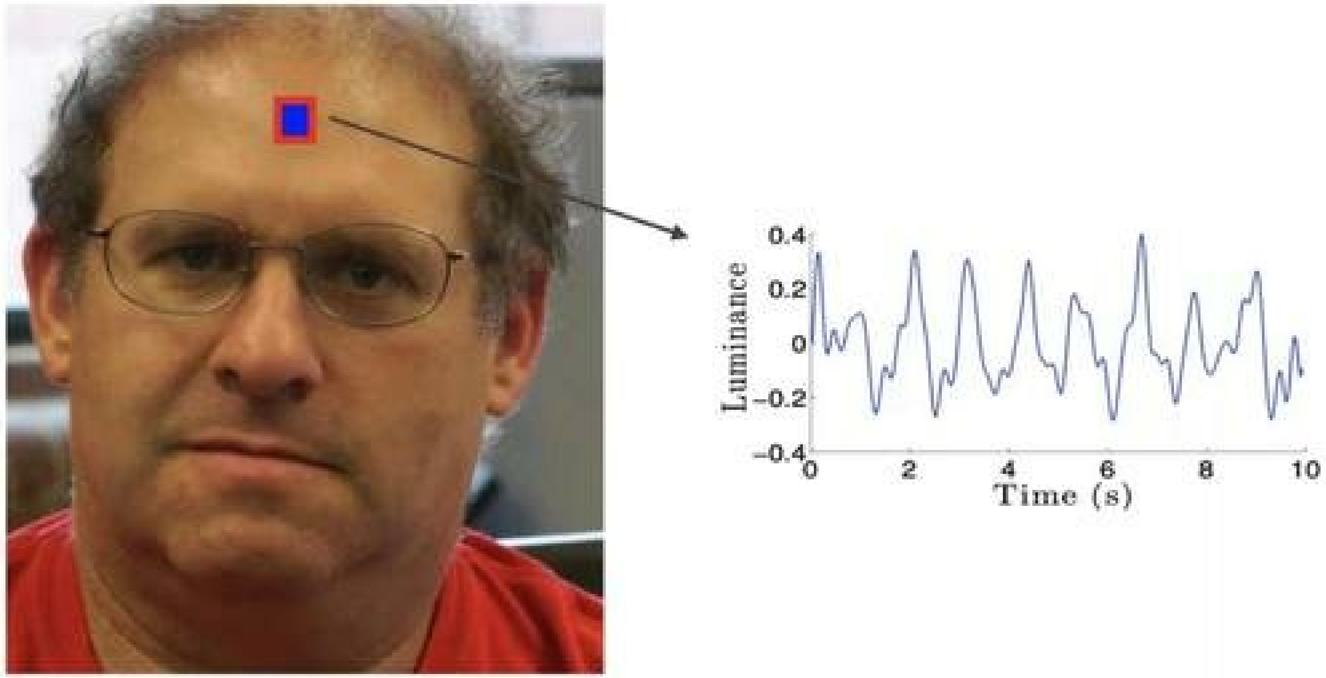

Wu et al. SIGGRAPH 2012

SUBTLE COLOR VARIATIONS

Input frame

SUBTLE COLOR VARIATIONS

- The face gets slightly redder when blood flows
- They use grayscale intensity value

Input frame

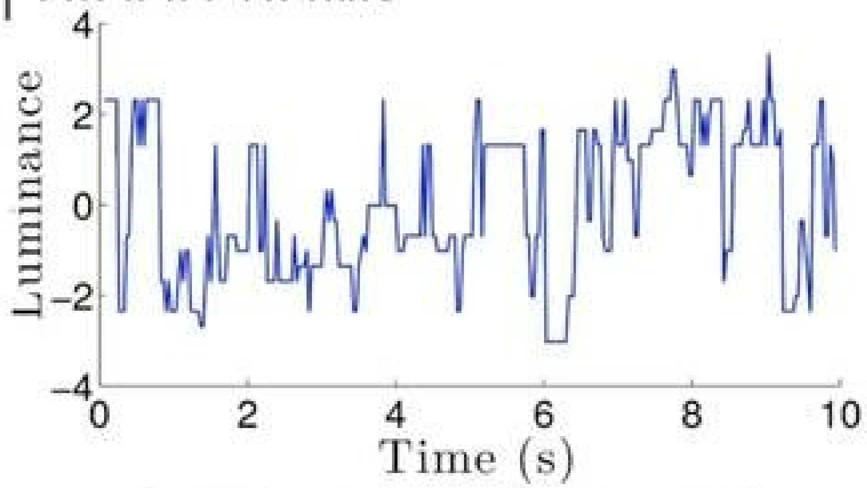

Luminance trace (zero mean)

SUBTLE COLOR VARIATIONS

1. Average spatially to overcome sensor and quantization noise

Input frame

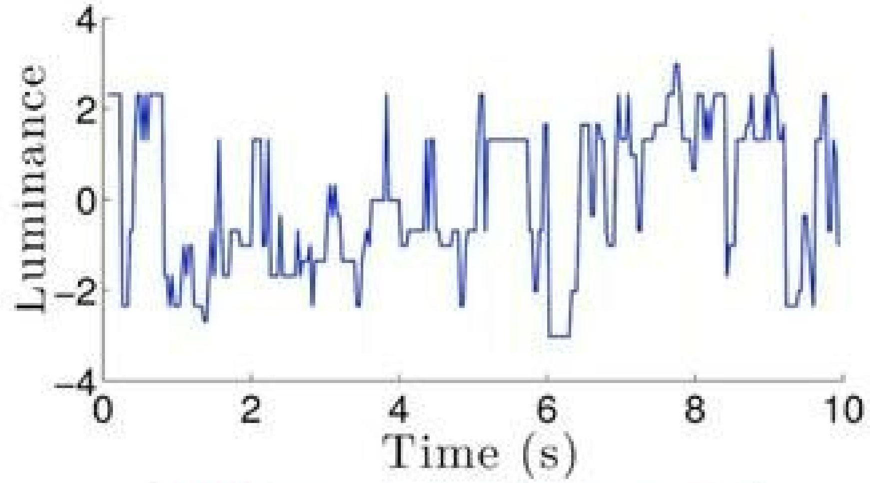

Luminance trace (zero mean)

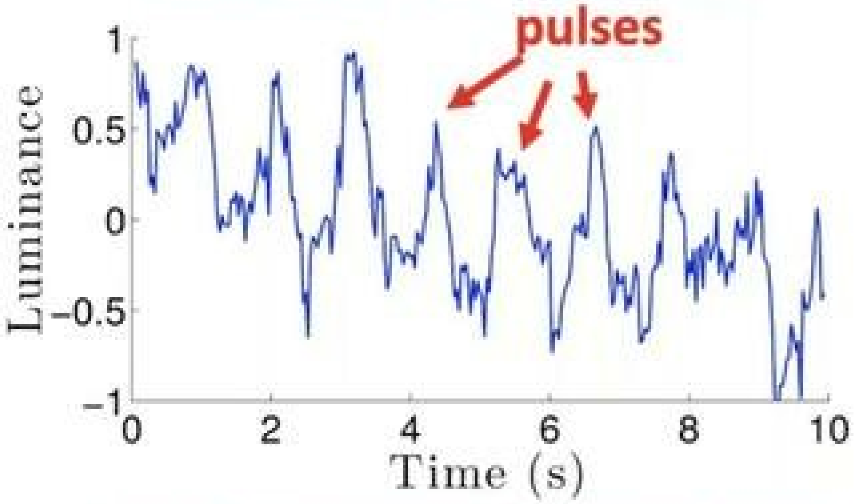

Spatially averaged luminance trace

AMPLIFYING SUBTLE COLOR VARIATIONS

2. Filter temporally to extract the signal of interest

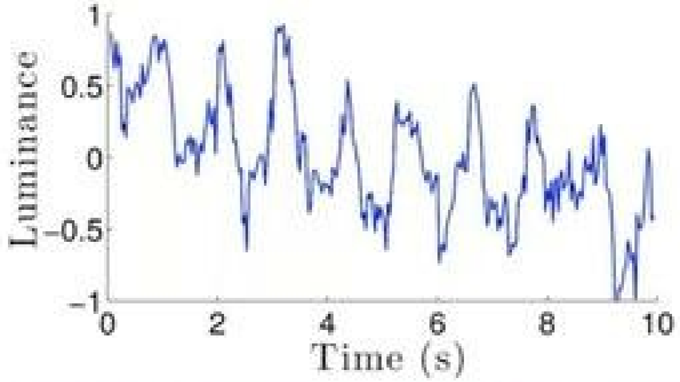

Spatially averaged luminance trace

⊗

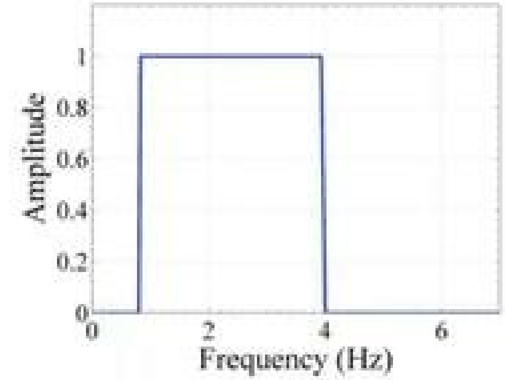

Temporal filter

=

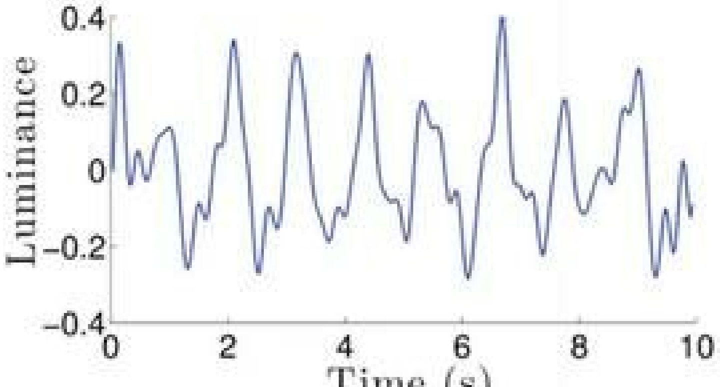

Temporally bandpassed trace

Heart Rate Extraction

Peak detection

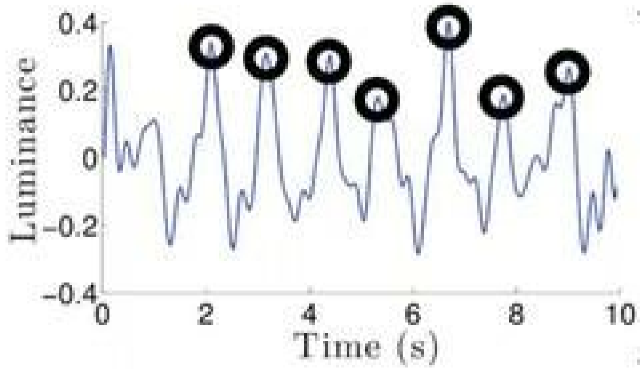

Temporally bandpassed trace (one pixel)

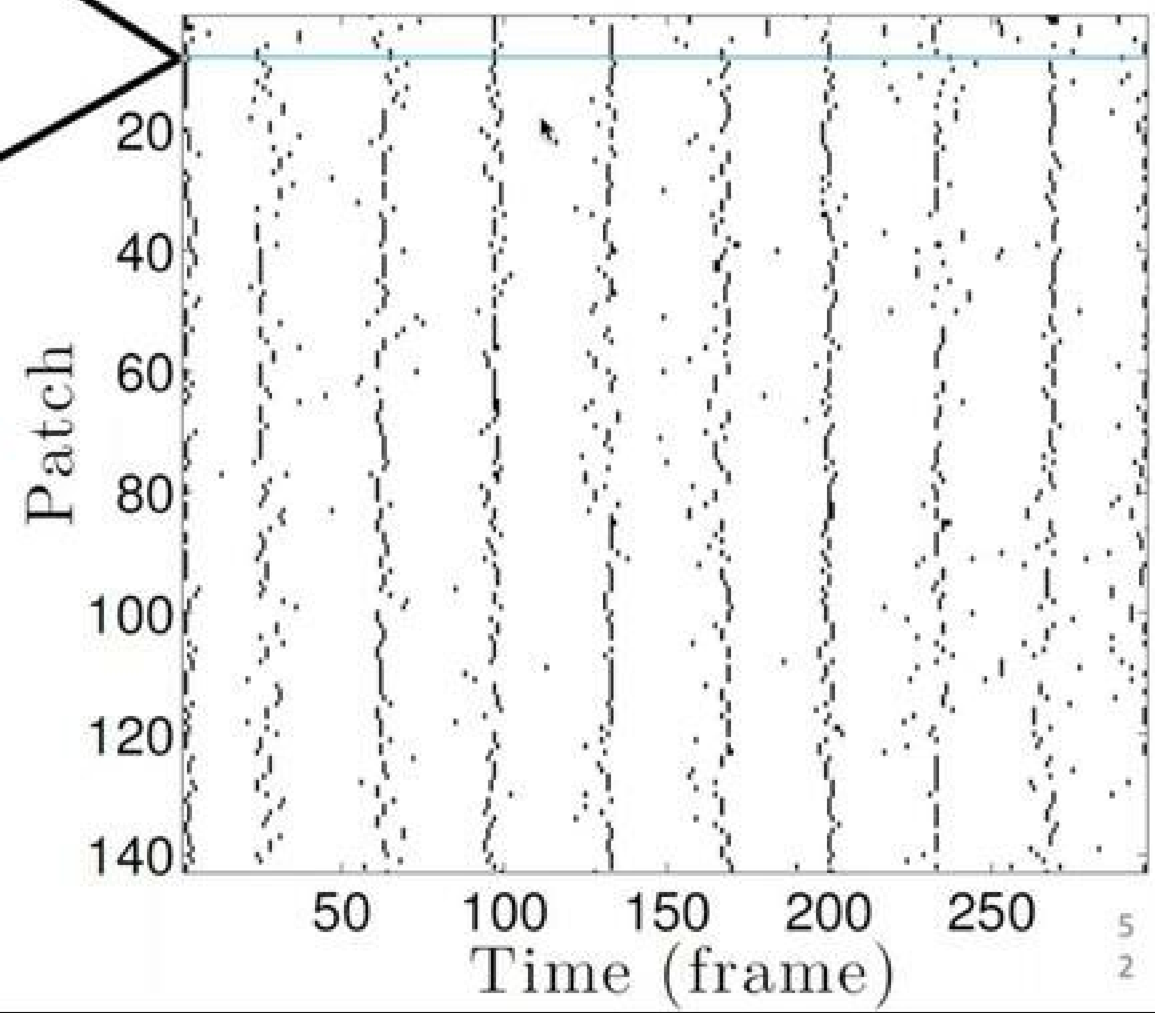

Heart Rate Extraction

Peak detection

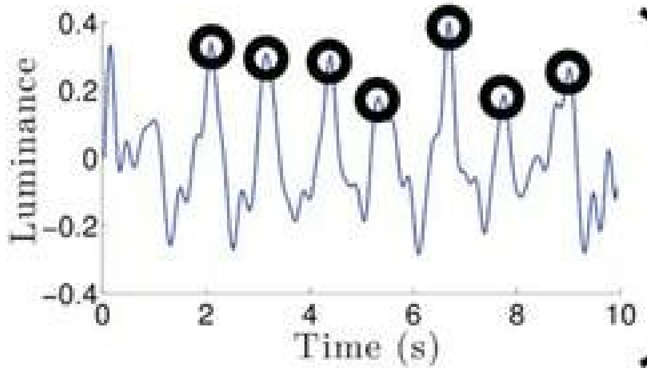

Temporally bandpassed trace (one pixel)

Pulse locations

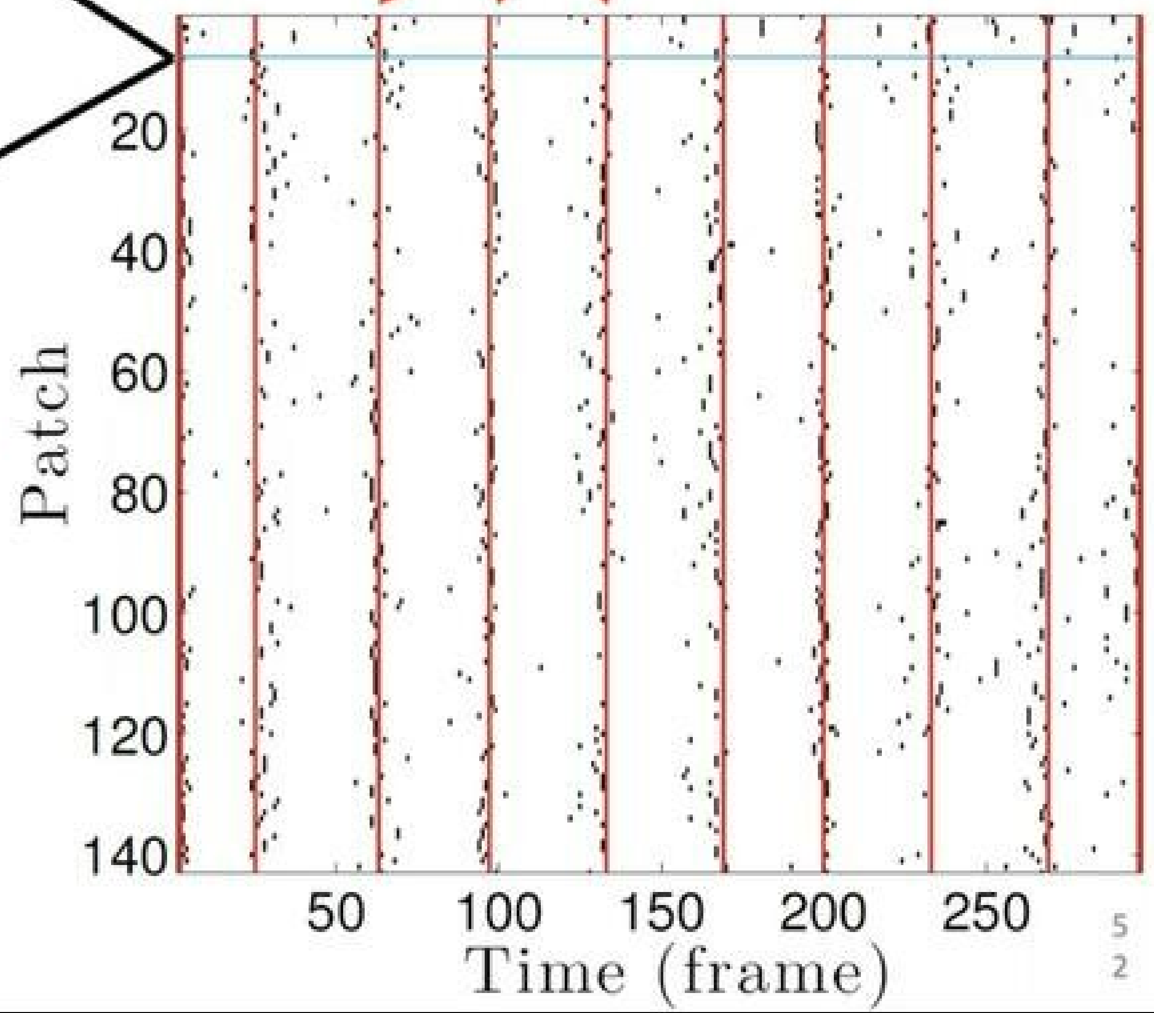

Heart Rate Extraction

Peak detection

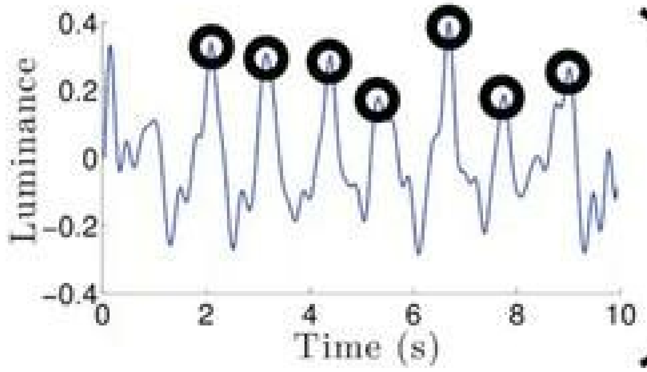

Temporally bandpassed trace (one pixel)

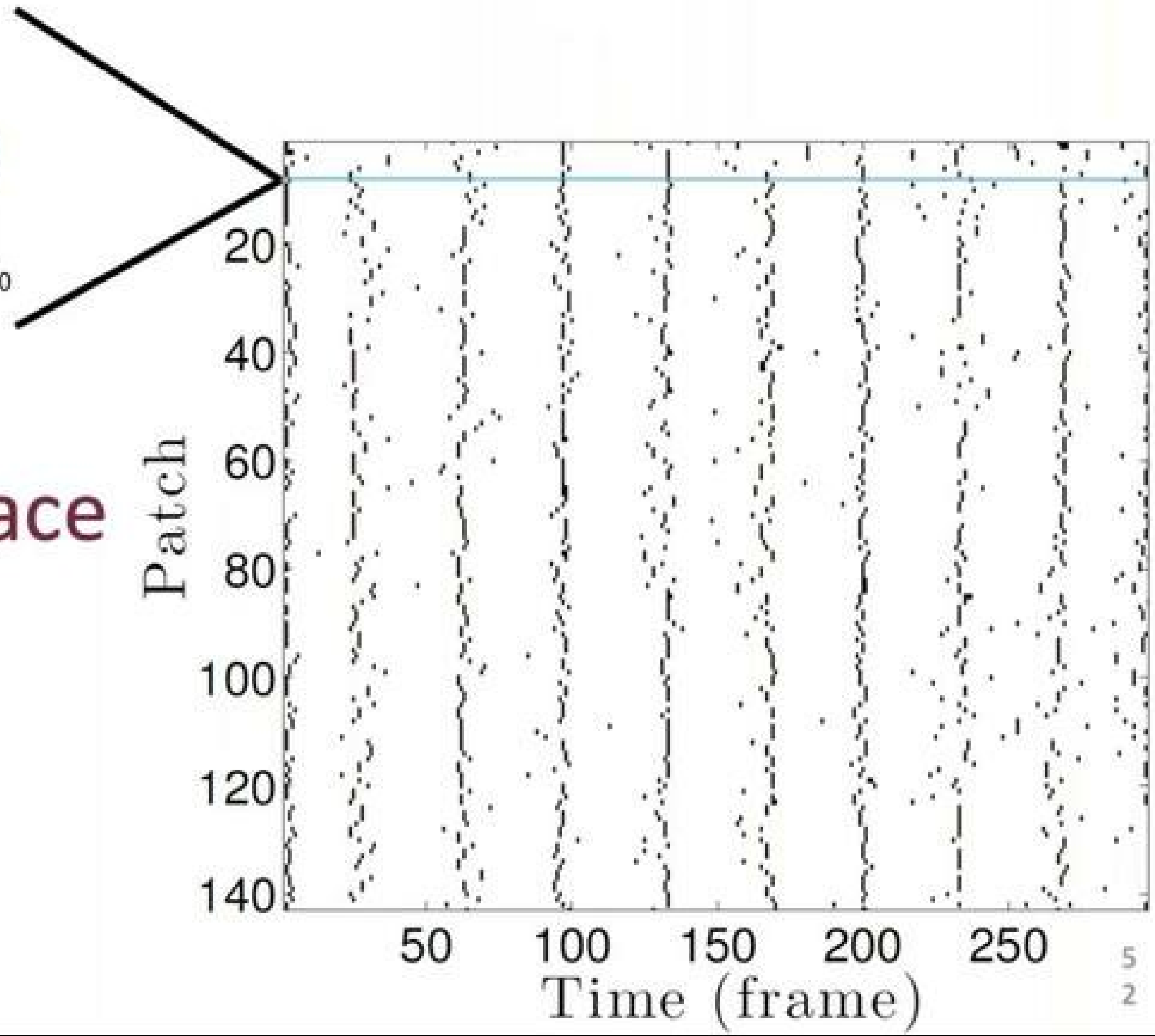

EXTRACT PHYSIOLOGICAL SIGNAL FROM VIDEOS

- Key challenges
  - Which color channels to use? (G vs RGB vs NIR vs IR)
  - How to extract the signal? (VidMag, ICA, CHROM, etc)
  - Effect of motion (Face detection and registration)
  - Face area selection (skin detection and preprocessing)
  - Effect of ambient illumination

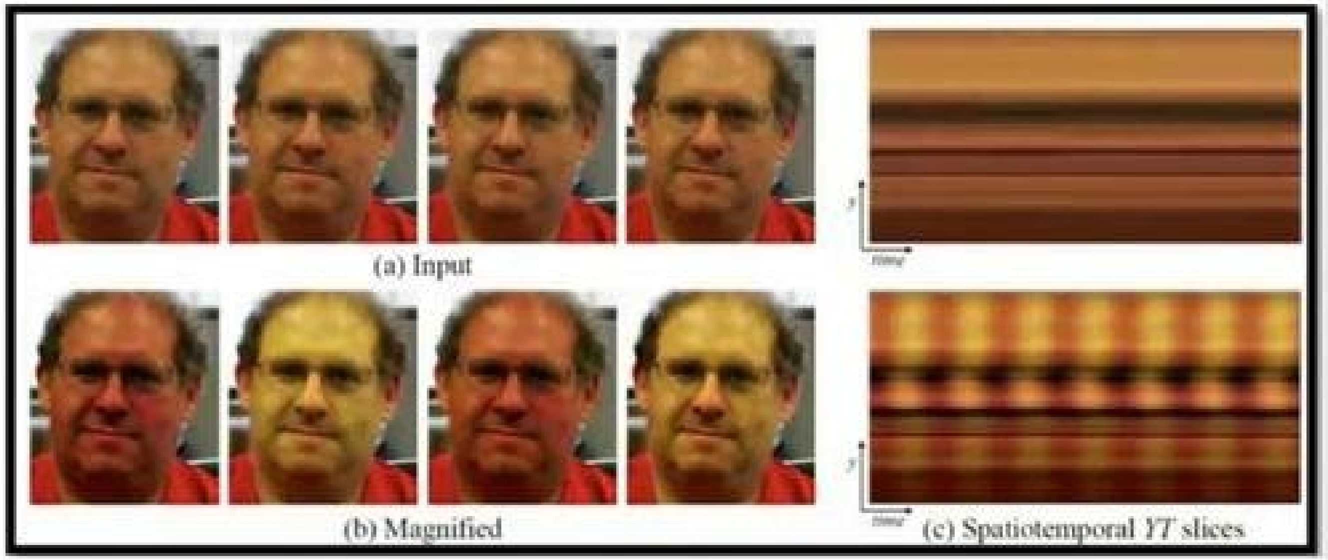

Picture from : Hao-Yu Wu, Michael Rubinstein, Eugene Shih, John Guttag, Fr'edo Durand, and William Freeman. Eulerian video magnification for revealing subtle changes in the world. ACM Trans. Graph. (Proceedings SIGGRAPH), 31(4), 2012.

STANDARD PIPELINE

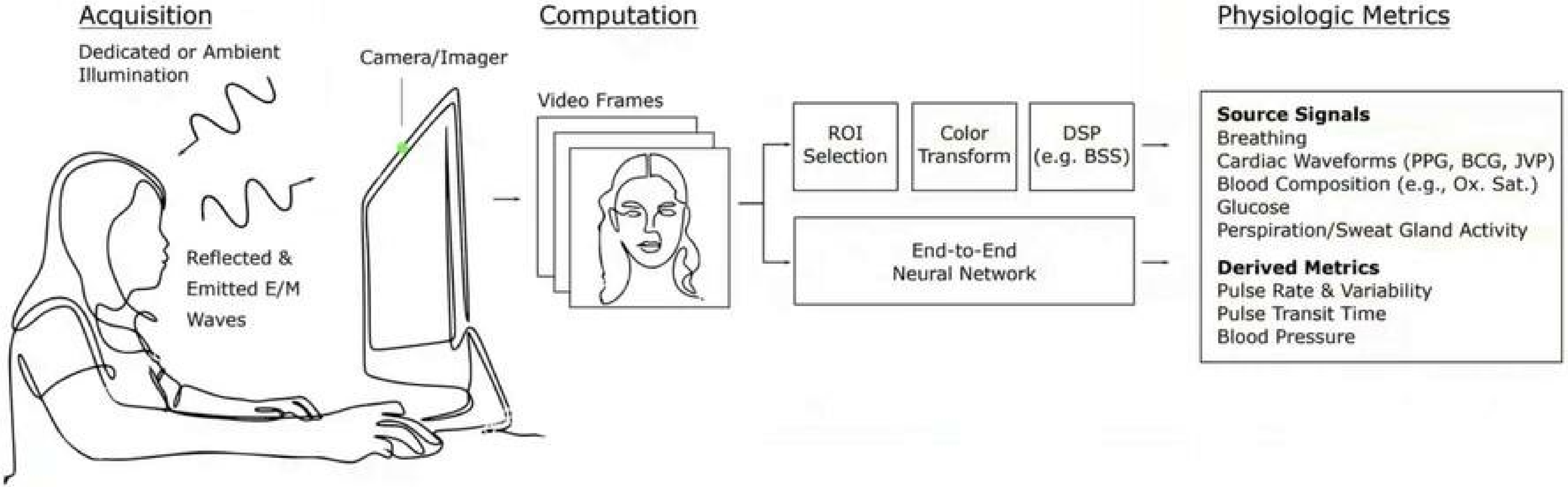

McDuff, D. (2023). Camera measurement of physiological vital signs. *ACM Computing Surveys*, *55*(9), 1-40.

MOTION

FACE DETECTION AND REGISTRATION

MOTION

FACE DETECTION AND REGISTRATION

MOTION

FACE DETECTION AND REGISTRATION

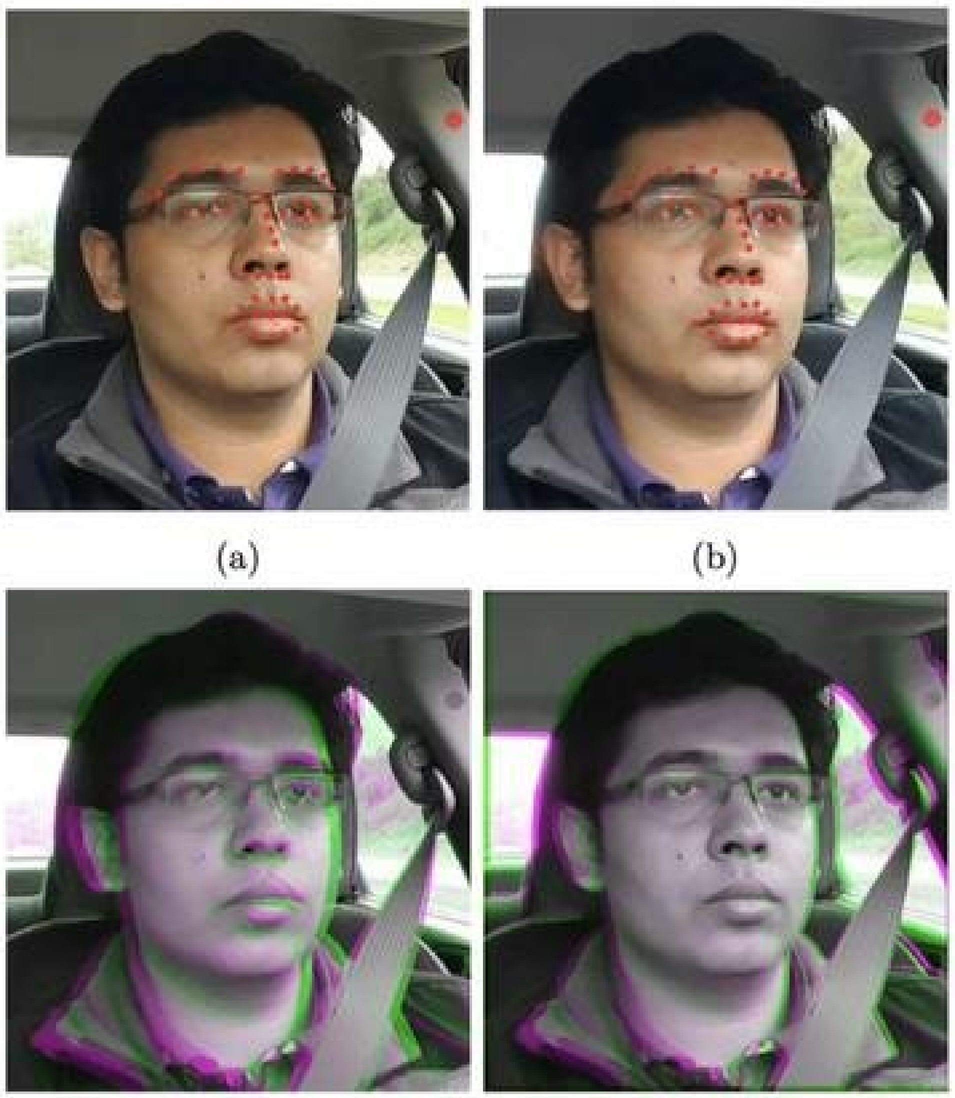

(a) (b)

(c) (d)

(a) Original points

(b) After homography

Sarkar, A. (2017). *Cardiac signals: remote measurement and applications* (Doctoral dissertation, Virginia Tech).

SKIN DETECTION

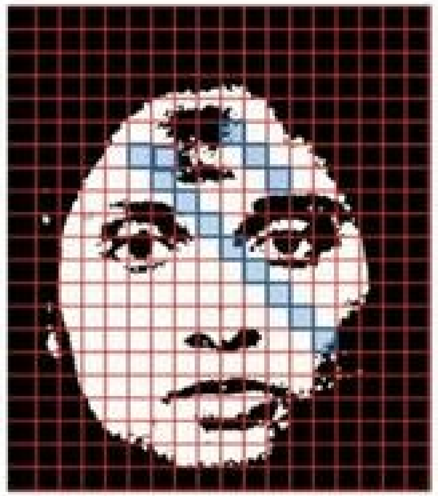

- Can we find out a universal skin detection algorithm for RGB and NIR?

SKIN DETECTION

SEARCH FOR UNIVERSAL SKIN DETECTOR

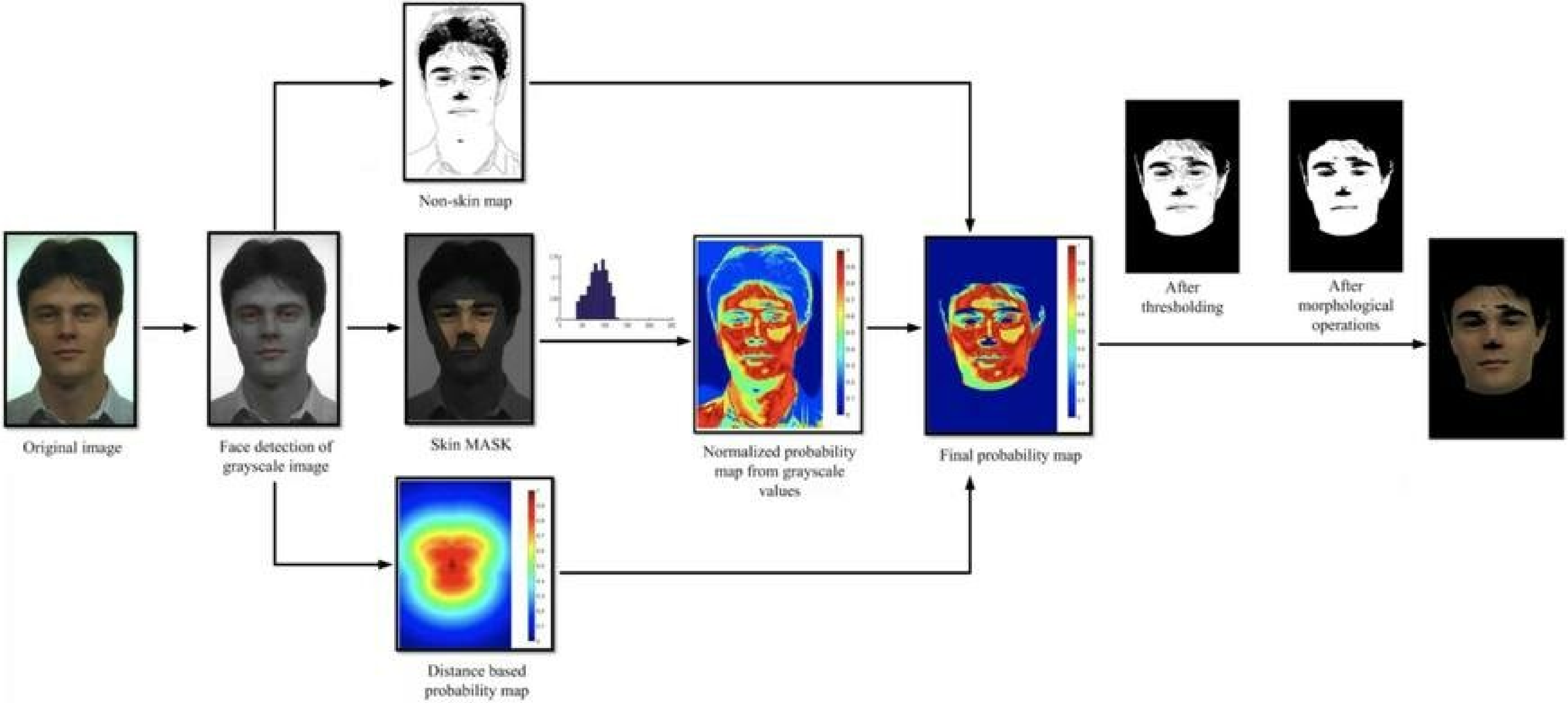

Sarkar, A., Abbott, A. L., & Doerzaph, Z. (2017, March). Universal skin detection without color information. In *2017 IEEE Winter Conference on Applications of Computer Vision (WACV)* (pp. 20-28). IEEE.

SKIN DETECTION
SKIN TEXTURE AND CONTEXTUAL INFORMATION

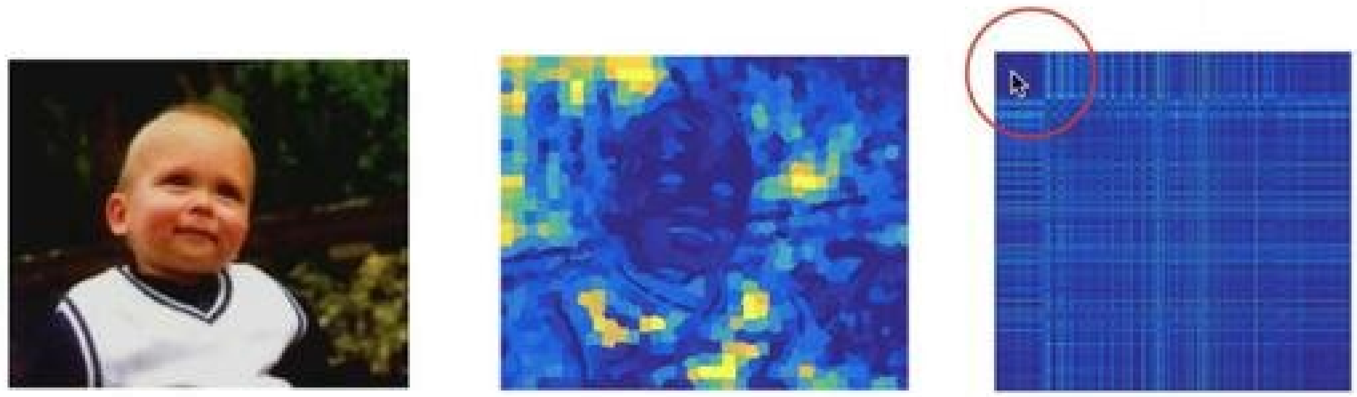

(a) (b) (c)

Sarkar, A., Abbott, A. L., & Doerzaph, Z. (2017, March). Universal skin detection without color information. In *2017 IEEE Winter Conference on Applications of Computer Vision (WACV)* (pp. 20-28). IEEE.

SKIN DETECTION

SKIN TEXTURE AND CONTEXTUAL INFORMATION

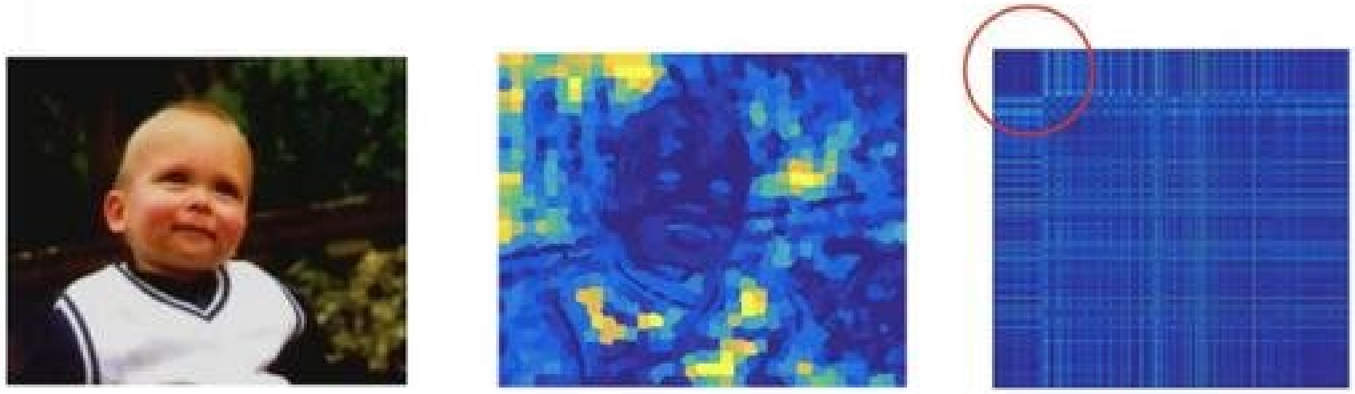

(a) (b) (c)

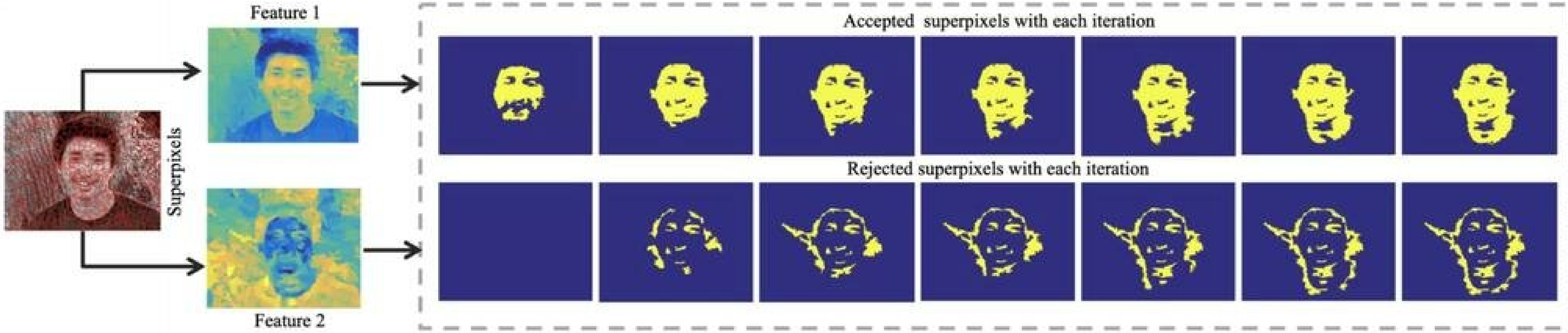

Sarkar, A., Abbott, A. L., & Doerzaph, Z. (2017, March). Universal skin detection without color information. In *2017 IEEE Winter Conference on Applications of Computer Vision (WACV)* (pp. 20-28). IEEE.

SKIN DETECTION

Sarkar, A., Abbott, A. L., & Doerzaph, Z. (2017, March). Universal skin detection without color information. In *2017 IEEE Winter Conference on Applications of Computer Vision (WACV)* (pp. 20-28). IEEE.

SKIN DETECTION
DEEP LEARNING BASED METHOD

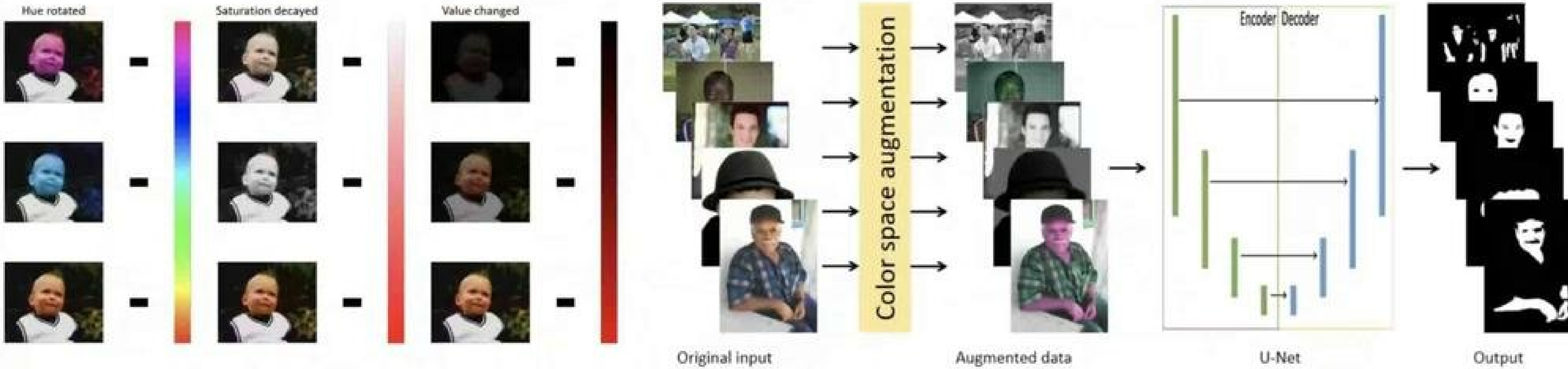

Xu, H., Sarkar, A., & Abbott, A. L. (2022). Color Invariant Skin Segmentation. In *Proceedings of the IEEE/CVF Conference on Computer Vision and Pattern Recognition* (pp. 2906-2915).

SKIN DETECTION

DEEP LEARNING BASED METHOD

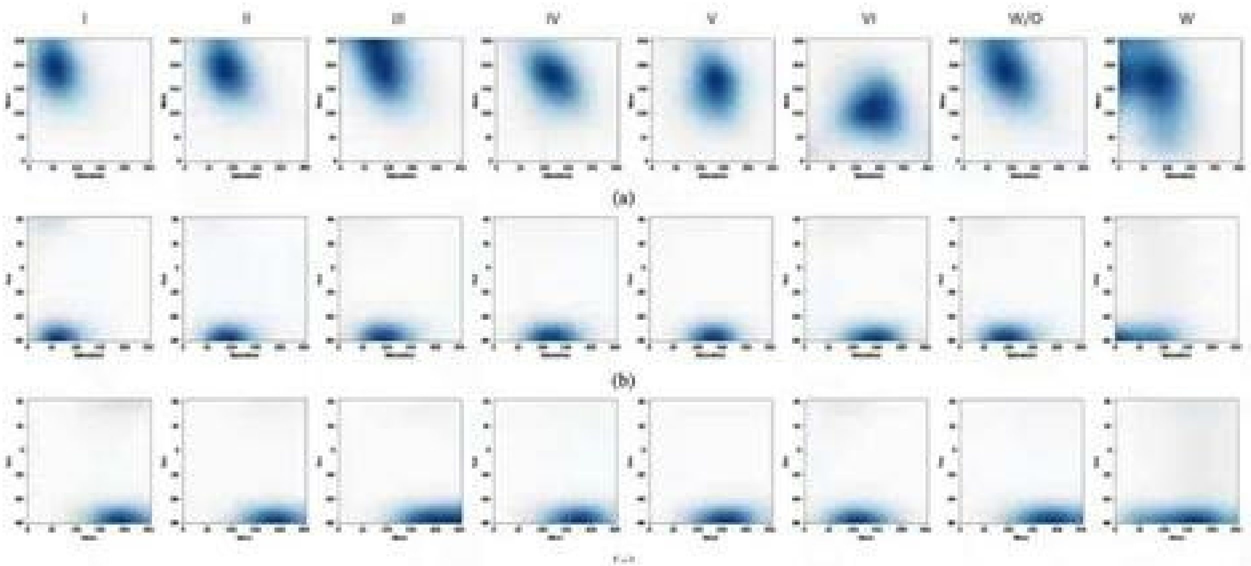

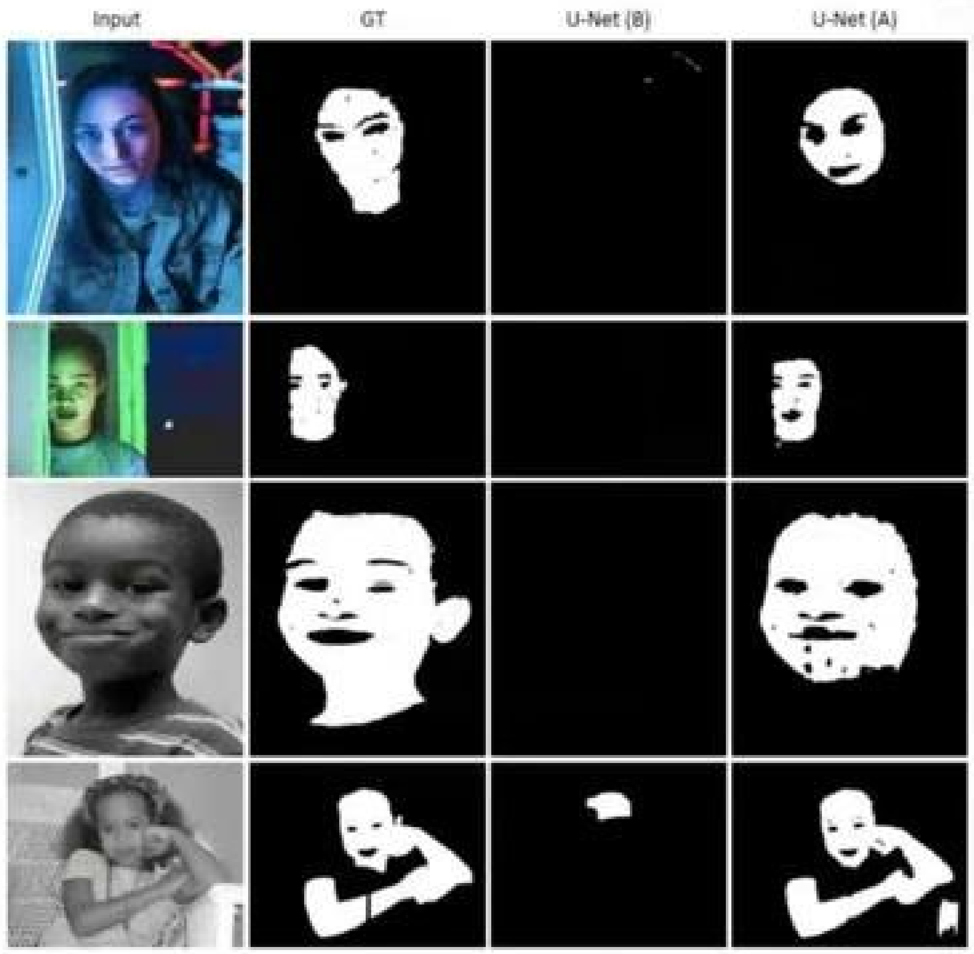

Methods	I	II	III	IV	V	VI	mix	σ
Kolkur *et al.* [24]	67.61	69.96	70.27	70.44	67.61	46.90	72.42	8.14
Dahmani *et al.* [8]	66.10	70.52	71.95	71.01	70.46	56.45	70.45	5.07
Jones *et al.* [21]	64.65	75.89	73.99	74.00	73.28	46.82	77.61	9.99
FCN before aug.	89.03	89.90	90.03	89.56	89.59	83.41	87.37	2.20
FCN after aug.	90.06	90.06	90.34	89.93	90.06	82.98	85.69	2.70
U-Net before aug.	87.16	89.58	90.38	**90.99**	**91.98**	84.72	88.82	2.29
U-Net after aug.	**90.88**	**91.34**	**91.21**	90.55	89.35	**86.05**	**89.60**	**1.84**

Xu, H., Sarkar, A., & Abbott, A. L. (2022). Color Invariant Skin Segmentation. In *Proceedings of the IEEE/CVF Conference on Computer Vision and Pattern Recognition* (pp. 2906-2915).

RESEARCH QUESTIONS FOR RPPG

- How accurately can we measure pulse rate?
- Which skin patches are useful?
- What limits the applications and how to assess them?

VALIDATION OF HRV

- HRV is the variation of RR intervals in ECG signal

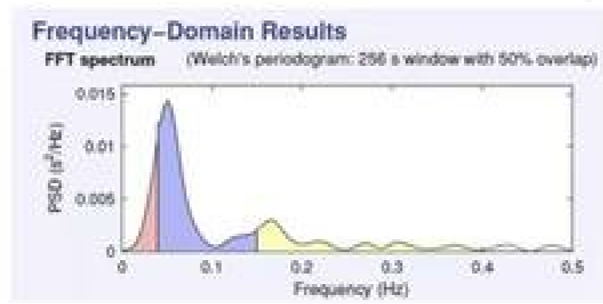

$$\frac{Area(LF)}{Area(HF)} \propto cognitive\ load$$

- We must know the accuracy of R-R measurement

VALIDATION OF HRV

- HRV is the variation of RR intervals in ECG signal

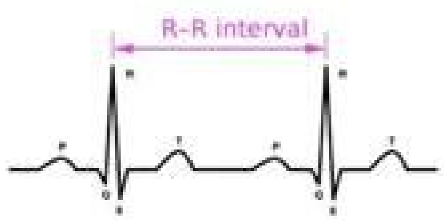

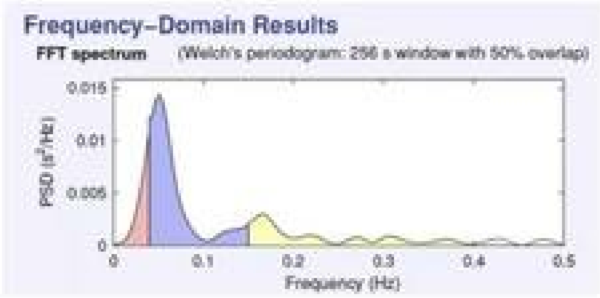

$$\frac{Area(LF)}{Area(HF)} \propto cognitive\ load$$

- We must know the accuracy of R-R measurement
- *Data collection*
  - *We have used GE S/5-Collect recorded at 100 Hz,* Video recorded at a rate of 30 fps using Canon Powershot on a tripod.

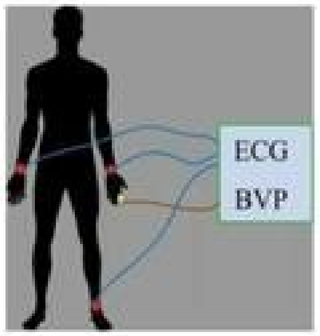

VALIDATION R-R INTERVAL

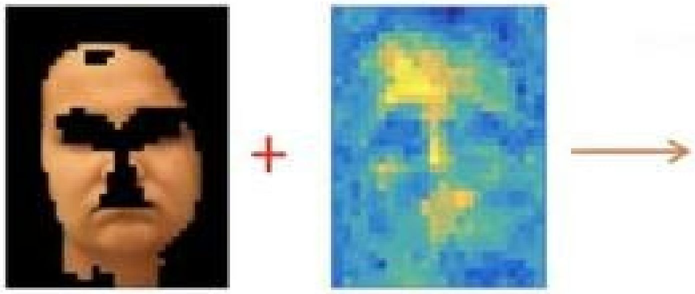

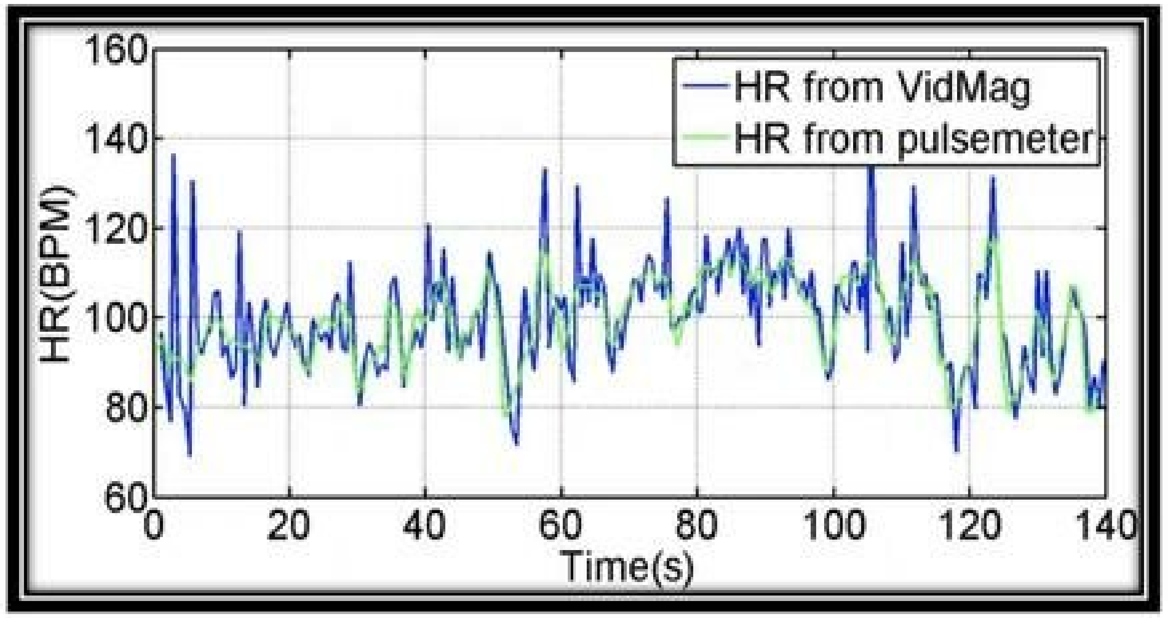

VALIDATION R-R INTERVAL

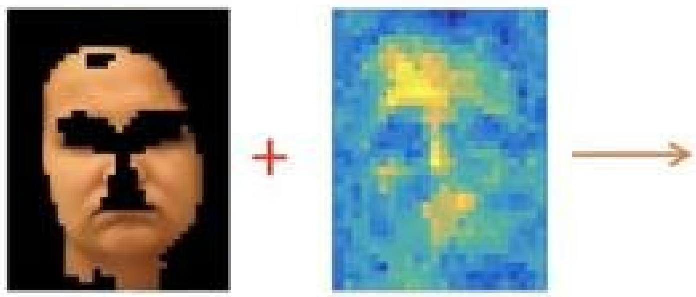

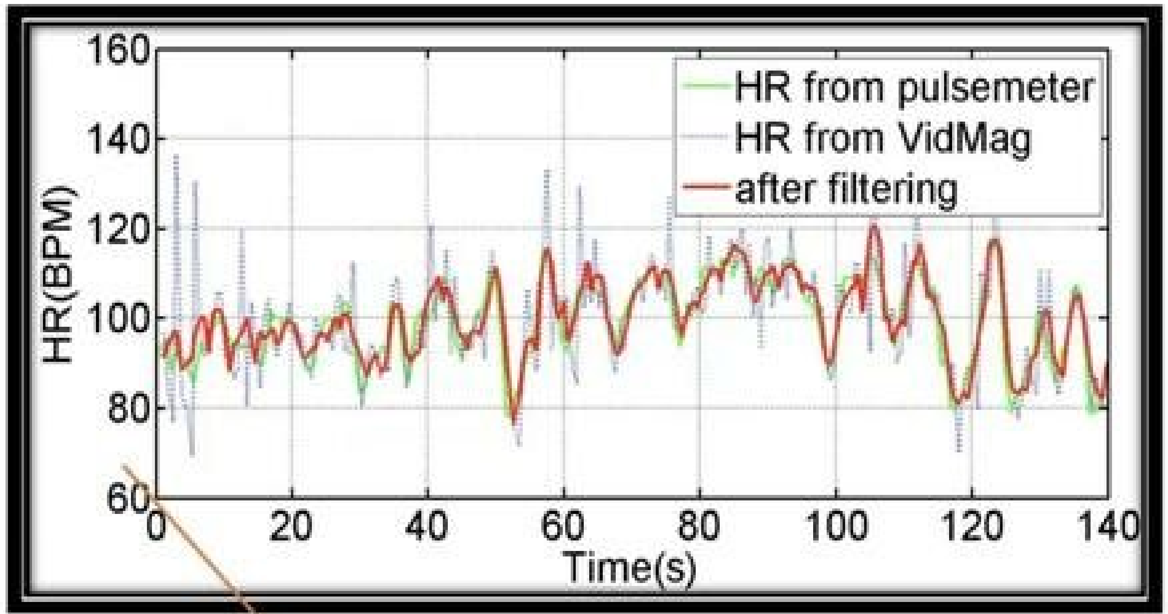

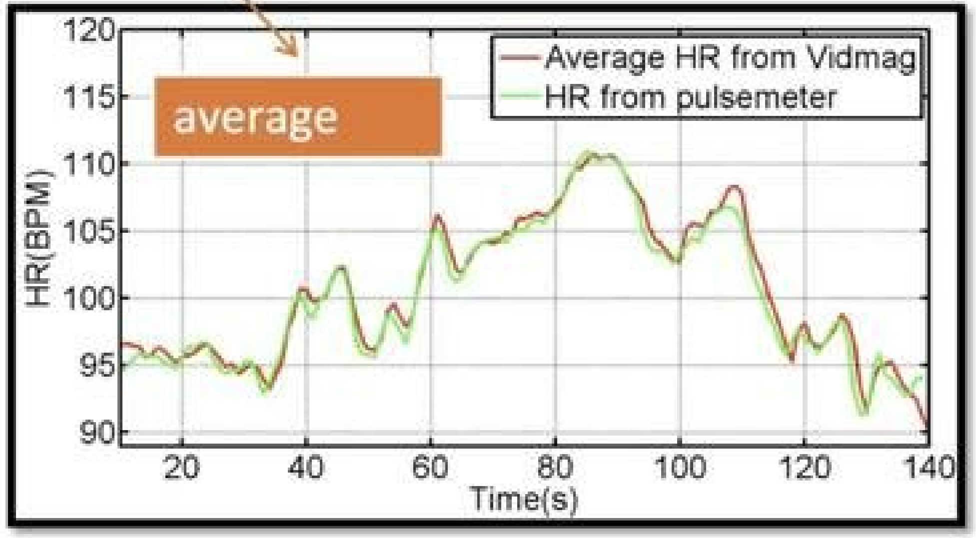

VALIDATION OF HRV

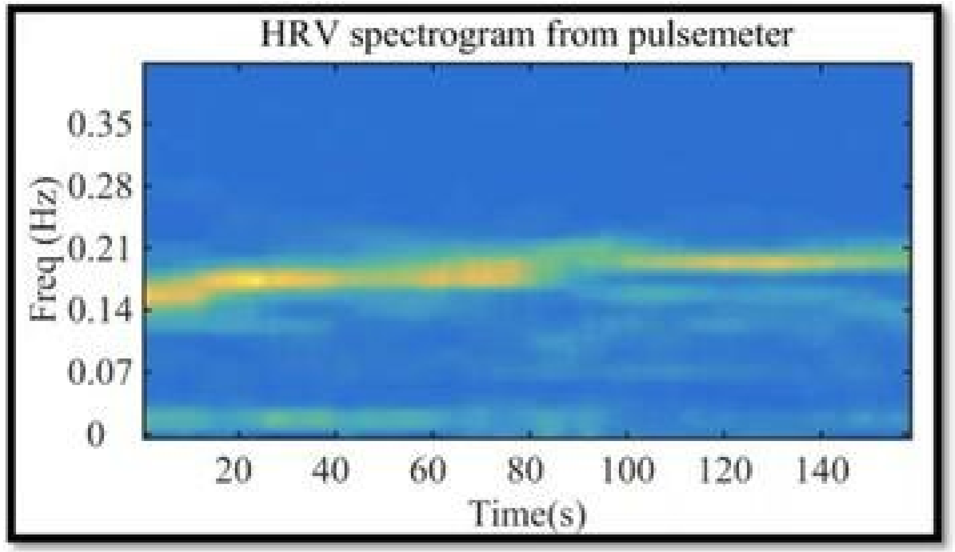

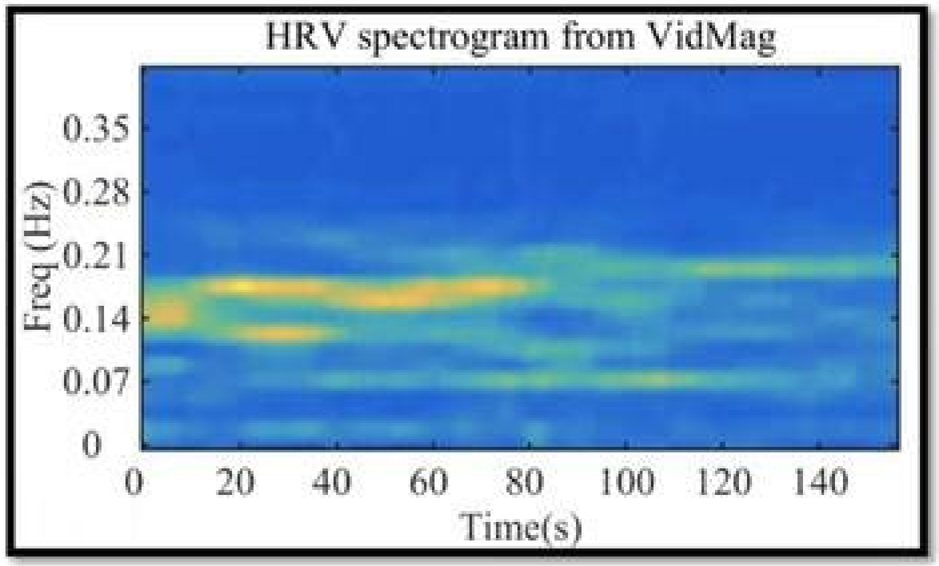

VALIDATION OF HRV

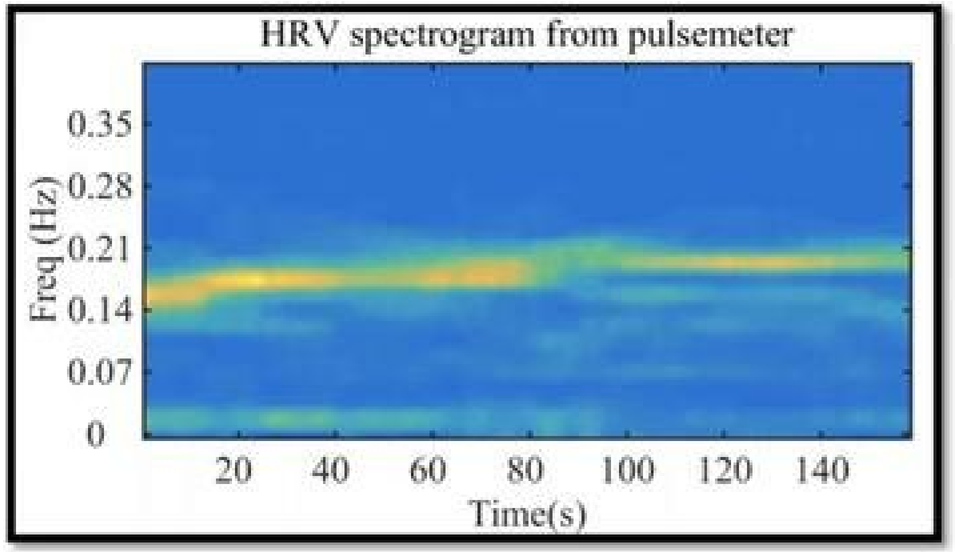

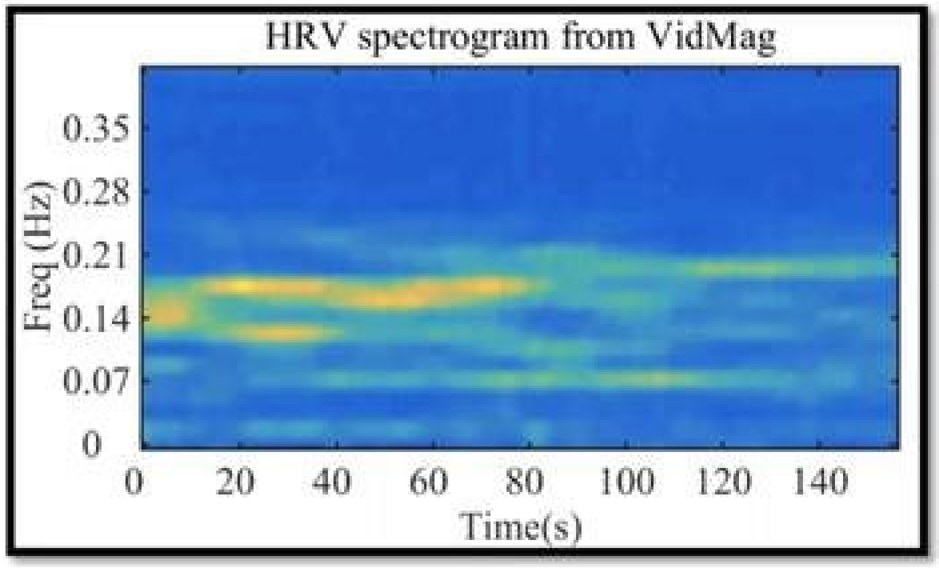

HR_{inst} $error$	**20 BPM**	**8.4 BPM**	**9.1 BPM**	**5.9 BPM**
HR_{avg} $error$	8.2 BPM	1.8 BPM	1.7 BPM	1.35 BPM

Blind Source Separation

Blind Source Separation

- Blind source separation (BSS) is the separation of a set of source signals from a set of mixed signals, without the aid of information (or with very little information) about the source signals or the mixing process.

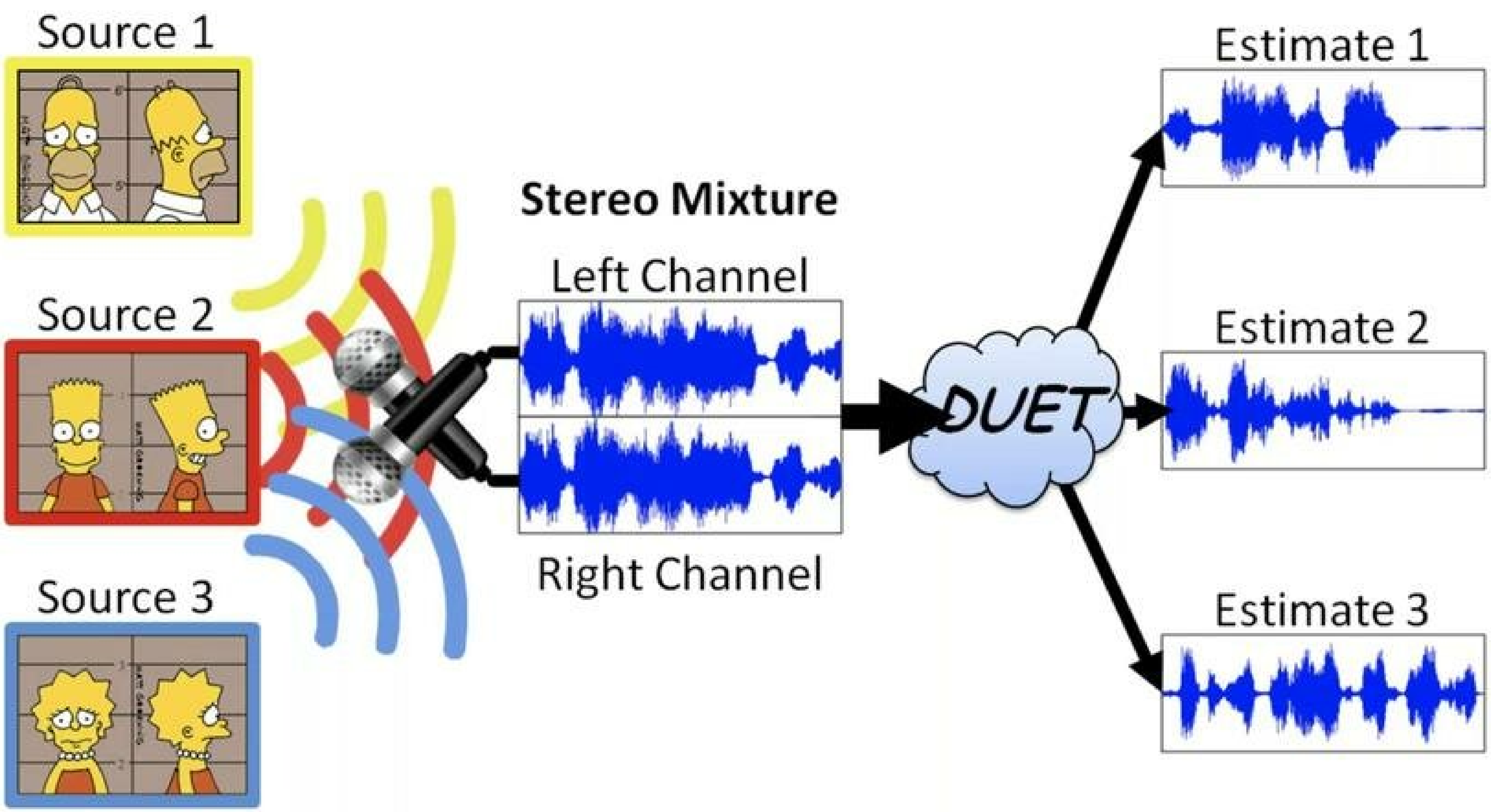
Source 1
Source 2
Source 3
Stereo Mixture
Left Channel
Right Channel
DUET
Estimate 1
Estimate 2
Estimate 3

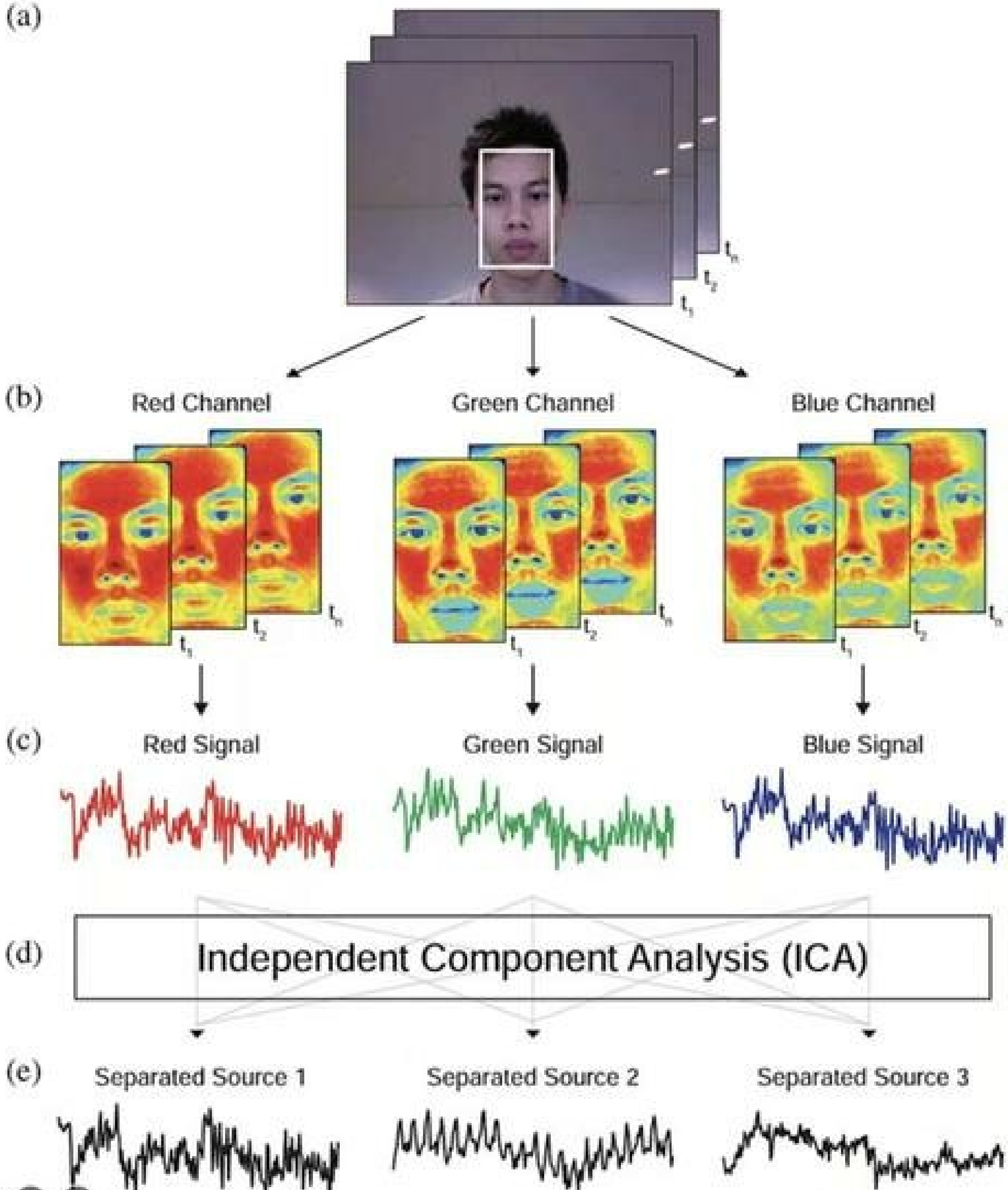

(a)
t_1
t_2
t_n
(b)
Red Channel
Green Channel
Blue Channel
(c)
Red Signal
Green Signal
Blue Signal
(d)
Independent Component Analysis (ICA)
(e)
Separated Source 1
Separated Source 2
Separated Source 3

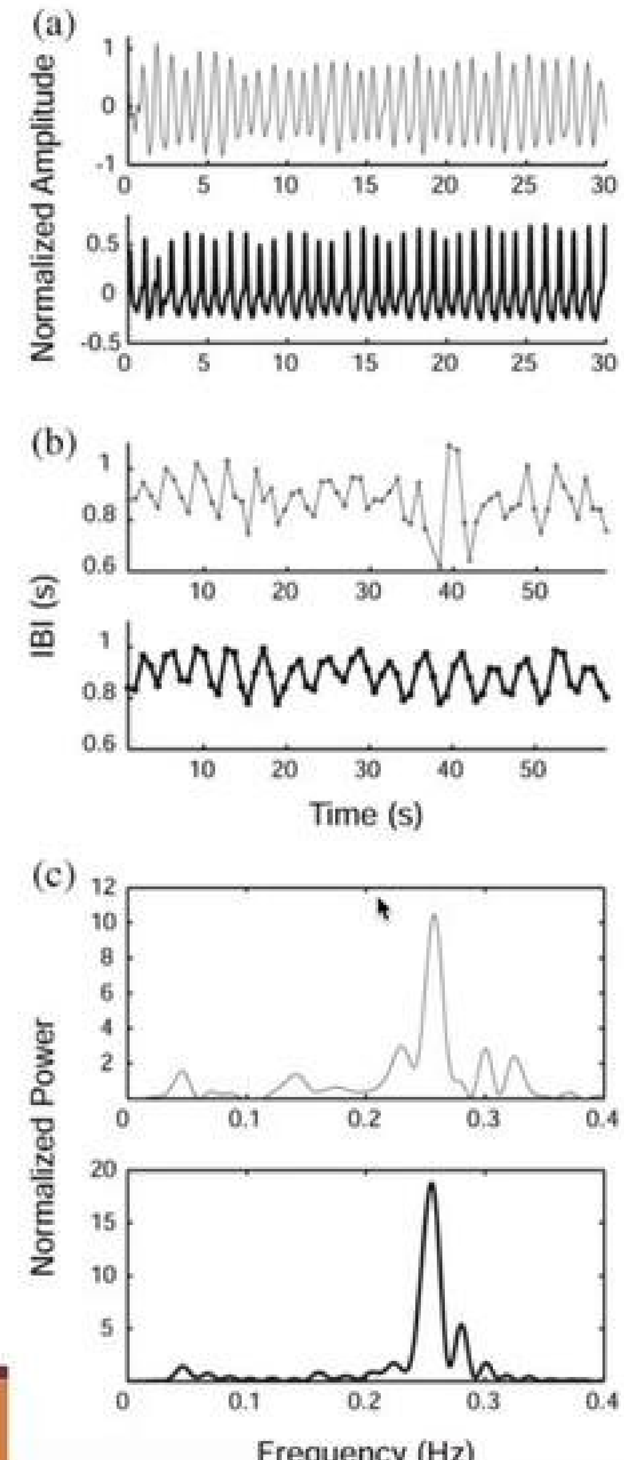

(a)
Normalized Amplitude
1
0
-1
0.5
0
-0.5
0 5 10 15 20 25 30
(b)
IBI (s)
1
0.8
0.6
10 20 30 40 50
Time (s)
(c)
Normalized Power
12 10 8 6 4 2
20 15 10 5
0 0.1 0.2 0.3 0.4
Frequency (Hz)

Five Channel Camera

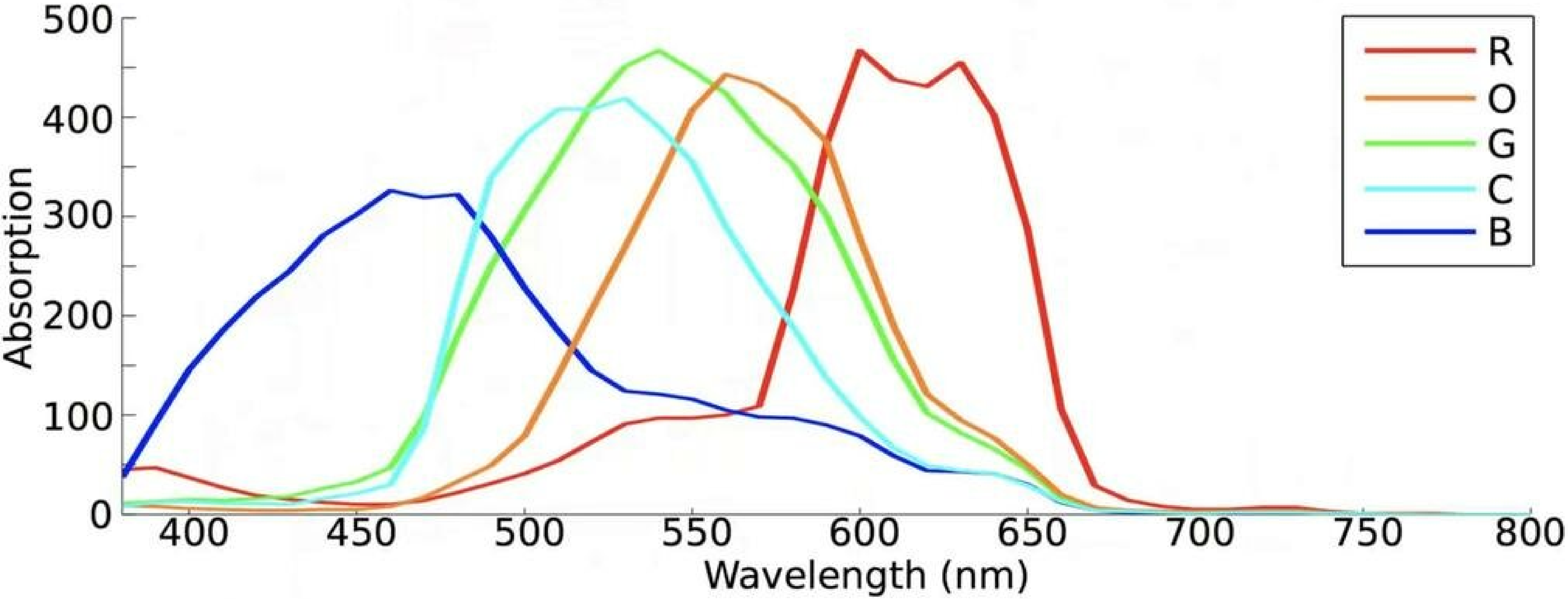

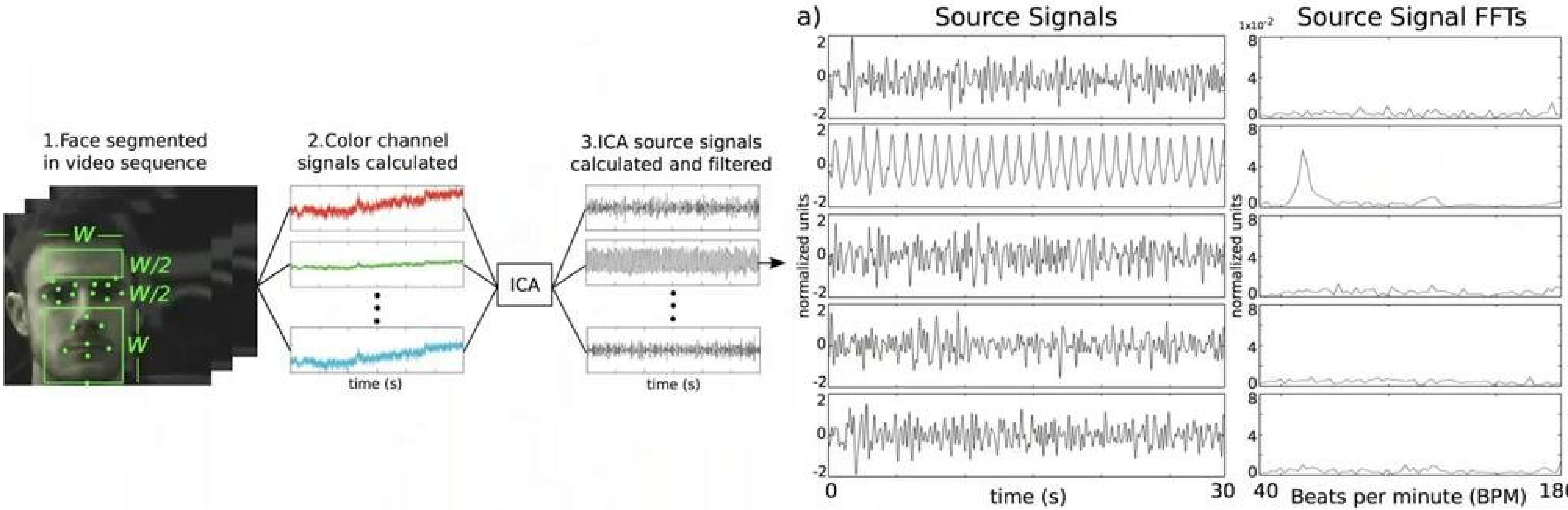

1.Face segmented in video sequence
W
W/2
W/2
W
2.Color channel signals calculated
time (s)
ICA
3.ICA source signals calculated and filtered
time (s)
a)
Source Signals
Source Signal FFTs
normalized units
time (s)
Beats per minute (BPM)

	HR	BR	LF	HF	LF/HF
R	0.99	0.95	0.60	0.60	0.57
G	0.99	0.91	0.63	0.63	0.63
B	0.99	0.93	0.68	0.68	0.70
C	0.85	0.44	0.64	0.64	0.64
O	0.83	-0.02	0.43	0.43	0.34
RG	0.97	0.66	0.72	0.72	0.74
RB	0.95	0.89	0.47	0.47	0.47
RC	0.99	0.67	0.69	0.69	0.73
RO	1.00	0.93	0.88	0.88	0.89
GB	0.89	0.75	0.44	0.44	0.44
GC	0.99	0.83	0.82	0.82	0.82
GO	1.00	0.98	0.88	0.88	0.88
BC	0.99	0.68	0.61	0.61	0.65
BO	1.00	0.92	0.87	0.87	0.87
CO	0.99	0.67	0.40	0.40	0.48
RGB	0.85	0.67	0.45	0.45	0.46
RGC	0.99	0.75	0.67	0.67	0.71
RGO	1.00	0.92	0.83	0.83	0.86
RBC	0.99	0.69	0.71	0.71	0.68
RBO	1.00	0.92	0.83	0.83	0.83
RCO	1.00	0.90	0.91	0.91	0.89
GBC	0.99	0.77	0.80	0.80	0.78
GBO	1.00	0.93	0.84	0.84	0.83
GCO	1.00	0.93	0.93	0.93	0.93
BCO	0.99	0.84	0.69	0.69	0.77
RGBC	0.99	0.89	0.72	0.72	0.68
RGBO	1.00	0.81	0.79	0.79	0.81
RGCO	1.00	0.90	0.87	0.87	0.86
RBCO	1.00	0.90	0.81	0.81	0.77
GBCO	1.00	0.72	0.83	0.83	0.80
RGBCO	1.00	0.74	0.81	0.81	0.79

Lowest $\overline{r}$
O
RGB
CO
GB
C
RB
BC
R
RC
RBC
G
RGC
RG
BCO
B
RGBC
GBC
RGBCO
GBCO
RGBO
GC
RBCO
RBO
GBO
RGO
RGCO
BO
RO
RCO
GO
GCO
Highest $\overline{r}$

Recorded green channel

PPG component from green channel

Background

$$\boldsymbol{g}_{\text{face}} = \boldsymbol{s} + \boldsymbol{y}$$

Component from Ambient Light

$$\boldsymbol{y} \approx h\boldsymbol{g}_{\text{bg}}$$

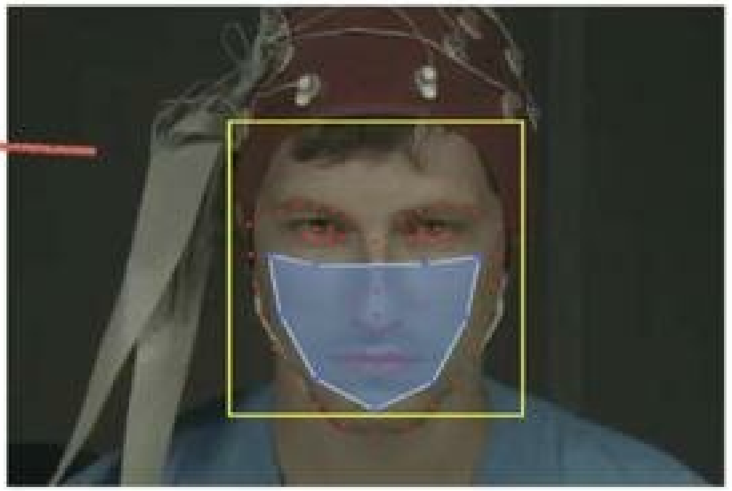

Recorded green channel

PPG component
from green channel

Component from Ambient Light

$$\boldsymbol{g}_{\text{face}} = \boldsymbol{s} + \boldsymbol{y}$$

$$\boldsymbol{y} \approx h\boldsymbol{g}_{\text{bg}}$$

Background

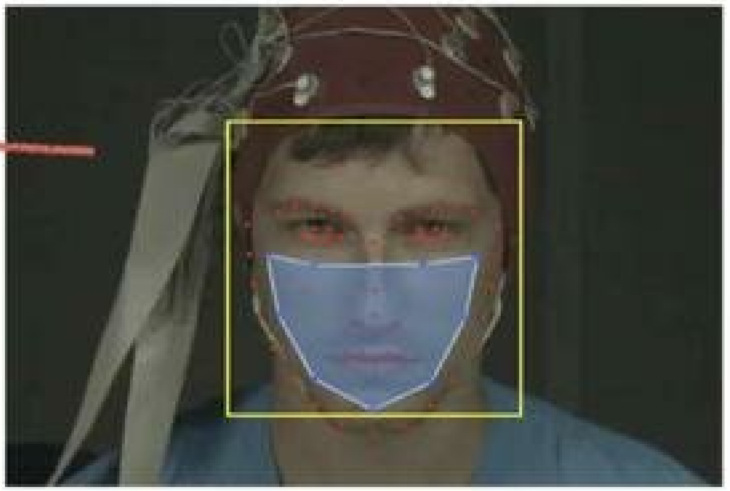

Illumination Rectified

$$\boldsymbol{g}_{\text{IR}} = \boldsymbol{g}_{\text{face}} - h\boldsymbol{g}_{\text{bg}}$$

$$\boldsymbol{g}_{\text{IR}} = \boldsymbol{s} + (\boldsymbol{y} - h\boldsymbol{g}_{\text{bg}})$$

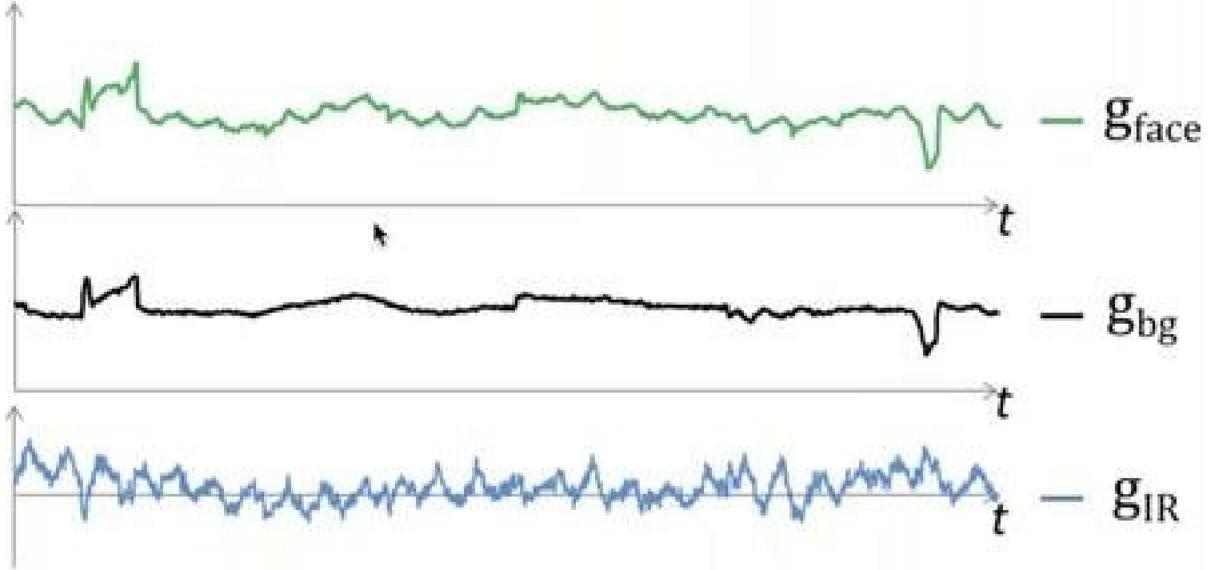

PATCH SELECTION

EFFECT OF ILLUMINATION

INFORMATION FROM EACH PATCH

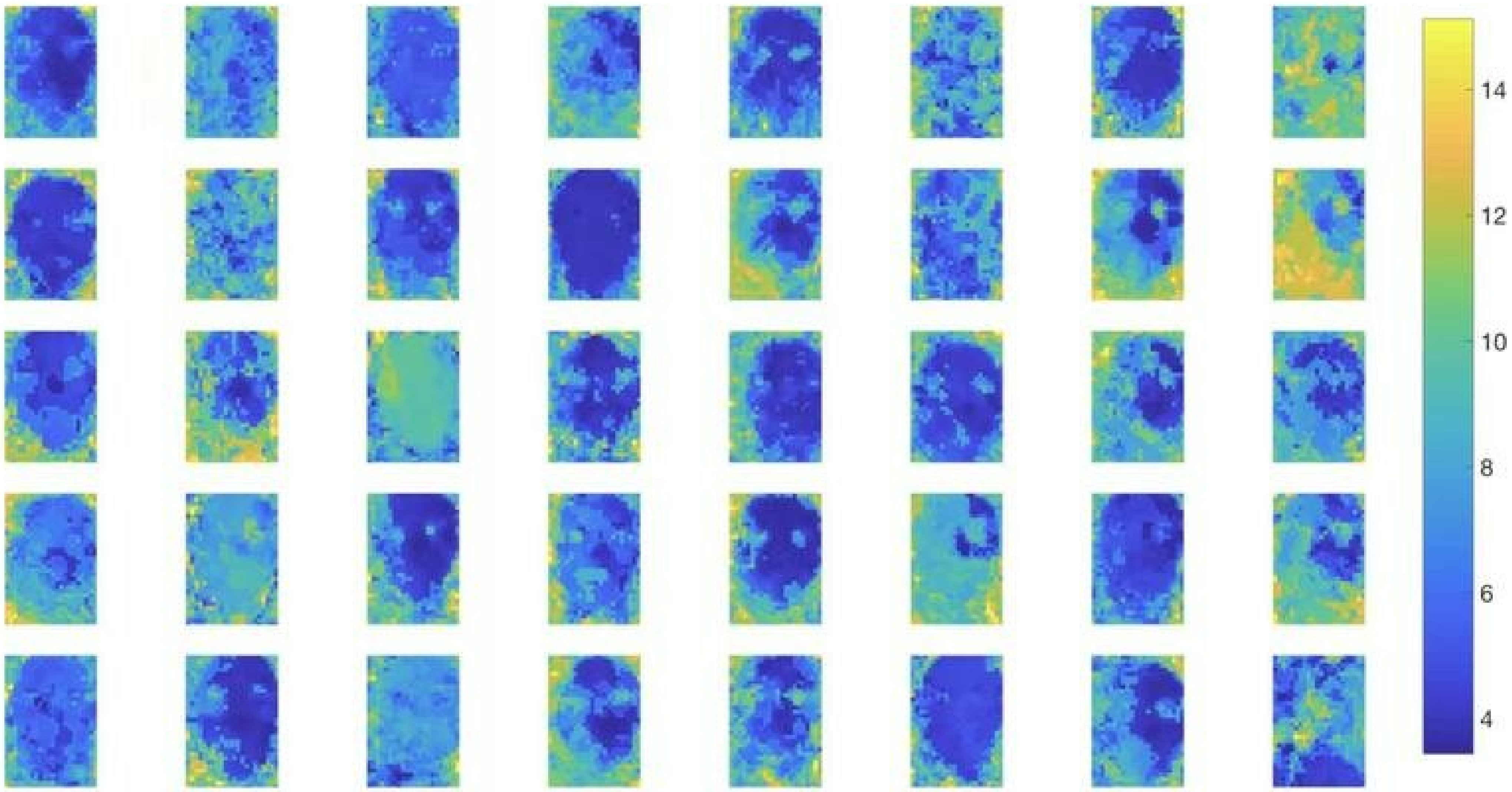

GOOD PATCH – BAD PATCH

- Heart rate is natural so tend to show normal distribution.
- We use this characteristics to compute entropy of the power spectrum.

Good patch

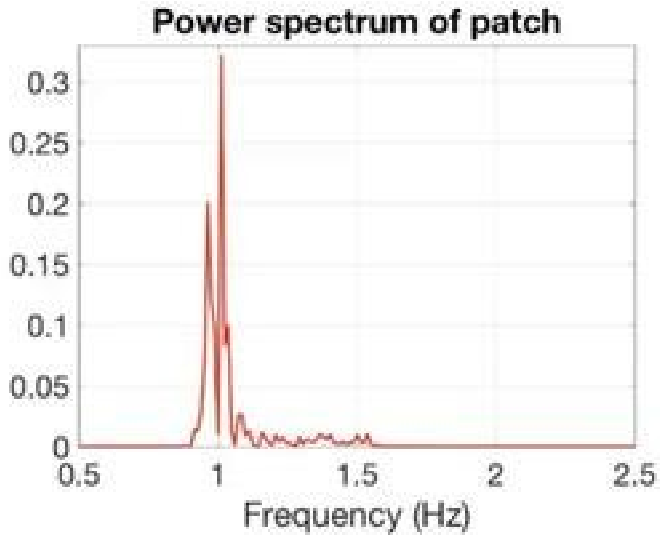

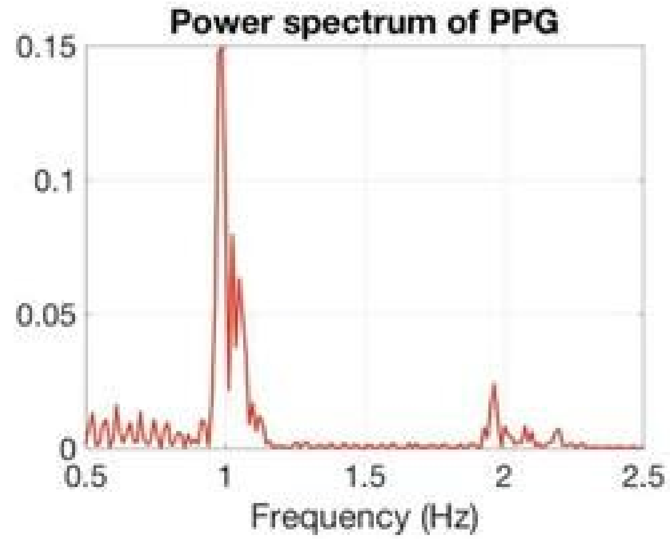

Bad patch

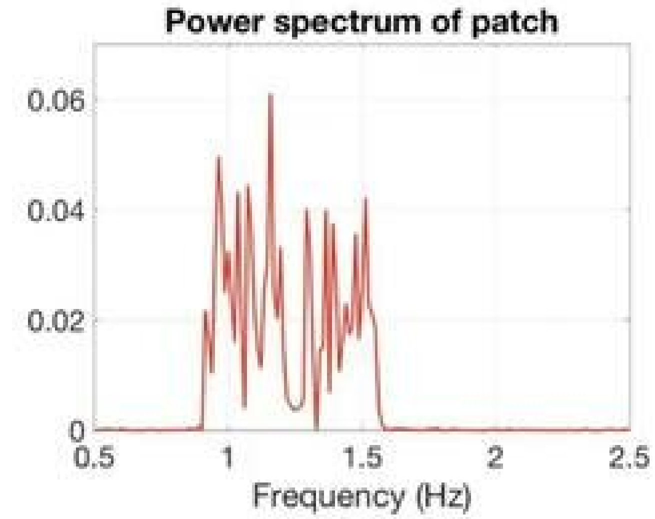

UNSUPERVISED RELATIVE PATCH WEIGHT

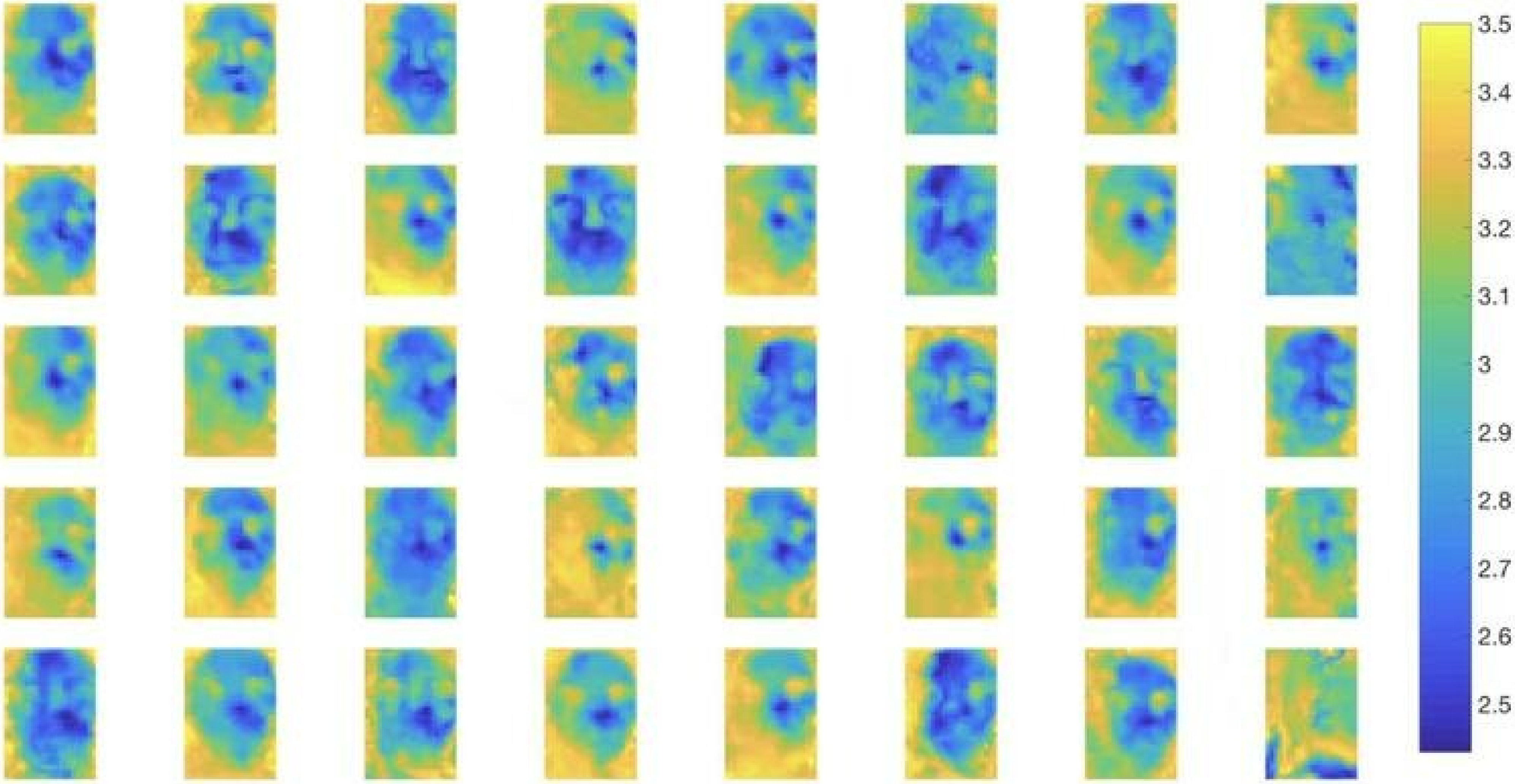

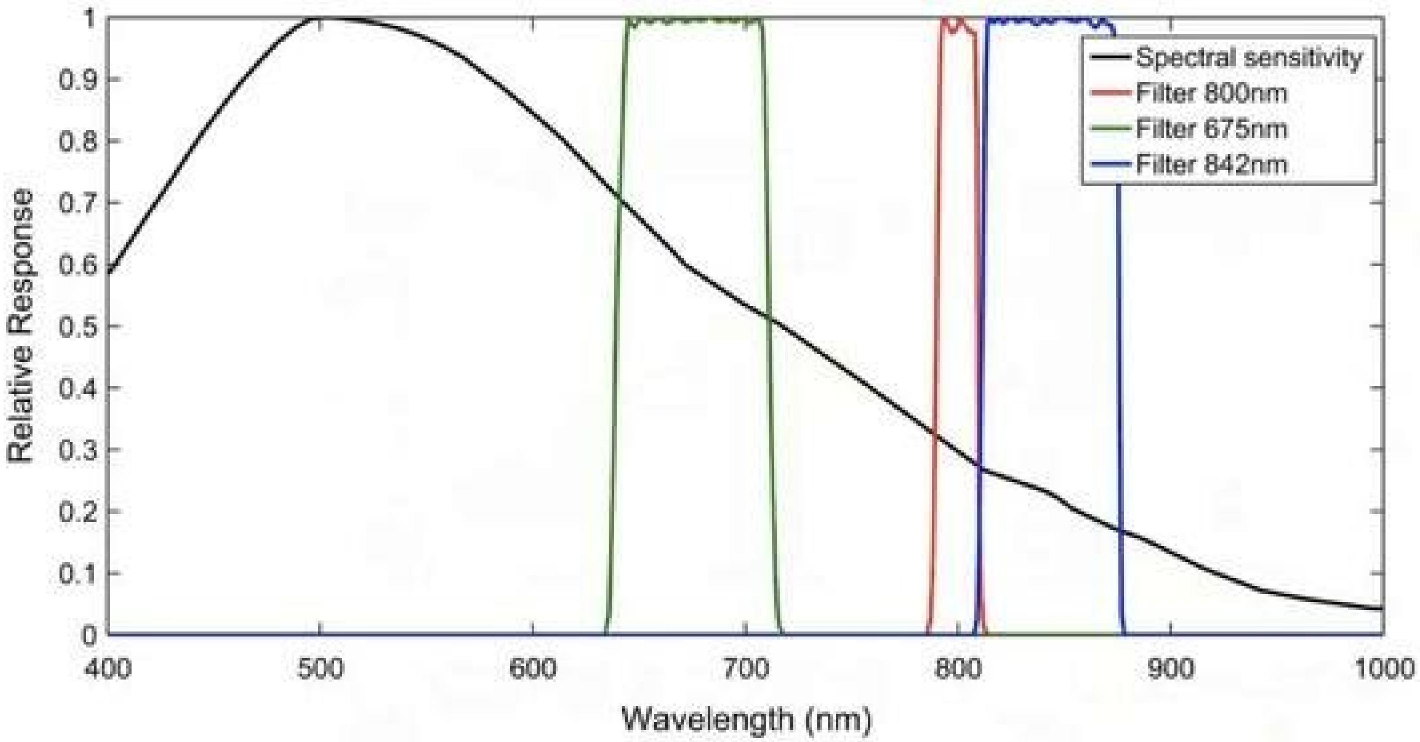

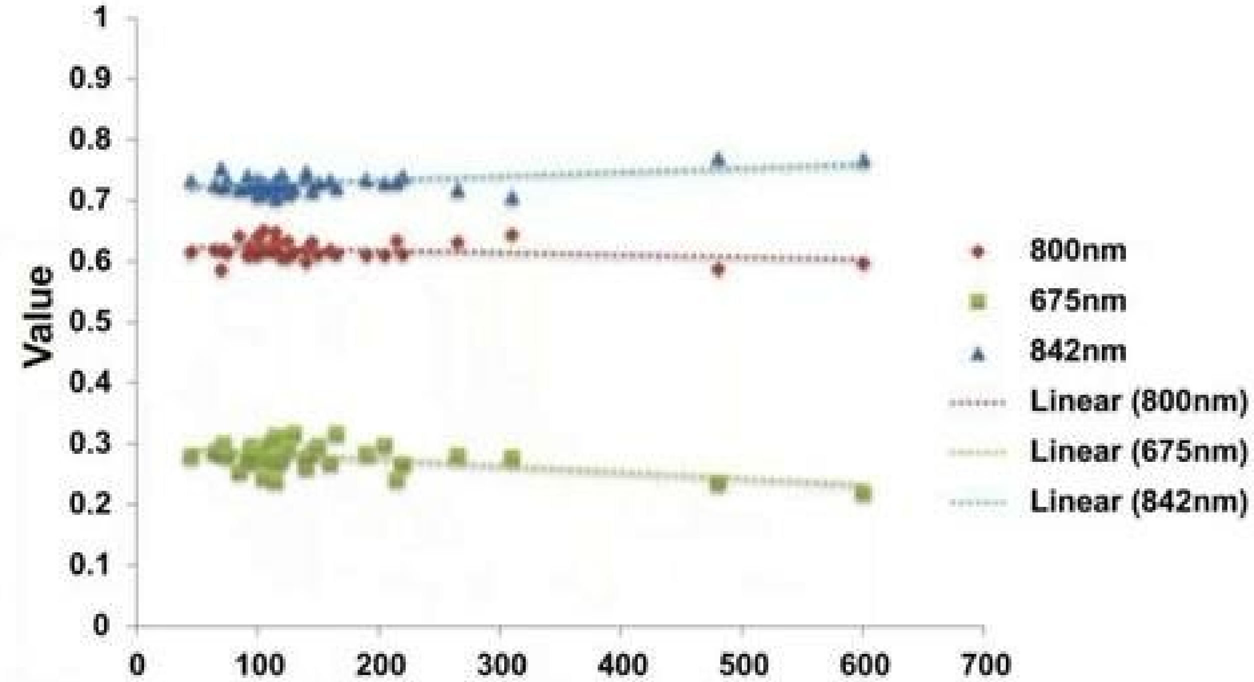

$$\vec{P}_{\mathrm{bv}} = [0.61, \quad 0.29, \quad 0.74]$$

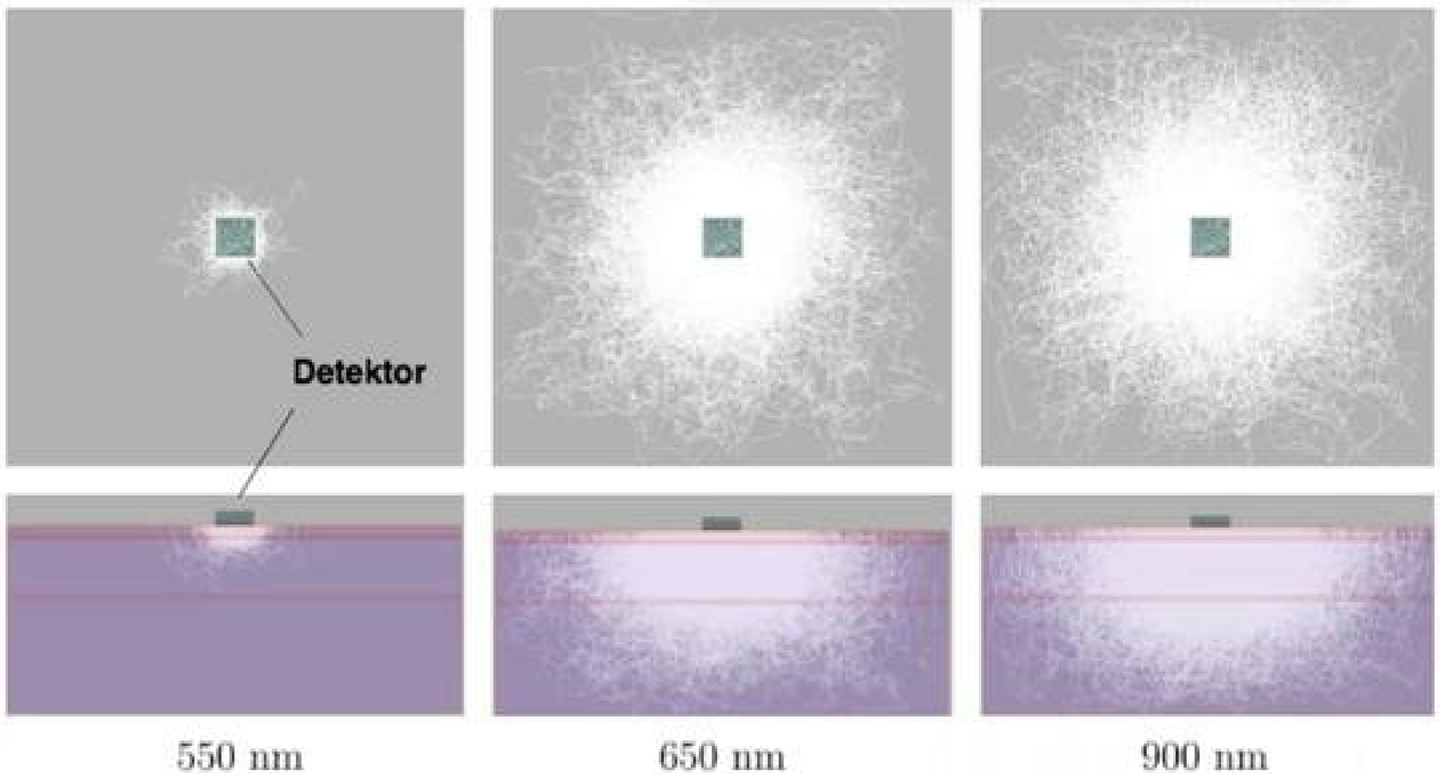
Detektor
550 nm
650 nm
900 nm

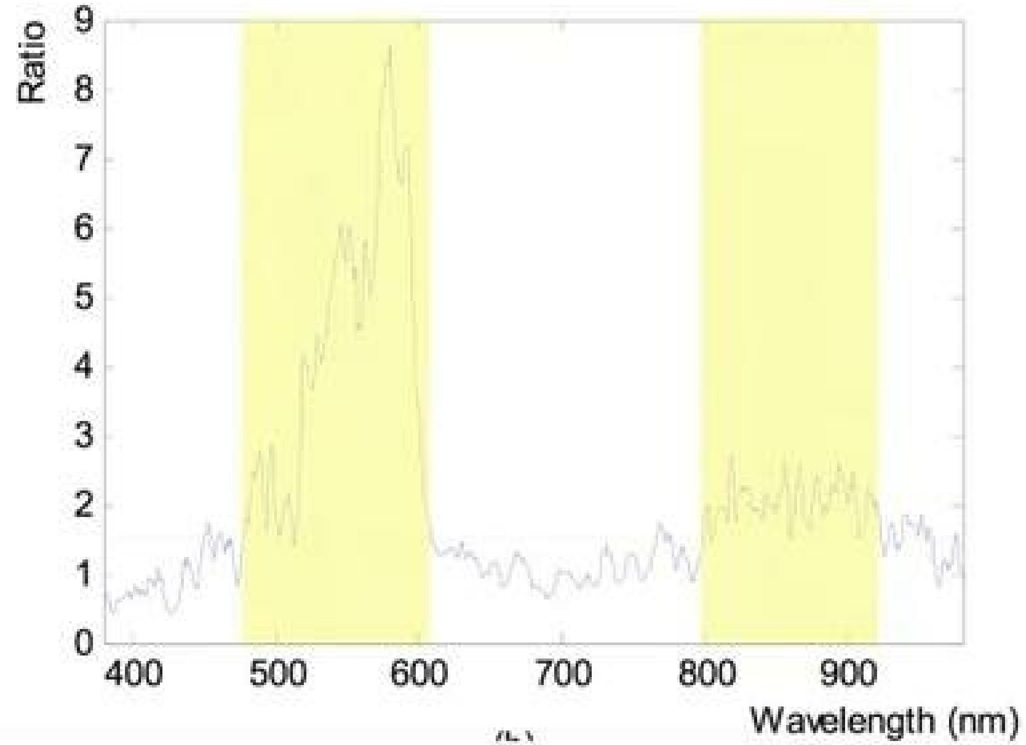
Ratio
0
1
2
3
4
5
6
7
8
9
400
500
600
700
800
900
Wavelength (nm)

DEEP LEARNING?

- What is a neural network?
- What is deep neural network?
- What is convolutional neural network and how it is used for object detection?
- Difference with traditional machine learning
  - Big data driven
  - Millions of parameters
  - High performance in speed and accuracy
  - Less interpretability

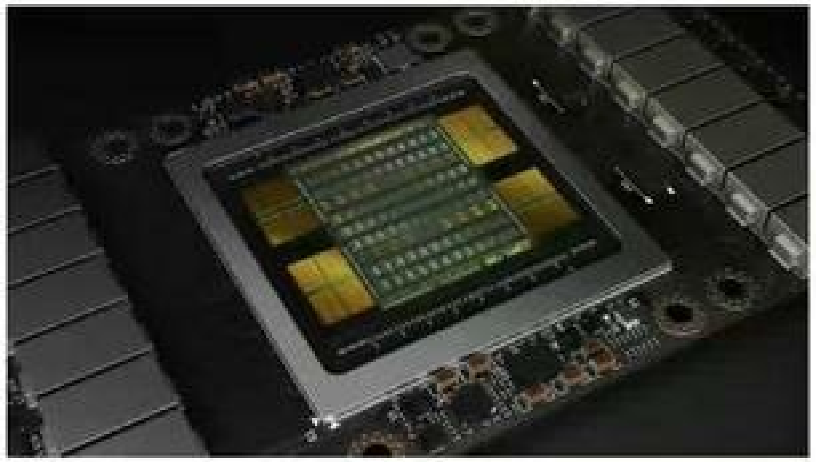

MLP VS CNN

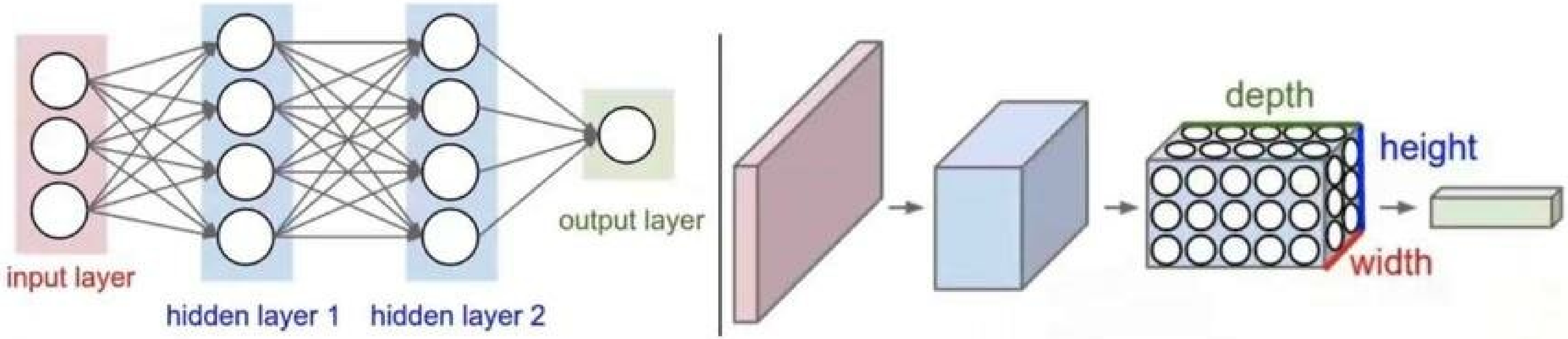

Left: A regular 3-layer Neural Network. Right: A ConvNet arranges its neurons in three dimensions (width, height, depth), as visualized in one of the layers. Every layer of a ConvNet transforms the 3D input volume to a 3D output volume of neuron activations. In this example, the red input layer holds the image, so its width and height would be the dimensions of the image, and the depth would be 3 (Red, Green, Blue channels).

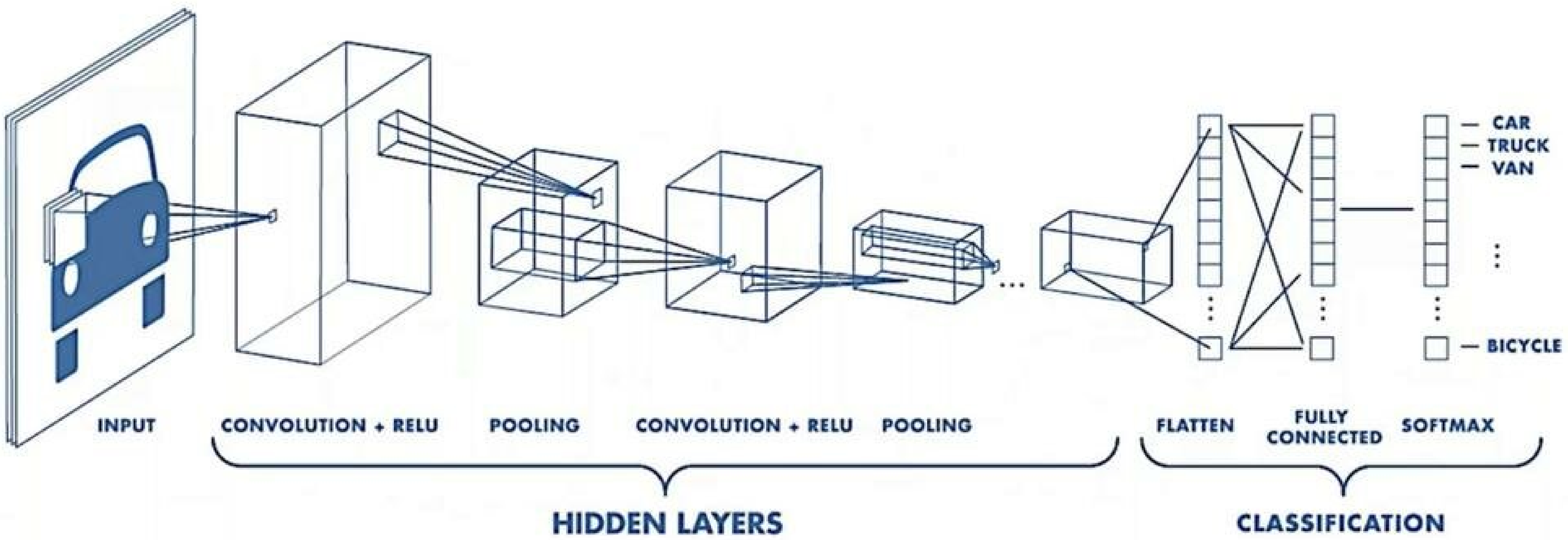

CAR
TRUCK
VAN
BICYCLE
INPUT
CONVOLUTION + RELU
POOLING
CONVOLUTION + RELU
POOLING
FLATTEN
FULLY CONNECTED
SOFTMAX
HIDDEN LAYERS
CLASSIFICATION

RHYTHMNET

- Paper: End-to-end Heart Rate Estimation from Face via Spatial-temporal Representation (link)

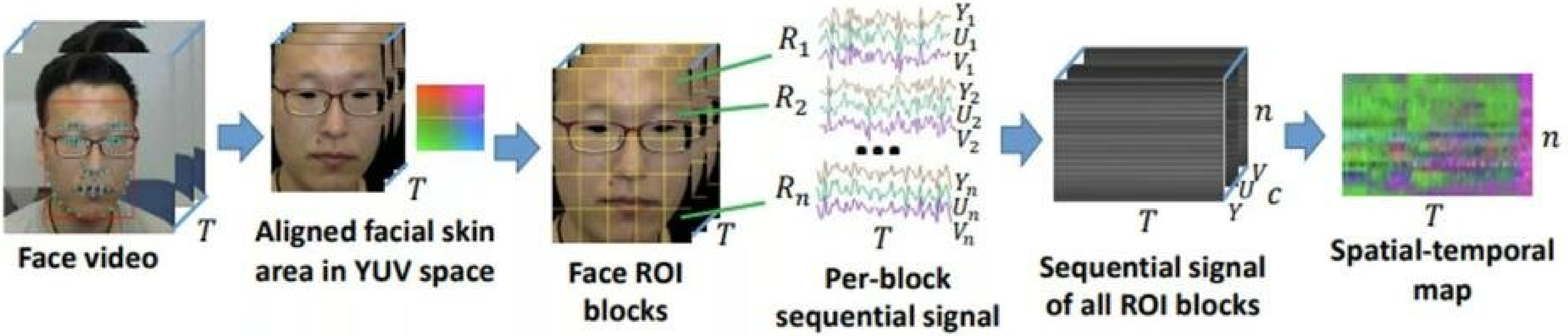

Niu, X., Shan, S., Han, H., & Chen, X. (2019). Rhythmnet: End-to-end heart rate estimation from face via spatial-temporal representation. *IEEE Transactions on Image Processing*, *29*, 2409-2423.

RHYTHMNET

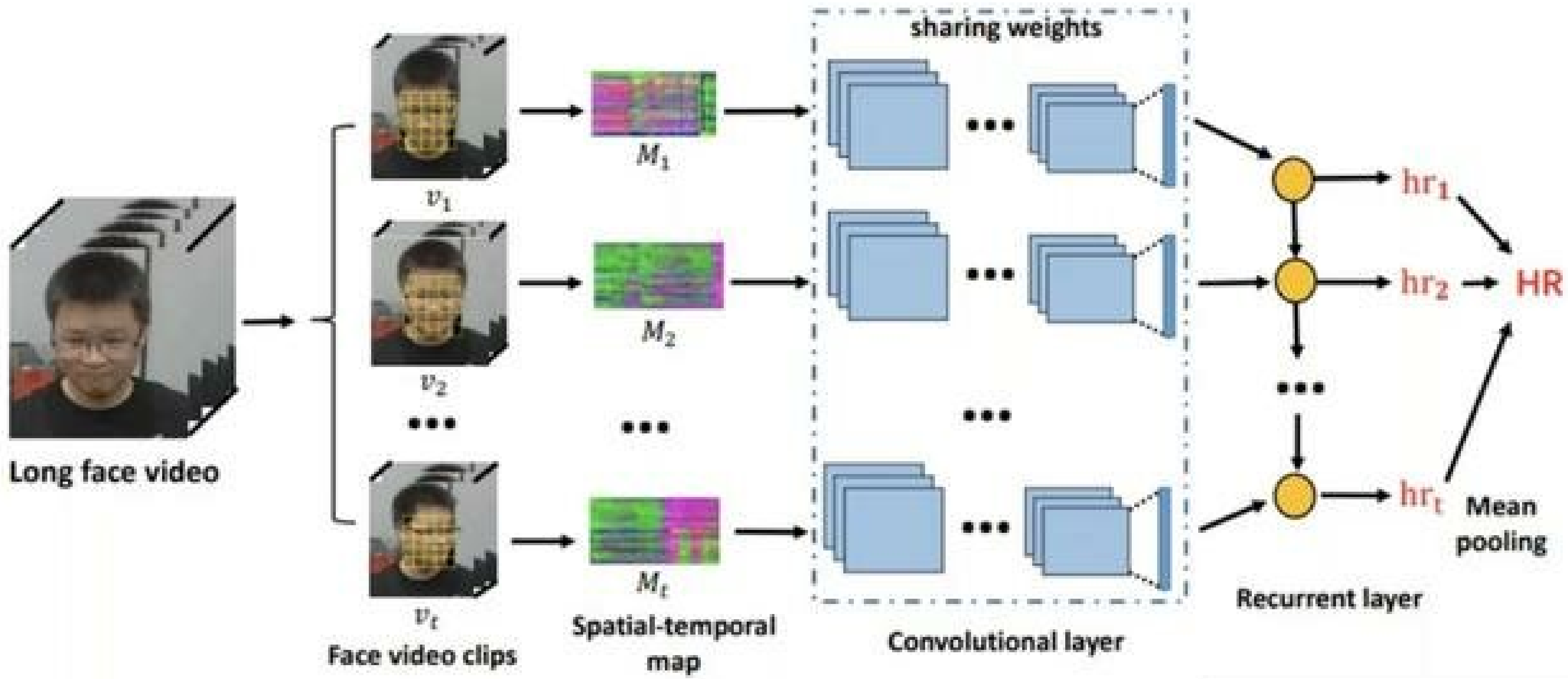

Method	Mean (bpm)	Std (bpm)	MAE (bpm)	RMSE (bpm)	MER	r
Tulyakov2016 [6]	10.8	18.0	15.9	21.0	26.7%	0.11
POS [7]	7.87	15.3	11.5	17.2	18.5%	0.30
Haan2013 [4]	7.63	15.1	11.4	16.9	17.8%	0.28
I3D [38]	1.37	15.9	12.0	15.9	15.6%	0.07
DeepPhy [26]	-2.60	13.6	11.0	13.8	13.6%	0.11
RhythmNet w/o GRU	1.02	8.88	5.79	8.94	7.38%	0.73
RhythmNet	**0.73**	**8.11**	**5.30**	**8.14**	**6.71%**	**0.76**

Niu, X., Shan, S., Han, H., & Chen, X. (2019). Rhythmnet: End-to-end heart rate estimation from face via spatial-temporal representation. *IEEE Transactions on Image Processing*, *29*, 2409-2423.

DEEPPHYS

- Attention
- Temporal patterns
- Signal recovery

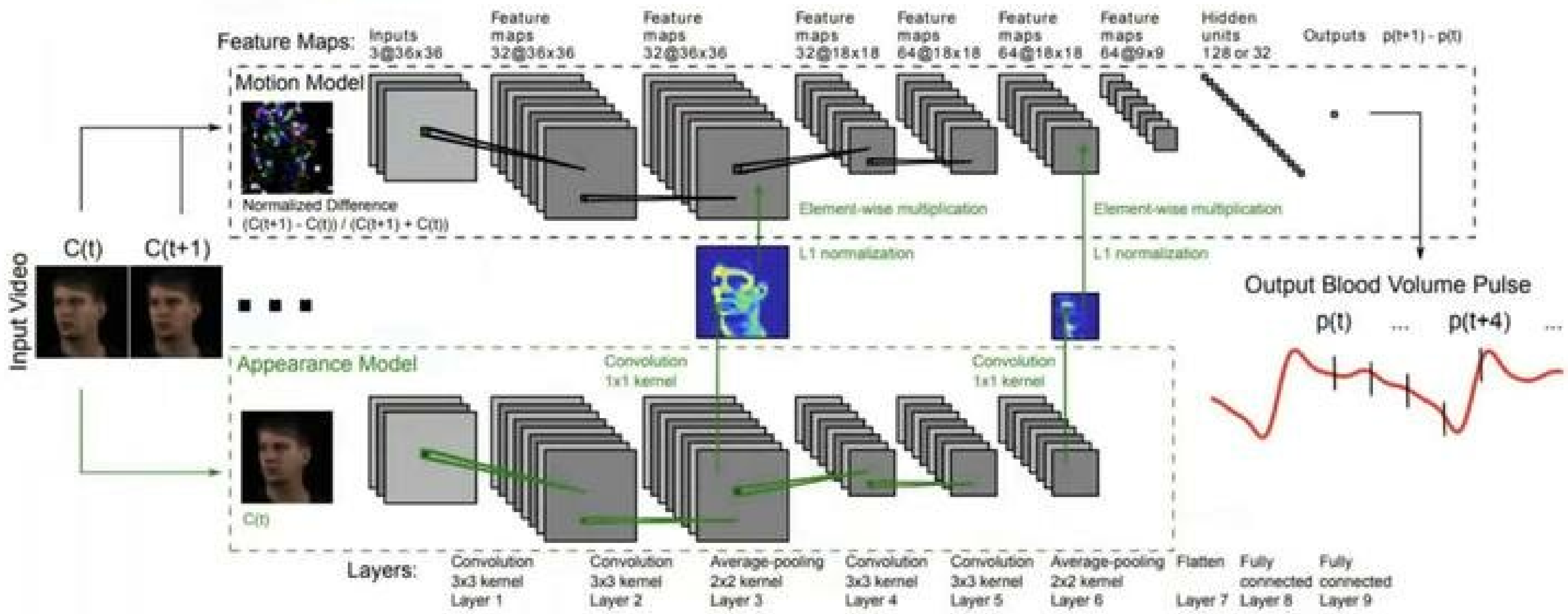

Chen, W., & McDuff, D. (2018). Deepphys: Video-based physiological measurement using convolutional attention networks. In *Proceedings of the european conference on computer vision (ECCV)* (pp. 349-365).

PPG FROM MULTIPLE SITES

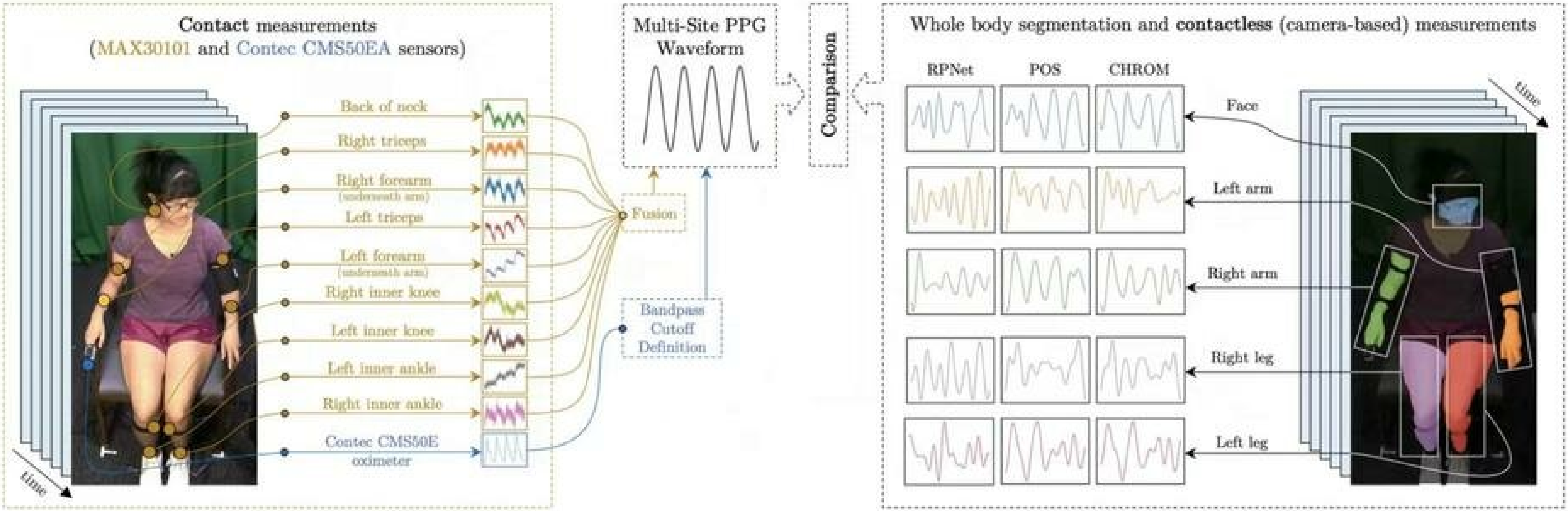

Niu, L., Speth, J., Vance, N., Sporrer, B., Czajka, A., & Flynn, P. (2023). Full-Body Cardiovascular Sensing with Remote Photoplethysmography. In *Proceedings of the IEEE/CVF Conference on Computer Vision and Pattern Recognition* (pp. 5993-6003).

PPG FROM MULTIPLE SITES

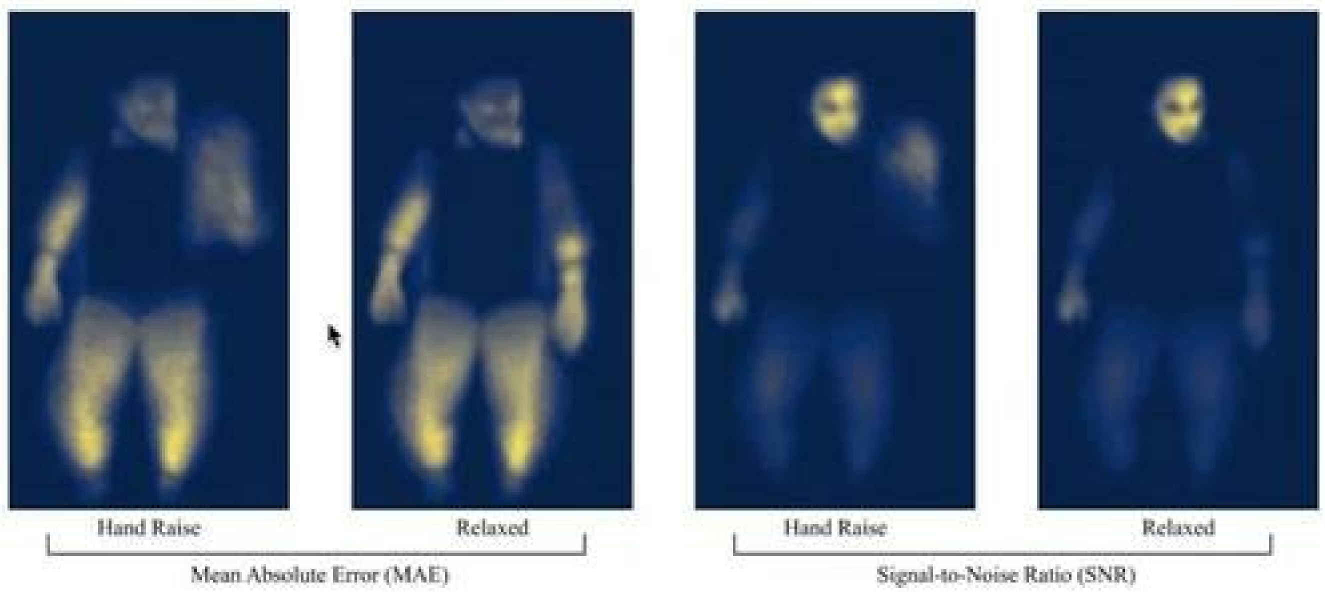

Methods	Both relaxed and hand raise										Relaxed		Hand raise			
	Face		Right leg		Left leg		Right arm		Left arm		Left arm		Left arm		Palm	
	MAE (bpm)	r	MAE (bpm)	r	MAE (bpm)	r	MAE (bpm)	r	MAE (bpm)	r	MAE (bpm)	r	MAE (bpm)	r	MAE (bpm)	r
CHROM [9]	2.38	0.85	10.92	0.42	11.07	0.41	9.13	0.50	9.81	0.41	11.57	0.35	4.26	0.71	5.01	0.67
POS [44]	**1.38**	**0.93**	**6.96**	**0.54**	**7.11**	**0.54**	**3.60**	**0.78**	**6.04**	**0.64**	**6.88**	**0.61**	**3.40**	**0.75**	**3.88**	**0.76**
RPNet [36]	2.27	0.87	29.50	0.14	30.42	0.11	23.94	0.15	23.15	0.16	27.01	0.11	11.06	0.38	6.70	0.52

Niu, L., Speth, J., Vance, N., Sporrer, B., Czajka, A., & Flynn, P. (2023). Full-Body Cardiovascular Sensing with Remote Photoplethysmography. In *Proceedings of the IEEE/CVF Conference on Computer Vision and Pattern Recognition* (pp. 5993-6003).

PPG FROM MULTIPLE SITES

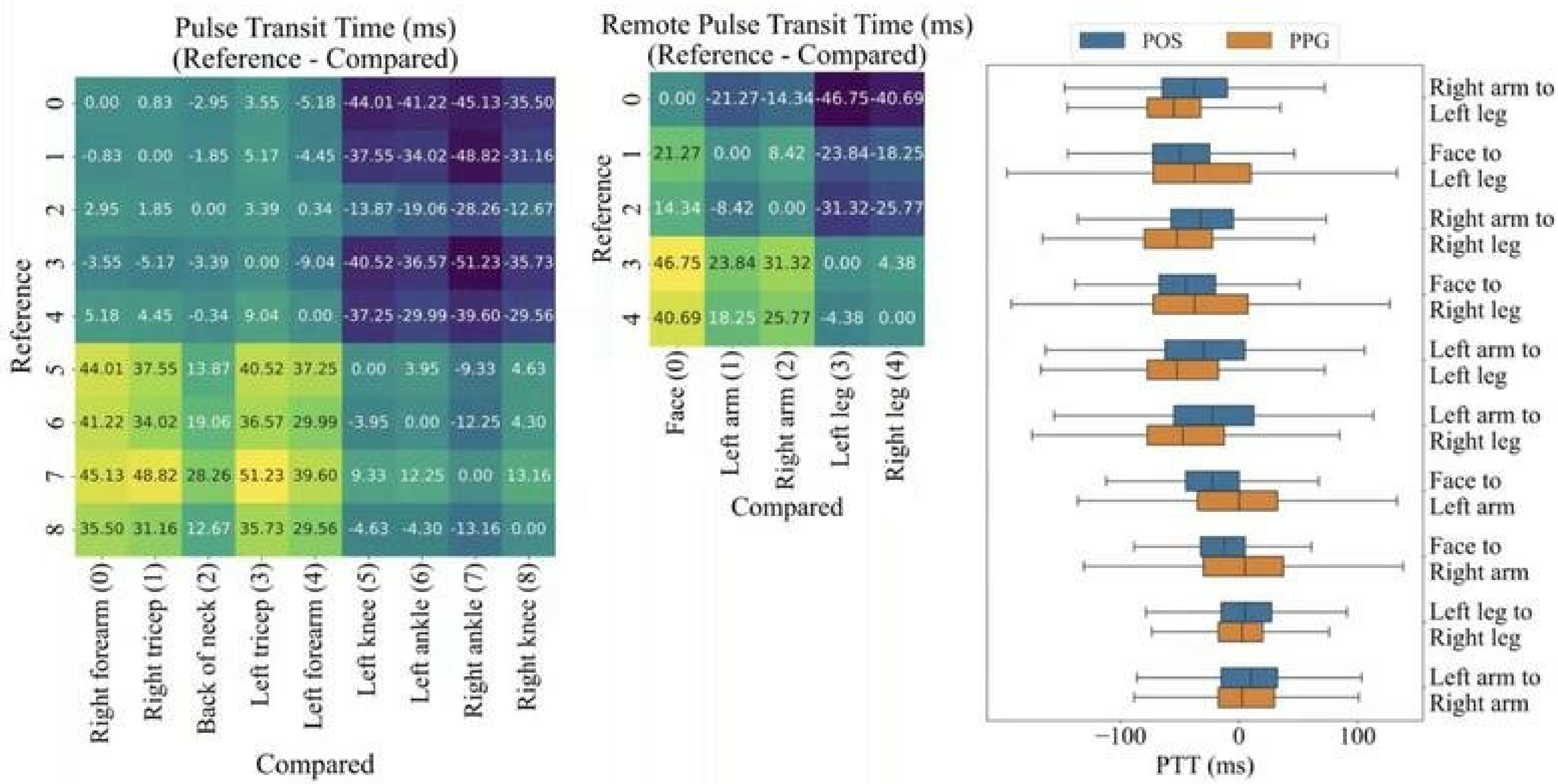

Niu, L., Speth, J., Vance, N., Sporrer, B., Czajka, A., & Flynn, P. (2023). Full-Body Cardiovascular Sensing with Remote Photoplethysmography. In *Proceedings of the IEEE/CVF Conference on Computer Vision and Pattern Recognition* (pp. 5993-6003).

SKIN PERFUSION MAP

- Skin perfusion during regional anesthesia
- Biophotonics Laboratory of the Institute of Atomic Physics and Spectroscopy (IAPS), University of Latvia.
- Patients undergoing hand surgery received ultrasound-guided axillary brachial plexus blocks with peripheral nerve stimulation support

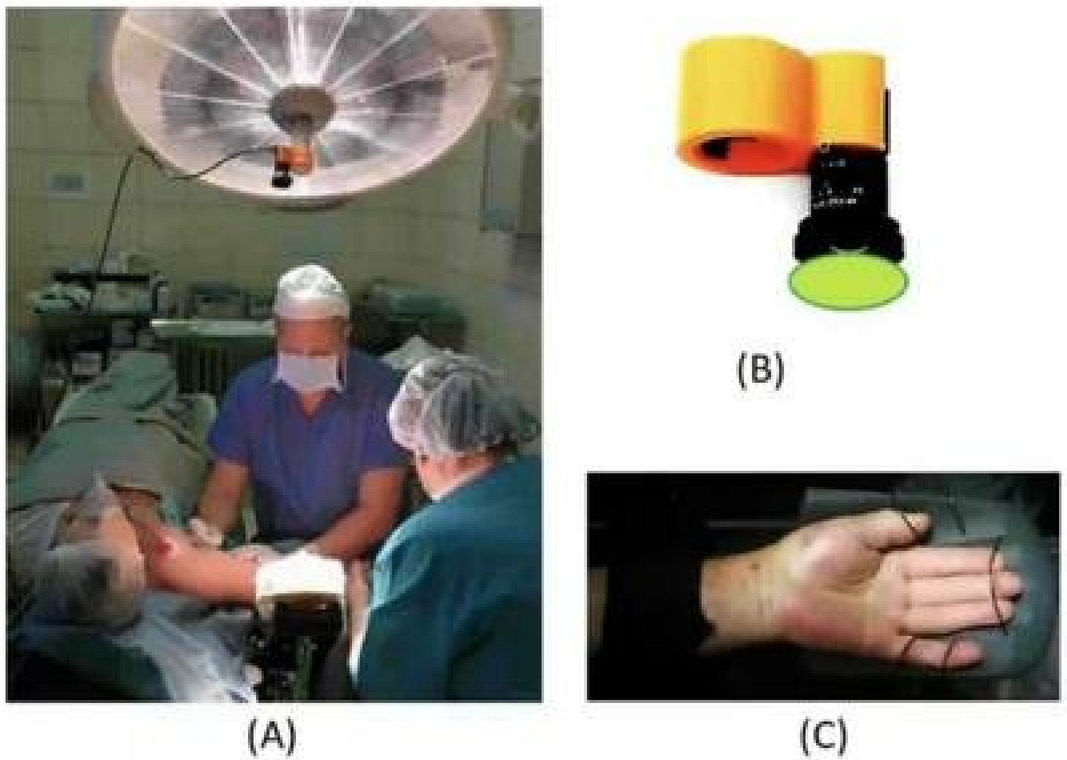

Rubins, U., Miscuks, A., Qawqzeh, Y., Marcinkevics, Z., & Grabovskis, A. (2023). Photoplethysmography Imaging Algorithm for Real-Time Monitoring of Skin Perfusion Maps. In *Proceedings of the IEEE/CVF Conference on Computer Vision and Pattern Recognition* (pp. 5949-5955).

SKIN PERFUSION MAP

- As the local anesthetic is administered in the brachial plexus during the procedure, it affects four different nerves, resulting in subsequent increases in blood circulation in distinct palm areas

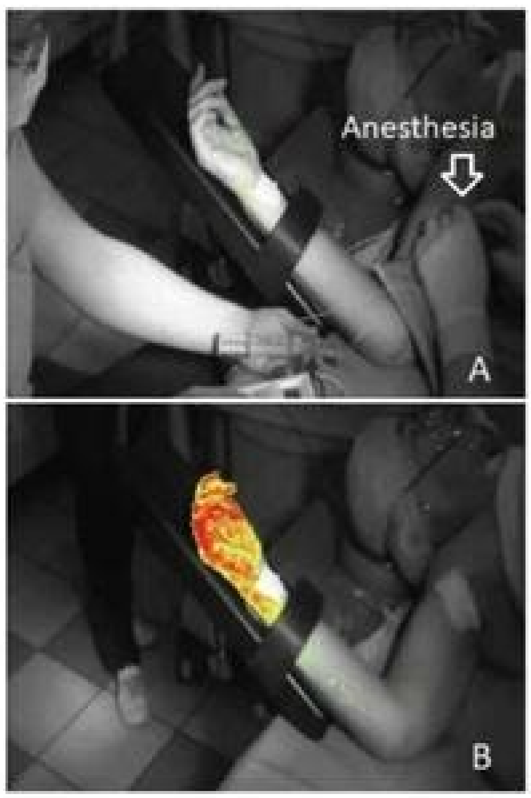

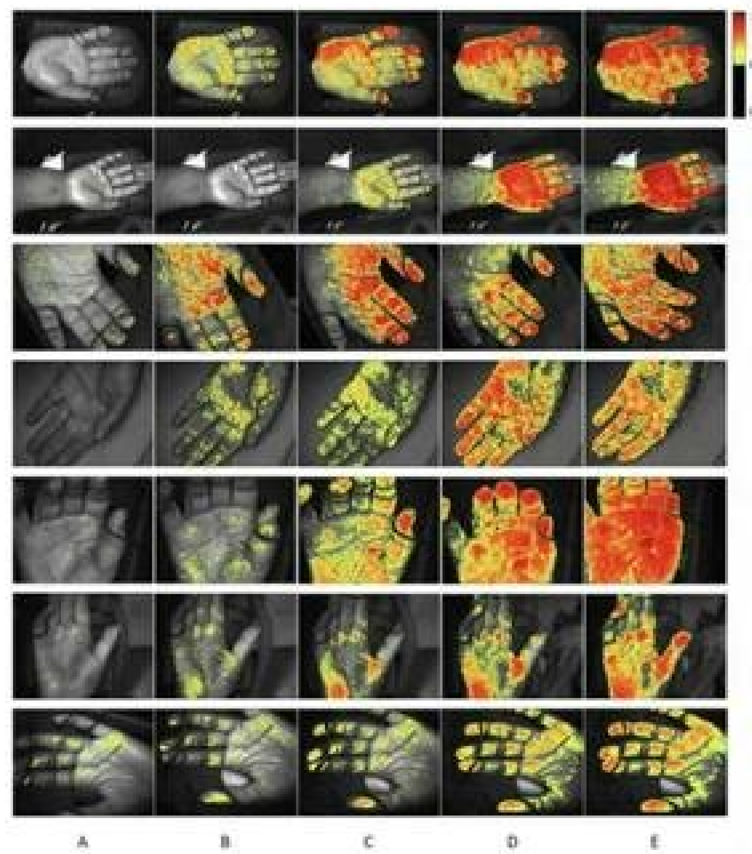

The perfusion maps overlaid with palm's image during 5 stages of measurement of 7 subjects: baseline (0-1 min) (a), 4th, 10th, 15th, and 20th minute after the LA administration (b-e).

Rubins, U., Miscuks, A., Qawqzeh, Y., Marcinkevics, Z., & Grabovskis, A. (2023). Photoplethysmography Imaging Algorithm for Real-Time Monitoring of Skin Perfusion Maps. In *Proceedings of the IEEE/CVF Conference on Computer Vision and Pattern Recognition* (pp. 5949-5955).

BREATHING RATE

- Patient monitoring
  - Fear of infection
  - Need specialists

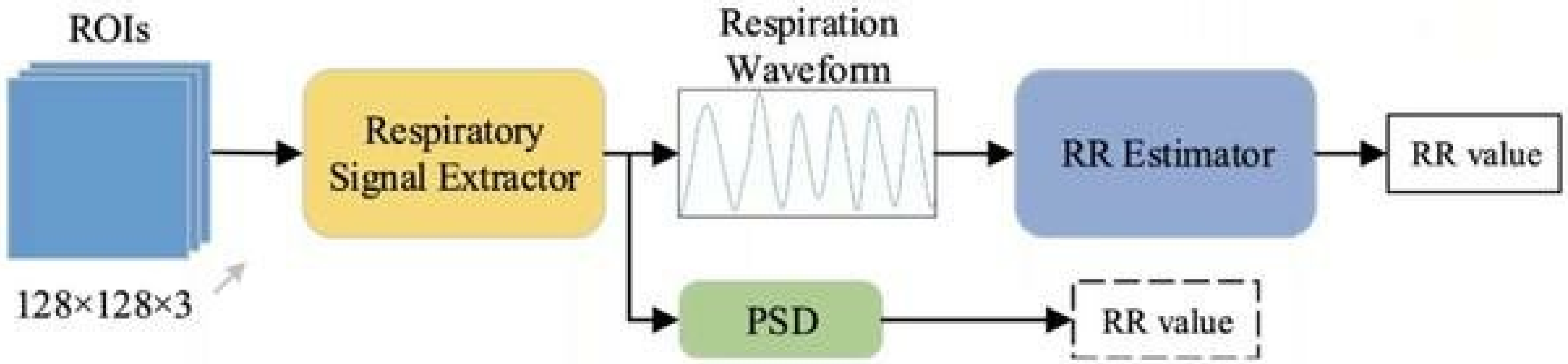

Liu, Z., Huang, B., Lin, C. L., Wu, C. L., Zhao, C., Chao, W. C., ... & Wang, Z. (2023). Contactless Respiratory Rate Monitoring for ICU Patients Based on Unsupervised Learning. In *Proceedings of the IEEE/CVF Conference on Computer Vision and Pattern Recognition* (pp. 6004-6013).

BREATHING RATE

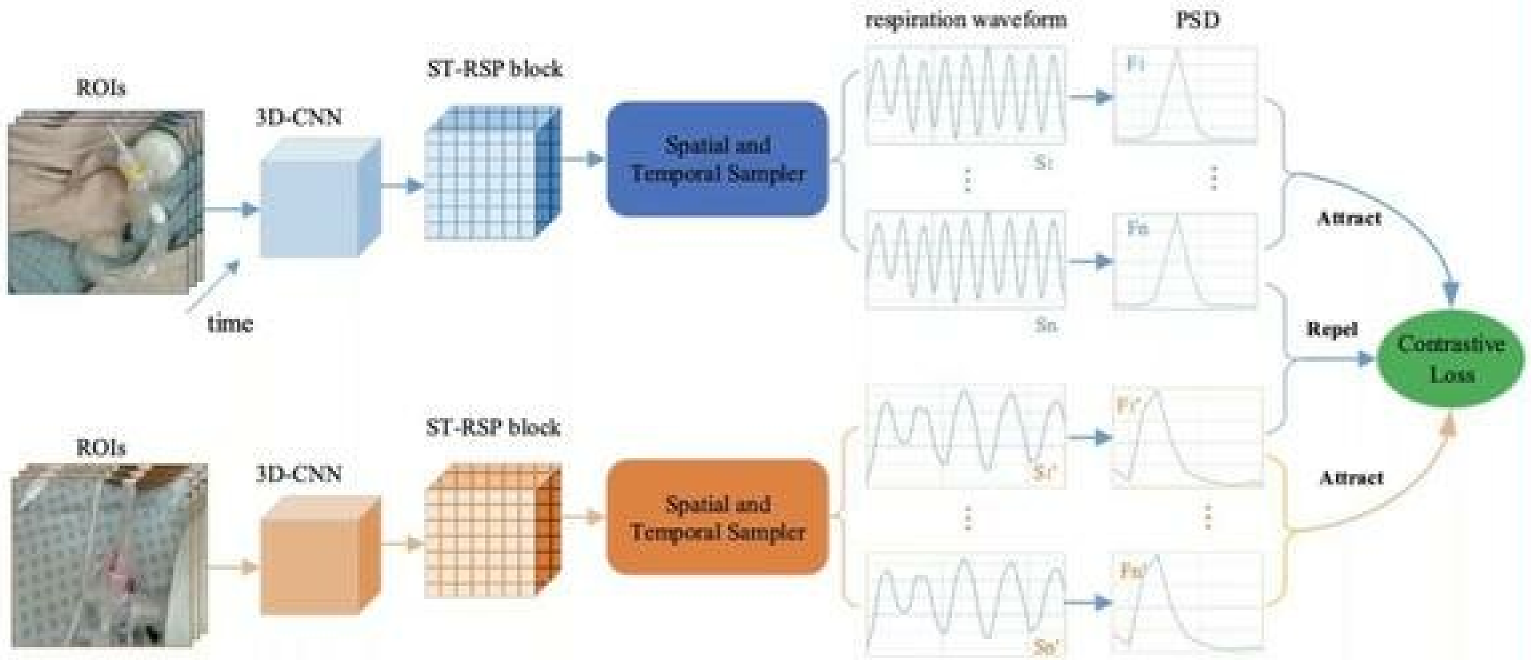

Method	MAE (bpm)	RMSE (bpm)	MAPE (%)	STD (bpm)
Ours	2.807	3.626	14.2	3.025
Massaroni et al. [19]	3.364	4.300	18.3	3.847

Liu, Z., Huang, B., Lin, C. L., Wu, C. L., Zhao, C., Chao, W. C., ... & Wang, Z. (2023). Contactless Respiratory Rate Monitoring for ICU Patients Based on Unsupervised Learning. In *Proceedings of the IEEE/CVF Conference on Computer Vision and Pattern Recognition* (pp. 6004-6013).

BREATHING RATE

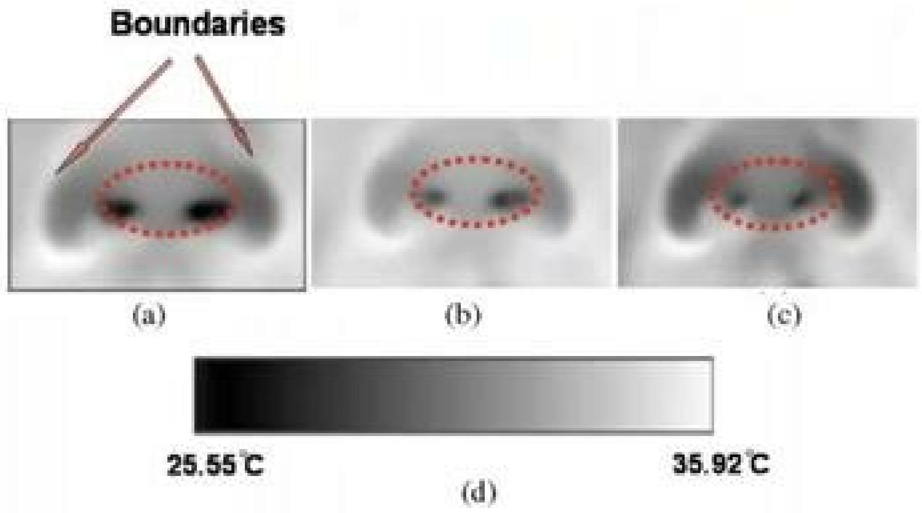

Temporal variance of nostril region in thermal imagery during breathing. (a) Inspiration phase. (b) Transition phase. (c) Expiration phase. (d) Thermal color map

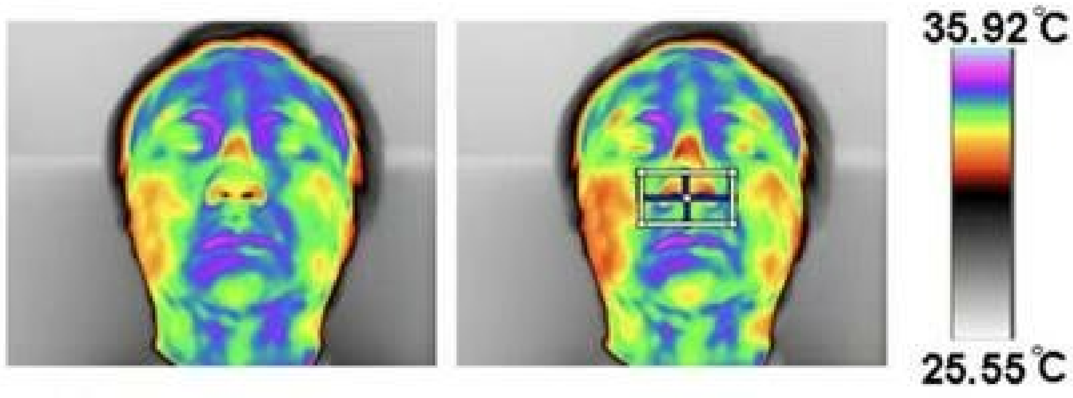

Fei, J., & Pavlidis, I. (2009). Thermistor at a distance: unobtrusive measurement of breathing. *IEEE transactions on biomedical engineering*, *57*(4), 988-998.

THERMAL IMAGING
PERINASAL PERSPIRATION

- Stress stimuli effects perinasal perspiration
- Stress induced perspiration vs physical activity-based perspiration
  - Transient vs long term
  - Thermoregulatory vs bioevolutionary

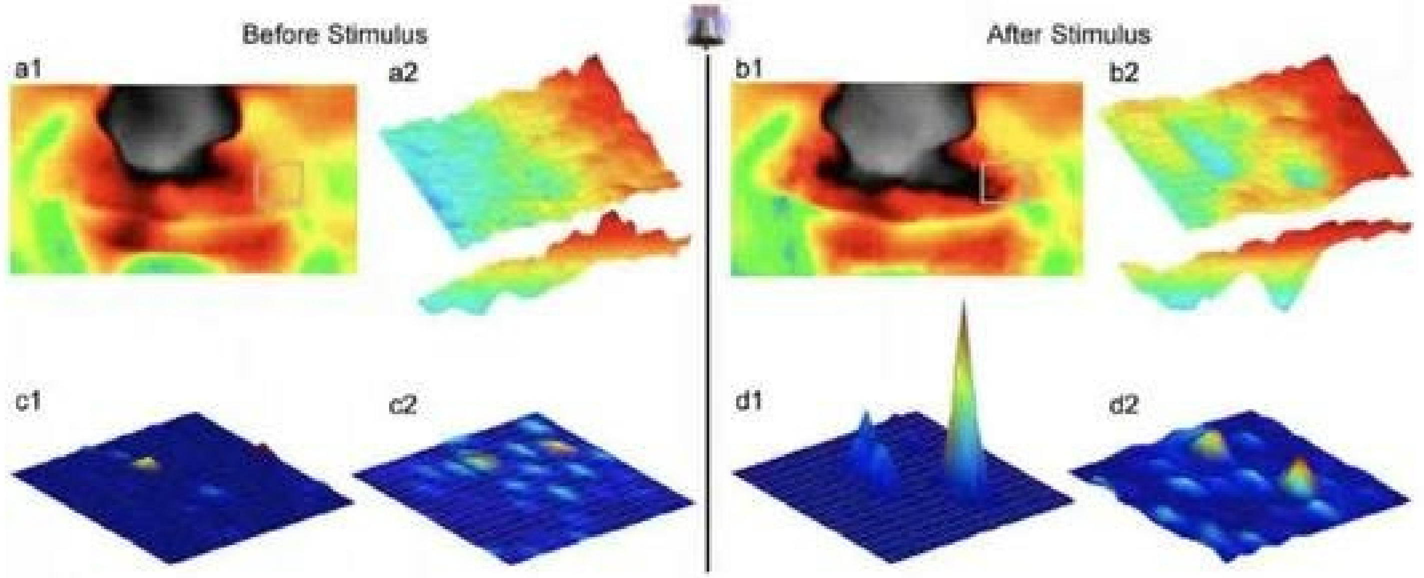

Fig. 1. (a1), (b1) Thermal image of a subject's face before and after an auditory startle stimulus; the gray rectangle delineates the region of interest. (a2), (b2) 3D thermal plots of ROI before and after stimulus. The smooth conic profiles of the emerging perspiration spots denote the gradual transition from a "cold" core to a "hot" surrounding background. (c1), (d1) and (c2), (d2) Nonnormalized 3D energy plots yielded by the morphological and wavelet extraction algorithms before and after stimulus.

SHASTRI ET AL.: PERINASAL IMAGING OF PHYSIOLOGICAL STRESS AND ITS AFFECTIVE POTENTIAL

A TEMPORAL ENCODER-DECODER APPROACH TO EXTRACTING BLOOD VOLUME PULSE SIGNAL MORPHOLOGY FROM FACE VIDEOS

FULAN LI, SURENDRABIKRAM THAPA, SHERYAS BHAT, ABHIJIT SARKAR, A. LYNN ABBOTT

MOTIVATION

RECOVERY OF SHAPE MORPHOLOGY

- iPPG can extract cardiovascular signals
  - Prior works show promises in identifying heart rate, breathing rate
- Recovery of the shape of the PPG
  - Prior works shows promises in detecting systolic/ diastolic peaks.
  - Limited work in finding exact shape morphology
- Shape morphology holds detailed information
  - Abnormalities, blood pressure, oxygen saturation
  - Person authentication and identification
  - Enhance HRV reliability

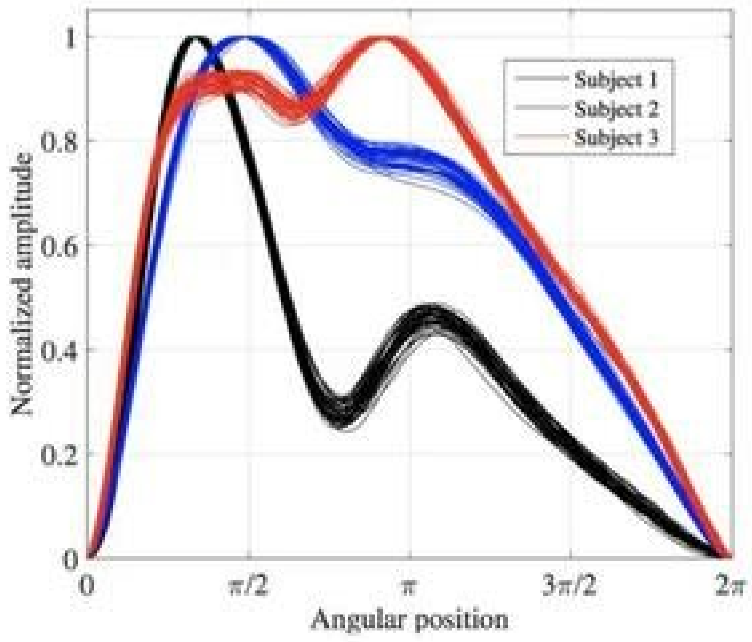

SUMMARY

TWO DIFFERENT METHODS TO RECOVER PPG

- Use manually selected ROIs v/s attention-based method

- Time series ROI data as input v/s images as input

MODEL ARCHITECTURE

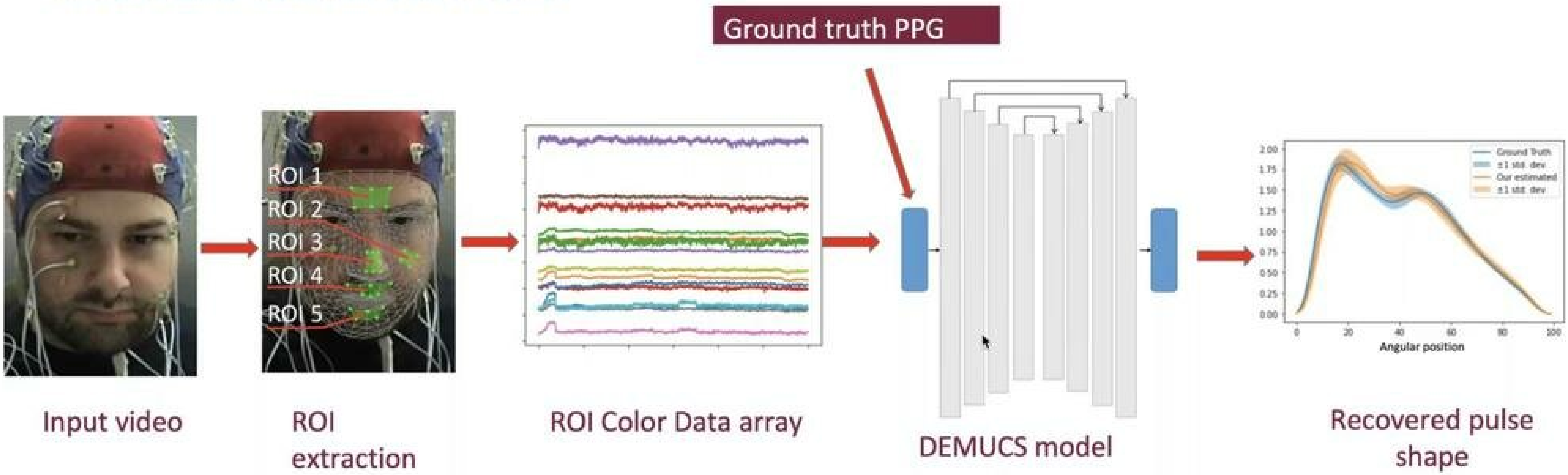

DEMUCS is an encoder-decoder model that are used for audio source separation.

$$L(y, \hat{y}) = (1-\lambda)\|y - \hat{y}\| + \lambda(\|Re(Y) - Re(\hat{Y})\| + \|Im(Y) - Im(\hat{Y})\|)$$

CAMERA-BASED RECOVERY OF CARDIOVASCULAR SIGNALS FROM UNCONSTRAINED FACE VIDEOS USING AN ATTENTION NETWORK

YOGESH DESHPANDEY, SURENDRABIKRAM THAPA, ABHIJIT SARKAR, A. LYNN ABBOTT

Traditional Pre-processing Flaws

Frames

Center Crop

Different Face Angles, Occlusion and Skin Tone Variations

Data Ref. – UBFC Phys

COMPLETE MODEL ARCHITECTURE

- Convolutional Attention Network
- Mean Square Error (MSE) Loss
- SGDM Optimizer

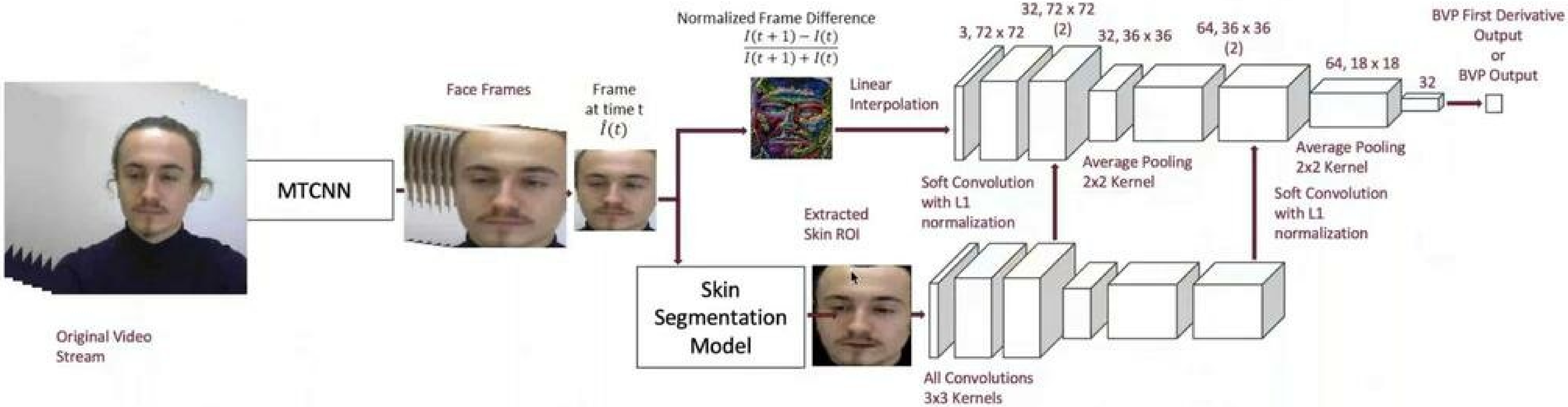

SHAPE MORPHOLOGY RECOVERY

Biometric identification

$$smm_t = \frac{1}{C}\sum_{i=1}^{C} ncr(x_i(t)_{gt}, x_i(t)_{op})$$

$$smm_f = \frac{1}{C}\sum_{i=1}^{C} ncr(x_i(f)_{gt}, x_i(f)_{gt})$$

$$smm_p = \frac{1}{C}\sum_{i=1}^{C} ncr(x_i(p)_{gt}, x_i(p)_{op})$$

Shape Morphology Metrics (Normalized Cross-Correlation) in time domain, frequency domain and power domain are given as smm_t, smm_f and smm_p respectively.

Metrics Domain	Our Model (First Der. BVP)	DeepPhys
Time↑	**0.120**	0.118
Frequency↑	**0.670**	0.645
Power↑	**0.594**	0.472

Shape Morphology Integrated Signal Metrics Domain Wise

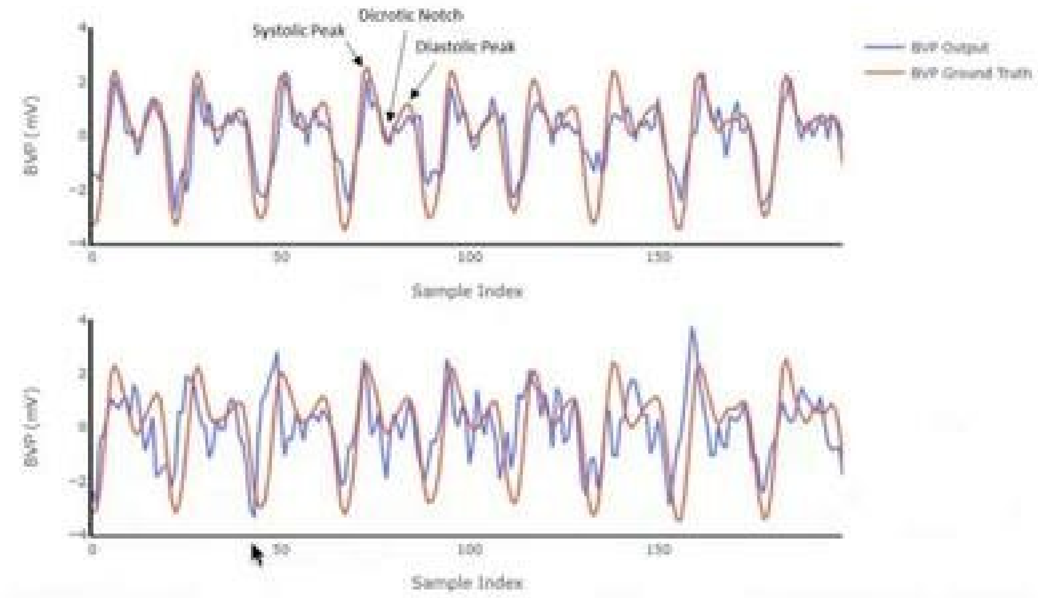

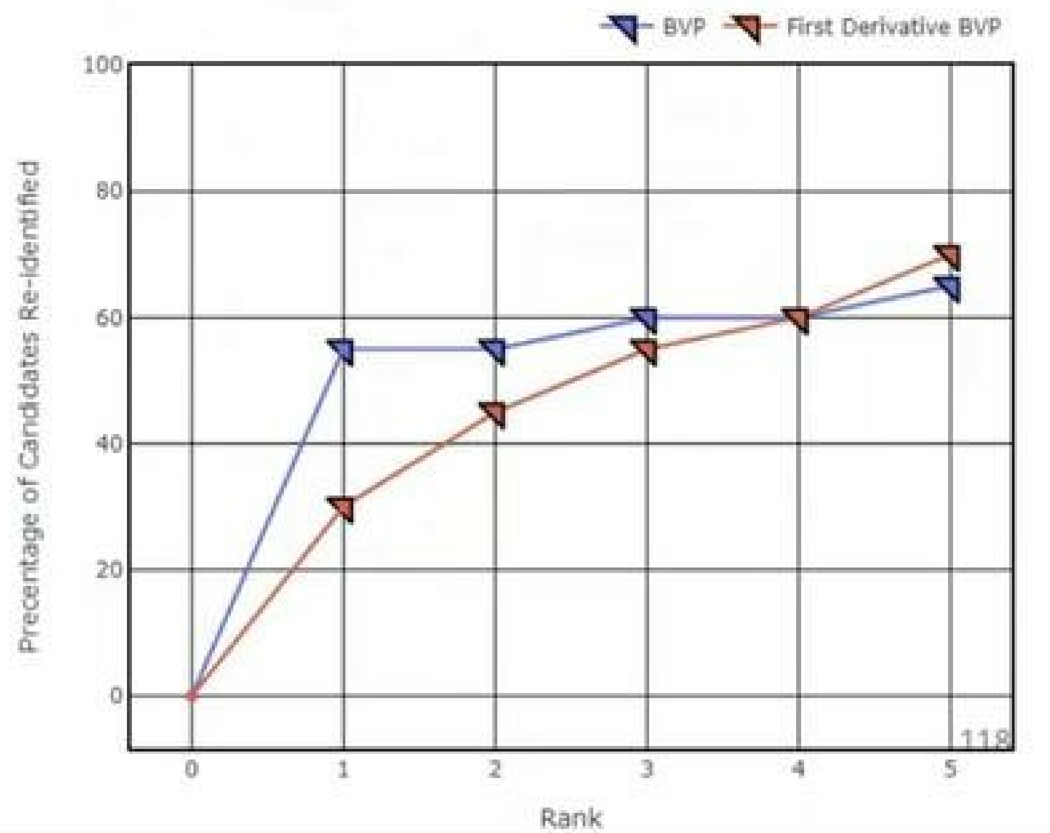

CONCLUSION

- rPPG has made significant progress in the last decade
- Research shows potential in neural network based methods
- However still question remains on HRV
- Scope of research remains in movement of head, unconstrained illumination.

CHALLENGES AND NEXT STEPS

CAMERA BASED METHODS

- Data collection
  - Create standard protocol
- Fairness
  - Biases stemming from data and methods
- Motion tolerance
- Ambient illumination
- Data privacy

DATASET

Dataset	No. of Subjects	No. of Videos	Variations	Ground Truth
PURE [8]	10	60	- Facial Expressions - Head Movements	PPG
MMSE-HR [9]	40	102	- Facial Expressions - Head Movements	HR
VIPL-HR [10]	107	2378	- Facial Expressions - Head Movements - Illumination - Camera Types (RGB and NIR)	HR and BVP
ECG-Fitness [3]	17	17 (YUV)	- Facial Expressions - Head Movements	ECG
MAHANOB-HCI [11]	27	527	- Facial Expressions	ECG
Vicar PPG2 [12]	10	20	- Facial Expressions - Head Movements - Camera Types - Occlusion	PPG
DEAP [13]	22	874	- Facial Expressions - Occlusion	PPG
MoLi-PPG [14]	30	170	- Facial Expressions - Head Movements - Illumination	ECG
COHFACE [15]	40	164	- Illumination	PPG
PFF [16]	13	104	- Head Movements - Illumination	
OBF [17]	100	200	- Camera Types (RGB, NIR)	ECG, BVP and RF
LGI [18]	25	100	- Facial Expressions - Head Movements - Illumination	PPG
UBFC-RPPG [19]	42	42	- Facial Expressions - Head Movements	PPG
UBFC-Phys [20]	56	168	- Facial Expressions - Head Movements - Facial Hair	BVP and EDA

- FDA approved equipment (Researchers require clinically approved ground truth values which could be further considered while training a models).
- Skin, age and gender variation with valid distribution.
- Health status of the candidates.
- Equipment Variation.
- Natural light and general light variability.

NEW DATASET

- Video collected
  - two NIR Cameras (940nm and 850nm), and one RGB Camera
  - Video Resolution: 2064 X 2464
  - 60 Hz
- Two different lighting conditions
- PPG Collected with [Biopac Sensor]
- 10 Subjects
- 7 Tasks in two sessions
  - Reading, watching videos
- Videos are collected raw as well with total dataset size to be around 20 TB.
- We will avail compressed versions as well (lesser dataset size).

Lighting Type 1 with RGB Camera

850 nm
Camera

950 nm
Camera

Candidate Revealing Neck Region

Lighting Type 2 with RGB Camera

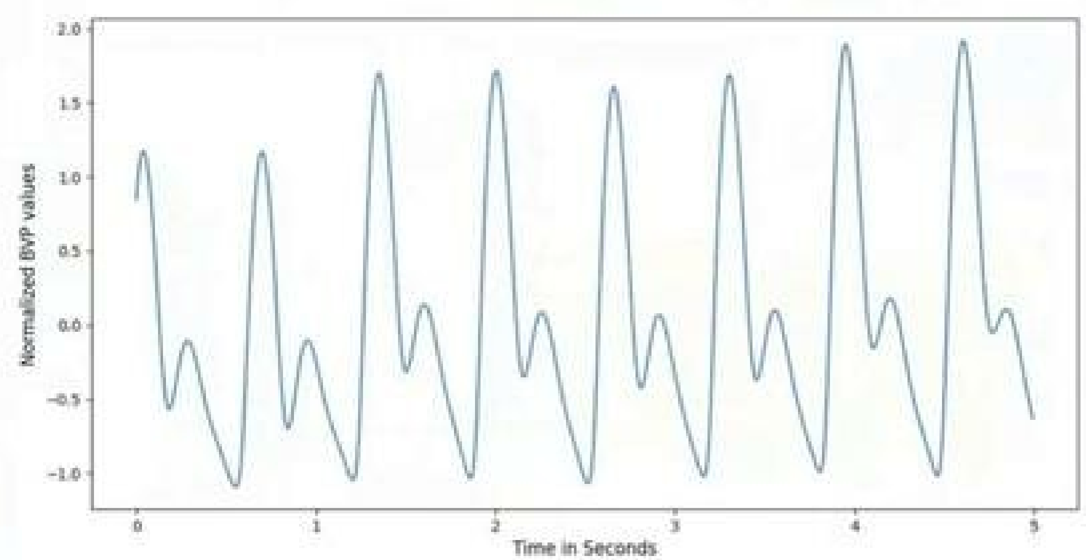

BVP Sample taken using [BioPac Sensor]

CODEBASE

- NVIDIA HeartRateNet

  A non-invasive heart rate estimation network, which aims to estimate heart rates from RGB facial videos.

- iphys-toolbox

  Toolbox for PPG analysis.

- PPGI-Toolbox

  Toolbox containing implementations of different models for image based Photoplethysmography.

- rppg.base package

  Baseline Algorithms for Remote Photoplethysmography (rPPG)

- https://sites.google.com/view/vt-tricam-ppg
  - Work of our team

CONTACT INFORMATION

Thank you!

- Dr. Lynn Abbott
  Abbott@vt.edu

- Dr. Abhijit Sarkar
  ASarkar@vtti.vt.edu
  asarkar1@vt.edu